UNIVERSIDAD D CÓRDOBA

Departamento de Agronomía
Área Ingeniería Hidráulica

Modelo integral de aprovechamiento de la energía solar fotovoltaica en riego

Integral model for the use of solar photovoltaic energy in irrigation

Tesis Doctoral presentada por

Aida Mérida García

para la obtención del título de

DOCTOR CON MENCIÓN INTERNACIONAL POR LA UNIVERSIDAD DE CÓRDOBA

Directores

Dr. Emilio Camacho Poyato

(Catedrático de la Universidad de Córdoba)

Dr. Juan Antonio Rodríguez Díaz

(Profesor Titular de la Universidad de Córdoba)

TITULO: *Integral model for the use of solar photovoltaic energy in irrigation*

AUTOR: *Aida Mérida García*

Campus de Rabanales
Ctra. Nacional IV, Km. 396 A
14071 Córdoba

https://www.uco.es/ucopress/index.php/es/
ucopress@uco.es

Mención de doctorado internacional

Esta tesis cumple con los requisitos establecidos por la Universidad de Córdoba para la obtención de la mención de doctorado internacional:

- Estancia de 3 meses realizada en Civil, Structural & Environmental Engineering Department of Trinity College Dublin (Irlanda), bajo la supervisión de Dr. Aonghus Mc Nabola.
- Informe previo de dos doctores externos y con experiencia investigadora acreditada de alguna institución de educación superior o instituto de investigación de fuera de España.
- Un miembro del tribunal pertenece a un centro de investigación extranjero.
- Parte de la tesis está escrita en inglés y castellano.

Tesis como compendio de publicaciones

Esta tesis se presenta como compendio de publicaciones, cumpliendo con los requisitos establecidos por la Universidad de Córdoba para este fin. Tres de los seis capítulos de esta tesis se corresponden con tres artículos científicos publicados en revistas incluidas en el primer cuartil según la última relación del Journal Cittation Reports (2018).

1. Mérida García A, Fernández García I, Camacho Poyato E, Montesinos Barrios P, Rodríguez Díaz JA (2018). Coupling irrigation scheduling with solar energy production in a smart irrigation management system. J. Clean. Prod. 175, 670-682. Índice de impacto: 5.651. 1er cuartil en el área de Ingeniería y Medioambiente, posición 7/50.
2. Mérida García, A., Gallagher, J., Mc Nabola, A., Camacho Poyato, E., Montesinos Barrios, P., Rodríguez Díaz, J.A., 2019. Comparing the environmental and economic impacts of on- or off-grid solar photovoltaics with traditional energy sources for rural irrigation systems. Renew. Energy 140, 895–904. Índice de impacto: 4.900. 1er cuartil en el área de Energía y Combustibles, posición 20/97; y en Tecnología y Ciencia de la Sostenibilidad (Green and Sustainable Science and Technology), posición 7/33.
3. Mérida García A, González Perea R, Camacho Poyato E, Montesinos Barrios P, Rodríguez Díaz JA, 2020. Comprehensive sizing methodology of Smart photovoltaic irrigation systems. Agricultural Water Management. Aceptado para publicación. Índice de impacto: 3.542. 1er cuartil en el área de Recursos Hídricos, posición 12/91; y en Agronomía, posición 9/89.

TÍTULO DE LA TESIS: Modelo integral de aprovechamiento de la energía solar fotovoltaica en riego.

DOCTORANDA: Aida Mérida García

INFORME RAZONADO DEL/DE LOS DIRECTOR/ES DE LA TESIS:

La tecnificación del regadío y su cada vez mayor dependencia energética, esencialmente debida a los bombeos de los sistemas de distribución de agua a presión, ha motivado que en los últimos años los regantes hayan experimentado un importante aumento en sus costes de producción que hacen que, en ocasiones, la rentabilidad de la producción agrícola se vea seriamente comprometida. Además de esto, en el contexto actual de cambio climático, la sociedad demanda de manera creciente alimentos producidos de una forma sostenible, con una huella ambiental mínima.

Ante esta situación, las energías renovables, y especialmente la energía solar fotovoltaica, están comenzando a jugar un papel importante en las redes de distribución de agua. Por un lado, la reducción de los costes de producción de los paneles hace que los períodos de amortización se hayan reducido a 4-6 años. Por

otro lado, la reducción en las emisiones asociadas a los bombeos permite reducir la huella de carbono asociada a la producción agrícola, lo que puede considerarse una ventaja competitiva en los mercados, de acuerdo con las demandas actuales de la sociedad.

No obstante, la energía solar fotovoltaica presenta ciertos inconvenientes que hacen que las prácticas de manejo del riego tradicionales no sean del todo válidas en las nuevas condiciones. Esto es debido principalmente a la imposibilidad de regar cuando la irradiancia es demasiado baja, lo que implica que sea necesario sincronizar el manejo del riego con la producción energética de la planta solar. Por otro lado, se hace necesario considerar la planta solar y el sistema de riego como un todo, que debe funcionar de forma conjunta para poder optimizar el uso de la potencia generada en cada momento y asegurar un uso eficiente del agua. Hasta la fecha, estos aspectos no se habían abordado en profundidad.

Con el objetivo de abordar esta problemática se ha desarrollado esta Tesis Doctoral, la cual se divide en tres grandes apartados claramente diferenciados, los cuáles abordan diferentes problemas relacionados con el riego solar y aportan soluciones para facilitar el manejo óptimo de dicha tecnología. La Tesis se ha elaborado como compendio de artículos científicos, que han dado lugar a publicaciones en revistas científicas con altos índices de impacto, en el primer cuartil de su área de conocimiento:

- Mérida García, A., Fernández García, I., Camacho Poyato, E., Montesinos Barrios, P., & Rodríguez Díaz, J. A. (2018). Coupling irrigation scheduling with solar

energy production in a smart irrigation management system. Journal of Cleaner Production, 175, 670-682. doi:10.1016/j.jclepro.2017.12.093

En este trabajo, como primer paso de la Tesis, se desarrolla un sistema de riego solar inteligente, el cual sincroniza la producción energética de la planta solar y el riego deficitario del olivar. Para ello, el sistema considera datos de irradiancia en tiempo real, modelo hidráulico del sistema de riego y un modelo suelo-agua-planta.

Este modelo se ha puesto en marcha y validado en una planta piloto instalada para este fin en la Finca Experimental del Campus de Rabanales de la Universidad de Córdoba.

- Mérida García, A., Gallagher, J., McNabola, A., Camacho Poyato, E., Montesinos Barrios, P., & Rodríguez Díaz, J. A. (2019). Comparing the environmental and economic impacts of on- or off-grid solar photovoltaics with traditional energy sources for rural irrigation systems. Renewable Energy, 140, 895-904. doi:10.1016/j.renene.2019.03.122

En el segundo de los trabajos se aborda el impacto ambiental y la huella de CO_2 del riego solar en comparación con otras fuentes convencionales tales como los generadores diésel y la red eléctrica. Este trabajo lo realizó en colaboración con investigadores del Trinity College de Dublin (Irlanda) durante su estancia predoctoral, necesaria para la obtención de la mención internacional de los estudios de doctorado.

- Mérida García, A., González Perea, R., Camacho Poyato, E., Montesinos Barrios, P., & Rodríguez Díaz, J. A. (2019). Comprehensive sizing methodology of

smart photovoltaic irrigation systems. Agricultural Water Management. Accepted for publication.

En el tercer trabajo se aborda la necesidad del diseño conjunto de la instalación de riego y de la planta solar simultáneamente. Para ellos se recurre a métodos heurísticos que permiten optimizar el diámetro de las tuberías, la gestión de riego en parcela y el tamaño de la planta solar.

Por último, complementando los trabajos anteriores, se añade un cuarto artículo como anejo, en el cual se muestran los detalles de la herramienta informática desarrollada para la implementación y operación del sistema de riego solar inteligente:

- González Perea, R. G., Mérida García, A., Fernández García, I., Poyato, E. C., Montesinos, P., & Rodríguez Díaz, J. A. (2019). Middleware to operate smart photovoltaic irrigation systems in real time. Water (Switzerland), 11(7) doi:10.3390/w11071508

En su conjunto, la investigación realizada representa un claro avance al estado del conocimiento actual en esta temática, sobre la cual prácticamente no existían trabajos previos. Además, la investigación desarrollada puede tener importantes repercusiones en el sector del riego, cada vez más interesado en el uso de la energía solar fotovoltaica para el suministro de agua por sus beneficios tanto económicos como ambientales.

Esta Tesis Doctoral se ha realizado al amparo de dos proyectos del Plan Nacional: “Tecnologías Innovadoras para mejorar el uso del agua y energía en el

regadío" (AGL2014-59747-C2-2-R) y "Eficiencia en la sostenibilidad del nexo agua y energía en el regadío" (AGL2017-82927-C3-1-R). Para la realización de la misma, la Doctoranda ha disfrutado de una beca de Formación de Personal Investigador (FPI), en la que, además de los trabajos de investigación, ha colaborado activamente en la docencia de diversas asignaturas en el ámbito de la Ingeniería Hidráulica y del Riego.

Por todo ello, se autoriza la presentación de la tesis doctoral.

Córdoba, 6 de Noviembre de 2019

Firma de los directores

Fdo.: Prof. Dr. Emilio Camacho Poyato

Fdo.: Prof. Dr. Juan Antonio Rodríguez Díaz

Agradecimientos

Hace cuatro años decidí comenzar una nueva etapa, gracias a la oportunidad que Emilio, Juan Antonio y Pilar me brindaron para hacer la tesis, una meta que hoy al fin, puedo ver conseguida. Han sido cuatro años cargados de emociones, esfuerzo, motivación y bastantes altibajos, pero sin lugar a duda, cuatro años tremendamente enriquecedores.

En primer lugar, no tengo palabras para agradecer la dedicación y confianza puesta en mi por parte de mis tres directores, gracias a los cuales hoy pongo fin a esta etapa. Gracias por contar conmigo para formar parte de este proyecto, por acompañarme y guiarme, por abrirme las puertas a un equipo de trabajo inmejorable. También, agradezco enormemente vuestra predisposición para hacerme partícipe de tantos congresos y actividades como os ha sido posible, y por supuesto, por permitirme comenzar la labor docente con la que desde pequeña había soñado. Esto me ha ayudado a crecer no solo profesionalmente, sino también en aspectos personales. A Emilio, por la cercanía, positivismo y alegría que desde el primer día me has transmitido, así como la motivación tras mis primeras experiencias dando clase. Por entrar cada mañana sonriente a la sala, compartir de vez en cuando un chiste y hacernos reír con alguna que otra trastada que gastar a Pilar. A Juan Antonio, por tener esa actitud comprensiva y empática con los que estamos empezando, por motivarme a luchar día a día y estar siempre dispuesto a ayudarme. Por nuestras infinitas reuniones con mi primer artículo, y las que han seguido. Y no puedo olvidar agradecerte el que me hayas acompañado en mi toma de contacto con las prácticas, siendo mi maestro. A Pilar, por nuestros ratitos mañaneros en los que cotilleábamos y nos poníamos al día. Por todo el tiempo dedicado a mis trabajos,

tus miles de correcciones coloridas y los cientos de enfoques y vueltas de tuerca que le hemos dado juntas al tercer artículo. Y por supuesto, por hacer de madre-postiza cuando lo he necesitado.

Al Ministerio de Economía y Competitividad y los Fondos Europeos de Desarrollo Regional, quienes han financiado el proyecto que ha sustentado el contrato predoctoral de Formación de Personal Investigador (FPI) gracias al cual ha sido posible el desarrollo de esta tesis doctoral.

A Aonghus y John, por recibirme con los brazos abiertos en su equipo durante los tres meses de mi estancia en Trinity College (Dublín), por haberme permitido aprender de vosotros y por brindarme vuestra ayuda y apoyo, así como seguir confiando en mí. Al Interreg Volunteer Youth, con quienes he disfrutado de mi primera experiencia en voluntariado durante esta misma estancia.

A Irene y Rafa, por estar siempre dispuestos a ayudarme, en especial, por sacarme del agujero negro de Matlab en tantísimas ocasiones. Por alentarme en mis días bajos, compartir risas y anécdotas y hacerme sentir una más desde el primer día. A Irene, por el tiempo compartido en Dublín, por hacer la experiencia aún mejor. A mis Cármenes y Jose, por llenarme cada día de alegría. A Carmen pequeña, por tu tremenda motivación y por transmitirme esas ganas, esa actitud de mirar todo en positivo. Mil gracias por hacerme sentirte siempre tan cerca. A Carmen grande, por haberme ganado en tan poco tiempo, por abrirte a mí y ofrecerte para escucharme en cualquier momento. Por hacer tan fácil el entendernos, mandarme una de esas frases que tanto nos gustan cuando más me hace falta y por los ratitos de risa en el coche. Y a Jose, por hacerme siempre reír, por tu actitud alegre y charlatana, por tu cercanía y predisposición para echarme una mano y compartir esos ratos en los que

el uno al otro nos contamos nuestro trabajo. Eso sí, muy equivocado al pensar que Cabra es la capital de la Subbética, pero en fin, buena gente. A Jorge, por haber formado parte de ese ambiente tan especial de trabajo que tenemos en la sala y apoyarme durante esta etapa. A mis hermanas favoritas, Victoria y Mari Paz, por compartir conmigo vivencias de hermanas que me hacen revivir las mías, por ese buen rollo y alegría que traéis cada día. Y a Manuel, pese al poco tiempo en que coincidimos en el despacho, gracias por los ratos que hemos compartido, porque, aunque te resistas, eres y siempre serás uno más del grupo de los hidráulicos.

A Félix y Manuela, por resolverme siempre los entuertos de papeleo y porque con vosotros, los ratos de laboratorio son mucho más divertidos. A, Pepe y Miguel, por los pequeños ratitos de charla mañaneros y animarme durante esta etapa. Y a Jose Emilio, por brindarme siempre tu ayuda.

A Alicia, mi compañera de batallas, mi amiga, confidente y apoyo diario. Por todo lo que haces por mí en el día a día, por demostrarme que estarás ahí siempre para lo que haga falta. Por tantas risas y llantos juntas en este tiempo. Porque la carrera nos unió y la tesis nos ha hecho inseparables. Y por nuestra lucha constante a ver quién es más desastre, en ese piso de abuela que hemos convertido en un pequeño hogar.

A Irina, por nuestras penas compartidas, para hacerlas medias.

Y a mis amigos, en especial a Silvia, Antonio y Soraya, por vuestro apoyo durante todo este tiempo.

Y por supuesto, a toda mi familia, por confiar siempre en mí. A mi padre, por motivarme a adentrarme en esta aventura, por interesarte por mi trabajo y empeñarte

en que te explique y entender mis modelos, por afirmar “hoy el día te irá bien” cuando sabes que necesito un empujón y por dibujar tu visión más positiva cuando los problemas no me dejan ver nada claro. A mi madre, por tu capacidad de ponerte en la piel de los demás, por tener siempre un abrazo de los que reconfortan, por convencerme en cada momento de que, si uno quiere, puede. Por escuchar atenta mis presentaciones y mostrar tanto entusiasmo por lo que hago. Porque sin vosotros, nunca habría llegado hasta aquí. Gracias por enseñarme cómo hacer frente a los problemas. A mi hermana Rosa, por tu incansable empeño en arrancarme una sonrisa cada mañana. Por tu apoyo, por transmitirme tus ganas y, sobre todo, por ser mi ejemplo a seguir. Por nuestros ratitos intentando enterarnos de la tesis de la otra, aunque luego resumas la mía en “riego solar inteligente”. Por cargarme las pilas con tu sobredosis de energía y estar siempre ahí, por difícil que lo pongan las circunstancias. Por nuestros ratos de risas infinitas que acaban mojados en lágrimas, esto también será siempre mi *Ahora* favorito. Y cómo no, gracias por esa maravillosa ecuación que resolvía todo el problema. Y a Juan, por tu infinita paciencia y por intentar transmitirme tu calma, aunque a veces te lo ponga bastante difícil. Por haberme acompañado en todo este camino, escuchando mis monólogos a cerca de mis modelos e intentando siempre echarme una mano. Por hacerme reír, animarme y confiar en mí, afirmando un “tranquila, acabarás consiguiéndolo”. Por hacer este recorrido mucho más llevadero. Y a mis abuelas, por haber hecho siempre evidente lo orgullosas que han estado de mí.

Gracias a todos, por hacerme sentir acompañada en este camino, y por hacerlo más fácil con vuestro apoyo.

Summary

Irrigated agriculture makes possible to increase the productivity of the cropped area, becoming a key activity to meet the growing food demand resulting from the increase of global population. The transformation of arable land from rain-fed to irrigated raises in turn the water demand by the agricultural sector, which currently accounts for 70% of total extractions, on a global scale.

The modernization of the irrigation sector led a substantial improvement in the efficiency of water use, although, in parallel, the replacement of systems based on open channels to pressurized networks resulted in a significant increase in energy demand. The main drawbacks of this growing demand are the higher farm operating costs and environmental impact linked to agriculture. In this context, there is a need to look for alternative energy sources with low greenhouse gas emissions, maintaining and even increasing the profitability of the agricultural activity.

This thesis is structured in 6 chapters and an annex, focused on the integration of photovoltaic technology in irrigation as energy supply source. Thus, the different chapters contemplate this integration from the point of view of irrigation management and schedule to the dimensioning of the system, taking into account economic, environmental and operational aspects. The first chapter contextualizes the reason of this thesis, which objectives are set out in chapter 2, in which the structure of the rest of the document is also detailed.

Chapter 3 presents a model for the management of photovoltaic irrigation. This model integrates crop, climatic, hydraulic and energy variables, accomplishing a real time synchronization of the photovoltaic power generated and the power and

irrigation times demanded by the network which supplies. The application of this model to a real case study (experimental olive orchard of the Rabanales Campus of the University of Córdoba) has achieved excellent results, being able to satisfy, automatically, more than 96% of the irrigation requirements of the crop during the irrigation season analysed. In addition, the substitution of the conventional electrical supply by photovoltaic energy avoided the emission of 1.2 t of CO_2 eq. corresponding to 602 h of irrigation (during a season), in the olive orchard field of the case study analysed.

In chapter 4 an analysis of the life cycle of the photovoltaic technology used as energy source in irrigation is carried out. In addition, it is also compared with the life cycle linked to the energy supply with traditional options, diesel generators and the electricity grid. Subsequently, a comparative analysis is carried out between the different supply options, establishing two possible scenarios: with and without grid connection. The results derived from this work, expressed in relation to the unit of energy in kWh, showed the importance linked to the percentage of photovoltaic energy produced that is actually used, thus having a great repercussion the seasonality of irrigation and the possibility of taking advantage of the surplus energy generated when irrigation is not required. This work was also complemented with an analysis of the life cycle cost for the different technologies. Thus, the photovoltaic option has the lowest total costs (63% and 36% lower than the diesel generator and electricity grid options, respectively, for a useful life of the project of 30 years), despite requiring a higher initial investment.

Chapter 5 presents a model for the optimal dimensioning of photovoltaic irrigation systems, which determines hydrants grouping in irrigation sectors, the pipe

diameters for each section of the network and the dimensioning of the photovoltaic plant. This model, based on evolutionary algorithms (specifically the genetic algorithm NSGAII) also integrates the first of the models presented, with which the operation of each generated sizing option is verified. The possible solutions are evaluated to select those that best fit the established objective functions. Therefore, the results provided by the model are those combinations of hydrant grouping, pipe sizes and PV plant dimensioning that minimize the investment costs while ensuring the proper operation of the system. Once the model was developed, it was simulated to carry out the dimensioning of the PV irrigation system of the experimental olive orchard field of the University of Córdoba. The results showed design solutions with investment cost reductions between 24 and 39%, compared to the original design of the installation, with an irrigation satisfaction equal or greater than the current 96% in all options.

Finally, chapter 6 synthesizes the main conclusions obtained after the development of this thesis, as well as the possible future avenues of research.

This thesis highlights the importance of the integration of photovoltaic energy in agriculture as energy supply source, with low environmental impact, alternative to traditional energy sources. Therefore, it presents innovative tools for photovoltaic irrigation management and jointly dimensioning of the system irrigation network-photovoltaic plant, taking into account the energy, hydraulic, economic, environmental and operational aspects of the system. Therefore, the purpose of providing the incorporation of this technology in the sector is combined with the objectives of reducing the environmental impact of this activity and improving the profitability of the farmer.

Resumen

La agricultura de regadío permite aumentar la productividad de la superficie agrícola, convirtiéndose en una actividad clave para satisfacer la creciente demanda de alimentos derivada del aumento de la población mundial. La conversión de superficie cultivable del secano al regadío a su vez incrementa la demanda de agua por parte del sector agrícola, la cual representa en la actualidad un 70% de las extracciones totales, a escala global.

La modernización del regadío ha permitido una mejora sustancial en la eficiencia del uso del agua, aunque, de forma paralela, la sustitución de los sistemas basados en canales abiertos por redes a presión ha dado lugar a un aumento significativo en la demanda de energía. Los principales inconvenientes derivados de esta creciente demanda se traducen en un mayor coste de operación en las explotaciones e impacto ambiental vinculado a la agricultura. En este contexto surge la necesidad de buscar fuentes de energía alternativas de baja emisión de gases efecto invernadero que permitan, además, mantener e incluso aumentar la rentabilidad de la actividad agrícola.

Esta tesis se estructura en 6 capítulos y un anexo, enfocados todos ellos a la integración de la tecnología fotovoltaica en el riego, como fuente de suministro energético. Así, los distintos capítulos contemplan esta integración desde el punto de vista de la gestión y programación del riego hasta el dimensionamiento del sistema, teniendo en cuenta aspectos económicos, ambientales y de operatividad. El primero de los capítulos contextualiza el porqué de esta tesis, estando los objetivos de la misma recogidos en el capítulo 2, donde además se detalla la estructura del resto del documento.

En el capítulo 3 se presenta un modelo para la gestión del riego fotovoltaico. Este modelo integra variables del cultivo, climáticas, hidráulicas y energéticas, llevando a cabo una sincronización en tiempo real de la potencia fotovoltaica generada y la potencia y tiempos de riego demandados por la red a la que abastece. La aplicación de este modelo a un caso de estudio real (parcela experimental de olivar del Campus de Rabanales de la Universidad de Córdoba) ha conseguido resultados excelentes, siendo capaz de satisfacer, de forma automática, más del 96% de los requerimientos de riego del cultivo durante la campaña de riego analizada. Además, la sustitución del suministro eléctrico convencional por energía fotovoltaica evitó la emisión de 1.2 t de CO_2 eq. correspondientes a 602 h de riego (durante una campaña), en el cultivo de olivar del caso de estudio analizado.

En el capítulo 4 se lleva a cabo un análisis del ciclo de vida de la tecnología fotovoltaica empleada como fuente de energía en el regadío. Además, también se compara con el ciclo de vida vinculado al suministro energético mediante las alternativas tradicionales, generadores diésel y la red eléctrica. Posteriormente, se lleva a cabo un análisis comparativo entre las distintas opciones de suministro, estableciendo para ello dos posibles escenarios: con y sin conexión a red. Los resultados derivados de este trabajo, expresados en relación a la unidad de energía en kWh, mostraron la importancia vinculada al porcentaje de energía fotovoltaica producida que es realmente aprovechado, teniendo por ello una gran repercusión la estacionalidad del riego y la posibilidad de aprovechar el excedente de energía producida en los momentos en los que no es necesario regar el cultivo. Este trabajo fue además complementado con un análisis del coste asociado al ciclo de vida de las distintas tecnologías. Así, la opción fotovoltaica presenta el menor de los costes totales (63% y 36% inferior a la opción de generador diésel y red eléctrica,

respectivamente, para una vida útil de proyecto de 30 años), a pesar de requerir una mayor inversión inicial.

En el capítulo 5 se presenta un modelo para el dimensionamiento óptimo de sistemas de riego fotovoltaico, el cual determina el agrupamiento de hidrantes en sectores de riego, el diámetro de tubería para cada tramo de la red y el dimensionamiento de la planta fotovoltaica. Este modelo, basado en algoritmos evolutivos (en concreto el algoritmo genético NSGAII) integra así mismo el primero de los modelos presentados, con el que se comprueba el funcionamiento de cada una de las opciones de dimensionamiento generadas. Las posibles soluciones son evaluadas con el fin de seleccionar aquellas que cumplen mejor las funciones objetivo establecidas. Por ello, los resultados facilitados por el modelo son aquellas combinaciones de agrupamiento de hidrantes, dimensiones de tuberías y tamaño de la planta FV que minimizan los costes de inversión y garantizan al mismo tiempo el correcto funcionamiento del sistema. Una vez desarrollado el modelo, éste fue simulado para llevar a cabo el dimensionamiento del sistema de riego FV de la parcela de olivar experimental de la Universidad de Córdoba. Los resultados obtenidos mostraron soluciones de diseño con ahorros en el coste de inversión de entre el 24 y el 39%, en comparación con el diseño original de la instalación, con una satisfacción del riego igual o superior al 96% actual en todas las opciones.

Finalmente, el capítulo 6 sintetiza las principales conclusiones obtenidas tras el desarrollo de esta tesis, así como las posibles futuras vías de investigación.

Esta tesis destaca la importancia de la integración de la energía fotovoltaica en la agricultura como medio de suministro energético, de bajo impacto ambiental, alternativo a las fuentes de energía tradicionales. Por ello, en ella se presentan

herramientas innovadoras de gestión del riego fotovoltaico y dimensionamiento conjunto del sistema red de riego-planta fotovoltaica, teniendo en cuenta los aspectos energéticos, hidráulicos, económicos, ambientales y de operatividad del sistema. Por tanto, el propósito de facilitar la incorporación de esta tecnología en el sector queda acompañado de los objetivos de disminuir el impacto ambiental de esta actividad y mejorar la rentabilidad del agricultor.

Table of Contents

List of Tables

List of Figures

List of Symbols and abbreviations

A: irrigated area

AC: ant colony

AP: acidification potential

ARDP: abiotic resource depletion potential

CD: crop density

C_p: pumping system cost

CRUD: create, read, update and delete

D: deep percolation (chap 3)

D: total days for month (chap 5)

DE: differential evolution

DF: emitter flow rate

Dr: soil moisture depletion in the root area

EAW: easily accessible water

EB: environmental burden

E_{gen}: total monthly energy production

E_{max}: maximum daily energy production

E_{mean}: mean daily energy production

E_{min}: minimum daily energy production

EPBT: energy payback time

E_{req}: total monthly energy required

$Et_{c\ adj}$: real crop adjusted evapotranspiration

ET_c: crop evapotranspiration

ET_o: reference evapotranspiration

FRDP: fossil resource depletion potential

GA: Genetic Algorithms

gen: generations

GGEs: greenhouse gas emissions

GHG: greenhouse gas

GP: genetic programming

GPE: genetic programming expression

GUI: graphical user interface

GWP: global warming potential

H: hydrants

H_i: minimum pressure head required for sector i

HS: harmony search

HTTP: human toxicity potential

i: sector index

I_{Ap}: applied irrigation depth

I_b: irradiance on the horizontal surface

ICTs: information and communication technologies

I_d: diffuse irradiance

ID: irrigation days of the month

IE: irrigation efficiency

$I_{n\,t}$: irradiance on the collector plane

I_{stc}: irradiance under standard conditions

JSON: JavaScript object notation

K: environmental burden associated to each material or process

K_c: crop coefficient

K_r: coefficient of soil evaporation reduction

LCA: life cycle assessment

LCC: life cycle cost

LCC_{inst}: total life cycle cost associated to the installation stage

LCC_{ope}: total life cycle cost associated to the operation stage

L_p: total length of each pipe type included in the network

MOPISS: model for optimal photovoltaic irrigation system sizing

n: day of the year

n_e: number of emitters in sector

NE: number of emitters per plant

NGSA: non-dominated sorting genetic algorithm

OF: objective function

P: pipes

PA: precision agriculture

PC_φ: unit cost of the commercial pipe diameters

PE: polyethylene

P_{eff}: effective precipitation

P_{effR}: real effective precipitation

$P_{min\ i}$: minimum power demand of sector i

P_n: net power transferred to the pump

pop: population

PP: peak power under standard conditions

$P_{pv\ n\ t}$: instantaneous photovoltaic power

PS: particle swarm

PV: photovoltaic

PVPP: photovoltaic peak power

q_e: emitters flow

Q_i: flow demand for sector i

R: runoff

rb: geometric factor which relates beam irradiation on the tilted plane to that on the horizontal surface

RDI: regulated deficit irrigation coefficient

RE: renewable energy

RESSIM: real time smart solar irrigation manager

S: energy source option (chap 4)

S: number of sectors (chap 5)

S_c: cultivated area

S_{hH}: sector for hydrant H

SPH: solar peak hours

SPIM: smart photovoltaic irrigation manager

Spv: PV modules surface

SQL: structured query language

SW: soil water content

t: time of day

TAW: total available soil water

T_{cell}: cell temperature in the modules

t_{req}: irrigation time required

T_{stc}: cell module temperature under standard conditions

U: total units for the material or process involved in each option

UC: unit cost

v: variables

V_{max}: maximum velocity rate

V_{min}: minimum velocity rate

V_{p_P}: flow velocity for pipe P in the network

V_{req}: daily irrigation volume required

WA: monthly water allocation

X: total number of different materials and processes

η_{am}: asynchronous motor efficiency

η_{fc}: converter efficiency

η_p: pumping system efficiency

$\Delta\ t_{req\ i\ n}$: time correction

β: performance decay coefficient due to the rising temperature of the module cells

γ: water specific weight

ρ, ω and γ: weighting coefficients for objective function 2

ρ: albedo

φ: tilt angle of the modules, in degrees

1. Introduction

1.1. Background

The global population increase is expected to reach 9.7 billion people by 2050. This fact will require substantial improvements in the use and conservation of resources, which should be enough to satisfy the growing food demand (Tubiello et al., 2014; FAO, 2017). In that way, the transformation of rainfed systems into irrigated lands allows for double and triple cropping, and also increases its production (FAO, 2011). Nowadays, irrigated agriculture, with around M 324 ha (FAO, 2014), represents 70% of global freshwater extraction, which must be considered under a climate change and limited resource context (FAO, 2017). In that way, the modernization of the agricultural sector implied some measures, as the transformation of open distribution networks into pressurized ones, among others. These water pressurized distribution systems allowed improving the efficiency in the use of water but also increased the energy requirements for pumping, which rose farm operation costs (Corominas, 2010; Fernández García et al., 2013). In this context, initiatives focussed on the optimization of both, water and energy use in agriculture, are specially required.

Higher farm energy requirements not only affect to the economic aspects, but also increases the greenhouse gas emissions (GGEs) due to agricultural activities. Moreover, high diesel and electricity costs and often unreliable energy services in isolated areas hinders pumping requirements satisfaction for irrigation for small and large farmers (Hartung and Pluschke, 2018). Due to these facts, and the social concern about global warming and climate change, renewable energies are being widely integrated in the agricultural sector. This alternative energy sources, as wind,

hydraulics and solar, allow reducing the environmental impact and grid-electricity or diesel dependency of farms (Carrillo Cobo et al., 2014).

1.2. The Spanish irrigation agriculture

The agricultural sector is one of the Spanish key activities for the economy, along with the service sector, construction and industry (INE, 2018). The total cropped area of the country is around M 17 ha, from which M 3.7 ha, representing 22% of the total, are irrigated (MAPA, 2018). The most representative crops are cereals, olive orchard and vineyard, with 25%, 21% and 10% of the area, respectively (MAPAMA, 2017). One of the most remarkable challenges facing the Mediterranean agricultural activities is defined by water scarcity and the irregular distribution of precipitation and droughts that characterises this climate, exacerbated by climate change. In that way, the Spanish National Irrigation Plan focused on the modernisation of the hydraulic infrastructures and the incorporation of research programs and innovative techniques, being the improvement of the sustainability one of the main principles of the initiative (MAPA, 2001). Thus, as a direct consequence of the modernization process, in addition to the pressurization of a large part of the distribution networks, irrigation systems, as drip or sprinkler, made possible to improve water use efficiency at farm level. These two irrigation systems currently represent around 39% and 27% of total water used by irrigated agriculture, respectively, which set at around 14.9 hm^3 (INE, 2016). Thus, irrigation modernization in the period from 2007 until 2017, showed a significant evolution on the main irrigation systems used. This was reflected in a 17% reduction of the area irrigated by gravity, while sprinkler, automotive irrigation and localised irrigation rose 23%, 27%, and 28%, respectively (MAPAMA, 2017). Moreover, irrigation

management based on climatic variables, crop characteristics and phenological stage, just as the application of deficit irrigation techniques, made it possible to adjust irrigation doses, reducing the total water volume used. Concurrently, the achieved improvements in water use efficiency derived from the pressurization translated into a higher energy dependency of farms, required not only for water abstraction but also for pumping (Corominas, 2010). These higher energy requirements together with the increase in the electric tariffs and fuel could endanger the profitability of some crops.

In Spain, the electricity sector currently accounts for almost a quarter of final energy consumption, only behind petroleum products (CES, 2017). In the last ten years, its final price has followed an upward trend. This continued growth of final electricity price, composed by the energy, entry fee and taxes prices, has been mainly explained by the evolution of the regulated costs: tolls and taxes, which represent 60% of the final price (CES, 2017). In addition to the economic aspects, in the CO_2 emissions context, the agricultural sector in Spain reached 33.75 Mt in 2016. This figure represents 17% of the emissions related to "diffuse sectors", which comprises agriculture, transport, residential and commercial activities (MITECO, 2016). In this same way, the generation structure of the electricity also plays an important role, since the higher the presence of renewable energies in the electricity mix is, the lower the environmental burden linked to its use will result. In the case of the Spanish grid electricity, in the last 8 years, renewable energies have represented on average 36% (REE, 2019a) of the total energy generated (Fig. 1.1).

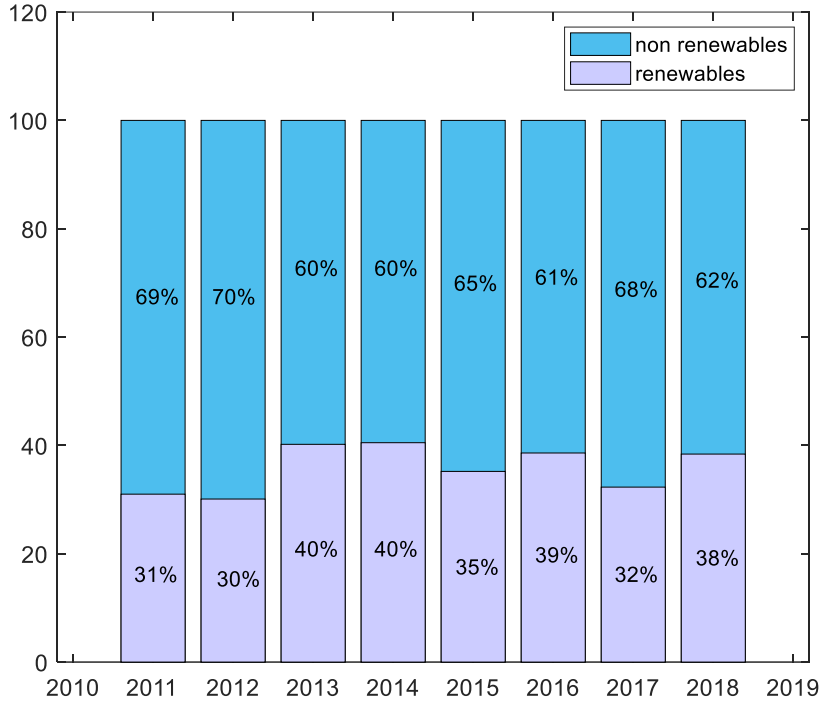

Fig. 1.1 Energy generation from renewable and non-renewable energy sources in Spain between 2011 and 2018. Source: Author´s elaboration based on REE (2019b)

From this 36% of energy, between 8-10% came from solar photovoltaic (PV) (REE, 2019b). Thus, PV energy represented the third renewable energy source related to its production, with around 8000 GWh yearly, following wind and hydraulics (Fig. 1.2). Nevertheless, renewable energies participation in the electricity grid should increase in the next years to achieve the proposed objectives of the environmental policies.

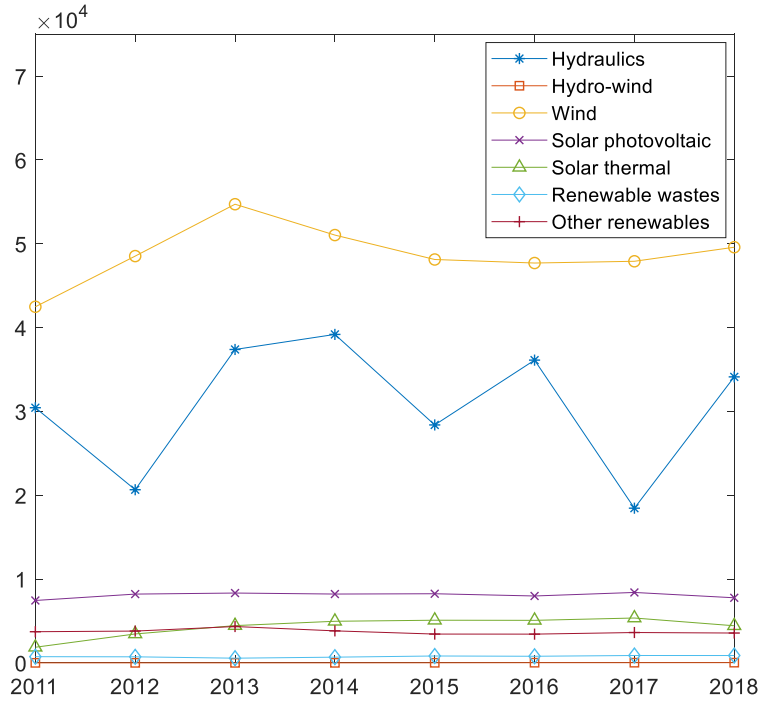

Fig. 1.2 Energy generation expressed as GWh, from the different renewable energy sources in Spain between 2011 and 2018. Source: Author´s elaboration based on REE (2019b)

The Integrated National Energy and Climate Plan addresses the policies and measures needed to contribute to the European target with a reduction of at least 20% of GHGs by 2030, compared to 1990 levels, which implies the contribution of the diffuse sectors, within which agriculture is included (MITECO, 2019). In this way, initiatives for reducing GHGs emissions already proposed by the national government include the substitution in the agricultural sector of fossil fuels by renewable energies, by using biomass boilers and solar irrigation, as example (MITECO, 2016). This proposal of integrating PV energy in irrigation in Spain is also favoured by high levels of radiation which are recorded in most of the Spanish area

throughout the year. Thus, PV technology shows a great potential as alternative energy source to the traditional ones for achieving a more sustainable and profitable agriculture.

1.3. Photovoltaic irrigation

The EU- 28 is currently the third largest emitter of GHGs on a global scale (Ministry of Defence, 2018). Its GHGs emissions evolution has followed a general decreasing trend from 1990, in which Spanish emissions have represented between 5.1 and 8.4% (Fig. 1.3). Even so, the transition to a competitive low-carbon European economy entails to reduce its internal emissions by 80% by 2050, compared to 1990 levels (EC, 2011).

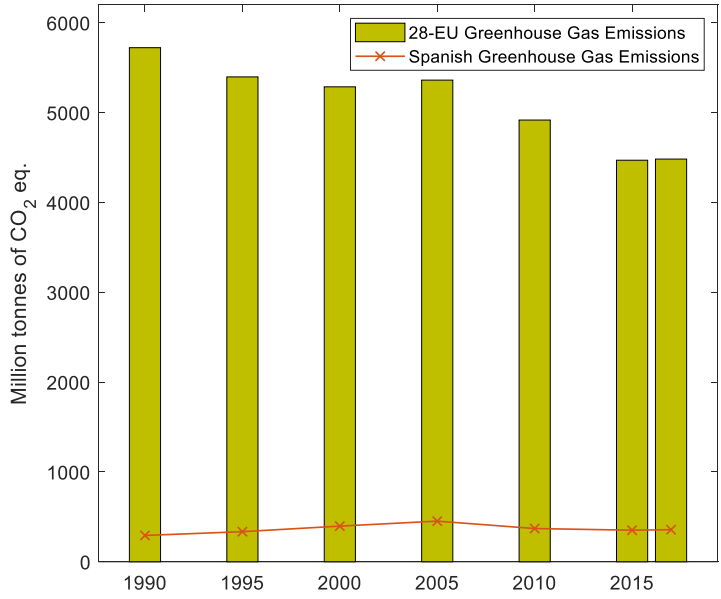

Fig. 1.3. European and Spanish Greenhouse gas emissions evolution in the period 1990-2017. Source: Author´s elaboration based on (Eurostat, 2019)

In this context, some countries are promoting solar PV irrigation systems in the framework of national action plans regarding climate change as a way to reduce emissions from agriculture. This fact is also fostered by the continuous reduction of solar panels cost, which makes its implementation in irrigation economically viable for farmers. Nevertheless, the integration of technology for solar pumping and irrigation is needed and is expected to be available in the future (Hartung and Pluschke, 2018).

To date, research works focused on the integration of renewable energies in irrigation have developed several methodologies and systems whose power source is based on solar PV. The most common configurations imply the hybridization with other renewable energies, as wind; the storage of potential energy, by pumping water from the supply point until a high reservoir or tank, from which the irrigation is subsequently applied by gravity; or the use of batteries/diesel generator as support system (Maheshwari et al., 2017; Ouachani et al., 2017; Yahyaoui et al., 2016). These options involve an increase in the investment cost of the system, space requirements and an important environmental burden related with the disposal of batteries or the use of diesel (Reca-Cardeña and López-Luque, 2018). For that reason, the study of the particularities of each project for the system configuration selection is crucial. Moreover, some crops can tolerate certain water stress, so they could operate with a direct injection system without any energy/water storage or support element. In this way, all solutions try to find the way of compensating the variability on PV power production, to meet the demand of the irrigation network during the irrigations season. In addition, the decrease in PV technology cost in recent years (Reca-Cardeña and López-Luque, 2018) facilitates its implementation in existing irrigation networks, substituting diesel or the electricity grid, as well as in

new irrigation projects. Usually, developed methodologies for the design of PV irrigation systems focus on the optimal PV plant dimensioning and do not take into account the need of considering both, the hydraulic (irrigation network) and energy components (PV plant) of the system jointly, in order to optimise the total cost of the installation, as well as its operability, in accordance to the particularities of this energy source. In the same way, works which objective was to optimize the irrigation network dimensioning did not usually consider the energy source nature. In both cases, the most common optimization developed methodologies include optimization algorithms as Genetic Algorithms (GA). GA is a tool to find optimal solutions to a multi-objective problem. This optimization algorithm performance relies on the generation of a series of possible solutions which are subsequently evaluated and selected. Selected solutions are then also evaluated, based, in both cases, on its fitness to the established objective functions (Deb et al., 2002). This process is repeated until the total generations of individuals are completed, which will show a set of optimal solutions.

In a general overview of PV irrigation systems, previous investigations have revealed that this technology shows potential reductions in GHGs emissions per unit of energy, compared with pumps powered by grid electricity or diesel (GIZ, 2016). Nevertheless, the design of the system will also reverberate on its environmental impact, due to the burden associated to the production of PV modules, principally (Desideri et al., 2012). The environmental burden associated to PV energy is frequently analysed with Life Cycle Assessment (LCA) methodology. This methodology allows accounting not only for the GHGs emissions, but also includes other environmental categories as acidification, abiotic and fuel resources depletion potentials, including the production, transport, operation and, in some cases, the

disposal of the devices at the end of its useful lifespan (IEA, 2011). The LCA works of PV installations usually shows the different burdens related to 1 kWh of generated energy, considering all potential energy production of the modules. Nevertheless, in the case of irrigation, not all the energy produced is used, so a specific study in which the operation time of the system is included would be necessary. In that way, related with the surplus of PV energy generated, Agrivoltaic production sustains that new agriculture should not only be self-sufficient energetically, but also it should generate an energy surplus, which would be injected in the grid, optimizing the economic returns of the farm (Reca-Cardeña and López-Luque, 2018). Thus, Agrivoltaic concept is known as the amalgamation between the crop and PV energy production in a same field. In this case, all energy produced would be used, although national legislation of each country would define the extra farm profits derived from the sale of the surplus of energy.

In essence, PV technology is going to play an important role as energy source in the new agriculture concept, as a more sustainable and profitable alternative to the traditional options. Nevertheless, drawbacks associated to the variability in the PV energy production, due to its dependency on climatic variables, will make necessary to develop new methodologies and tools. Thus, the integration of PV energy production with hydraulic and agronomic aspects of the irrigation sector in a specific smart management system allows for the energy self-sufficiency of the farm. Moreover, the lower dependency on diesel or electricity grid of farms and the development of specific designing PV irrigation system methodologies, which involve economic and operation aspects, allows for the resources consumption optimization and thus, the environmental economy of agriculture.

1.4. References

Carrillo Cobo, M.T., Camacho Poyato, E., Montesinos, P., Rodríguez Díaz, J.A., 2014. New model for sustainable management of pressurized irrigation networks. Application to Bembézar MD irrigation district (Spain). Sci. Total Environ. 473–474, 1–8. https://doi.org/10.1016/j.scitotenv.2013.11.093

CES Consejo Económico y Social, 2017. Informe el sector eléctrico en España.

Corominas, J., 2010. Agua y energía en el riego en la época de la sostenibilidad. Ing. del agua 17, 219–233.

Deb, K., Pratab, S., Agarwal, S., Meyarivan, T., 2002. A Fast and Elitist Multiobjective Genetic Algorithm: NGSA-II. IEEE Trans. Evol. Comput. 6, 182–197. https://doi.org/10.1109/4235.996017

Desideri, U., Proietti, S., Zepparelli, F., Sdringola, P., Bini, S., 2012. Life Cycle Assessment of a ground-mounted 1778kWp photovoltaic plant and comparison with traditional energy production systems. Appl. Energy 97, 930–943. https://doi.org/10.1016/j.apenergy.2012.01.055

EC European Commission, 2011. Comunicación de la Comisión al Parlamento Europeo, al Consejo, al Comité Económico y Social Europeo y al Comité de las Regiones. Hoja de Ruta hacia una economía hipocarbónica competitiva en 2050.

Eurostat, 2019. Greenhouse gas emission statistics - emission inventories. Eurostat. Eur. Com.

FAO, 2017. The future of food and agriculture. Trends and challenges. El Futur. la Agric. y la Aliment. https://doi.org/10.1515/nleng-2015-0013

FAO, 2014. Superficie equipada para el riego. Superf. equipada para el riego 1.

FAO, 2011. Energy-Smart Food for People Climate 66. https://doi.org/2/3/2017

Fernández García, I., Rodríguez Díaz, J.A., Camacho Poyato, E., Montesinos, P., 2013. Optimal Operation of Pressurized Irrigation Networks with Several Supply Sources. Water Resour. Manag. 27, 2855–2869. https://doi.org/10.1007/s11269-013-0319-y

GIZ Deutsche Gesellschaft für Internationale Zusammenardbeit, 2016. Frequently asked questions on Solar Powered Irrigation Pumps.

Hartung, H., Pluschke, L., 2018. The benefits and risks of solar-powered irrigation. A global overview.

IEA, 2011. Methodology Guidelines on Life Cycle Assessment of Photovoltaic Electricity. Int. Energy Agency. Photovolt. power Syst. Program.

INE. Instituto Nacional de Estadística, 2018. España en cifras 2018.

INE Instituto Nacional de Estadística, 2016. Encuesta sobre el uso del agua en el sector agrario [WWW Document]. URL https://www.ine.es/dyngs/INEbase/es/operacion.htm?c=Estadistica_C&cid=1254736176839&menu=ultiDatos&idp=1254735976602 (accessed 6.27.18).

Maheshwari, T.K., Kumar, D., Kumar, M., 2017. Solar Photovoltaic Irrigation Pumping System 6, 1884–1889.

MAPA; Ministry of Agriculture; Fisheries and Food, 2001. National Irrigation Plan-Horizon 2008.

MAPA, 2018. Encuesta sobre Superficies y Rendimientos de Cultivos ESYCE.

MAPAMA. Ministerio de Agricultura y Pesca Aimentación y Medio Ambiente, 2017. Encuesta sobre superficies y rendimientos de cultivos. Informe sobre regadíos en España.

Ministry of Defence. Instituto Español de Estudios Estratégicos. Comité español del Consejo Mundial de la Energía. Club Español de la Energía., 2018. Energía y Geoestrategia 2018.

MITECO, 2016. Emisiones de gases de efecto invernadero de los sectores difusos [WWW Document]. URL https://www.miteco.gob.es/es/cambio-climatico/temas/mitigacion-politicas-y-medidas (accessed 4.7.19).

MITECO Ministerio para la Transición Ecológica, 2019. Borrador del Plan Nacional Integrado de Energía y Clima 2021-2030.

Ouachani, I., Rabhi, A., Yahyaoui, I., Tidhaf, B., Tadeo, T.F., 2017. Renewable Energy Management Algorithm for a Water Pumping System. Energy Procedia 111, 1030–1039. https://doi.org/10.1016/j.egypro.2017.03.266

Reca-Cardeña, J., López-Luque, R., 2018. Design Principles of Photovoltaic Irrigation Systems, Advances in Renewable Energies and Power Technologies. https://doi.org/10.1016/B978-0-12-812959-3.00009-5

REE Red Eéctrica de España, 2019. Evolución de la generación renovable y no renovable. Sistema Eléctrico Nacional [WWW Document]. URL

https://www.ree.es/es/datos/generacion/evolucion-renovable-no-renovable (accessed 11.7.19).

REE Red Eléctrica de España, 2019. Generación renovable por tecnología/combustible (%). Sistema Eléctrico Nacional. [WWW Document]. URL https://www.ree.es/es/datos/generacion/estructura-renovables (accessed 11.7.19).

Tubiello, F.N., Salvatore, M., Cóndor-Golec, R.D., Ferraca, A., Rossi, S., Biancalani, R., Federici, S., Jacobs, H., Flammini, A., 2014. Agriculture, Forestry and Other Land Use Emissions by Sources and Removals by Sinks. Climate, Energy and Tenure Division, FAO.

Yahyaoui, I., Tadeo, F., Segatto, M.V., 2016. Energy and water management for drip-irrigation of tomatoes in a semi- arid district. Agric. Water Manag. 183, 4–15. https://doi.org/10.1016/j.agwat.2016.08.003

2. Objectives and thesis structure

2.1. Objectives

The general objective of this thesis is to develop new tools for the integration of photovoltaic energy in the irrigation sector considering economic, environmental and operability aspects.

To achieve this goal, the specific objectives are detailed below:

1. Develop a smart photovoltaic irrigation system to apply crop irrigation requirements based on the synchronization of the photovoltaic power production with the power requirements and the water demand of the irrigation sectors of the network.
2. Determine the environmental impact and economic costs associated to photovoltaic energy in irrigation systems and compare with the use of traditional energy sources.
3. Develop a model for the optimal sizing of photovoltaic irrigation systems based on economic and operability aspects.

2.2. Thesis structure

According to these objectives, this thesis comprises six chapters and one appendix. Following the introduction (**Chapter 1**) and objectives (**Chapter 2**), the chapters are:

Chapter 3 presents a model to manage photovoltaic irrigation by the synchronization of the photovoltaic power production and the hydraulic power and irrigation water demands of the sectors that make up the network. This model

considers climatic, hydraulic, energetic variables and the specific characteristics of the crop, soil and the selected irrigation scheduling. This chapter has been published under the title "Coupling irrigation scheduling with solar energy production in a smart irrigation management system" (2018) by Mérida García A, Fernández García I, Camacho Poyato E, Montesinos Barrios P, Rodríguez Díaz JA in *Journal of Cleaner Production*.

Chapter 4 includes an environmental an economic analysis of photovoltaic energy in irrigation and compares these results with those obtained for the use of traditional energy sources (diesel generators and grid electricity). This chapter has been published under the title "Comparing the environmental and economic impacts of on- or off- grid solar photovoltaics with traditional energy sources for rural irrigation systems" (2019) by Merida García A, Gallagher J, McNabola A, Camacho Poyato E, Montesinos barrios P, Rodríguez Díaz JA in the journal *Renewable Energy*.

The methodology developed to resolve the optimal dimensioning of the photovoltaic irrigation system is integrated in the model presented in **Chapter 5**. This methodology, which includes economic and operability aspects, is based on evolutive algorithms and incorporates also the model previously stated in Charter 3, which is used to check the operation aspects of the possible designs evaluated. The model offers as results the hydrants grouping, pipes size and the photovoltaic plant peak power required. This chapter corresponds to the paper "Comprehensive sizing methodology of smart photovoltaic irrigation systems" (2020) by Merida Garcia A, Gonzalez Perea R, Camacho Poyato E, Montesinos Barrios P, Rodríguez Díaz JA, published in the journal *Agricultural Water Management*.

Appendix A includes the paper "Middleware to operate smart photovoltaic irrigation systems in teal time" (2019) by González Perea R, Mérida García A, Fernández García I, Camacho Poyato E, Montesinos P, Rodriguez Diaz JA, published in the journal *Water*. It shows the tool developed for the real on field management of the smart photovoltaic irrigation system. Thus, this work provides a useful middleware to control and supervise smart photovoltaic irrigation systems operation. This is a platform which connects several information sources as agroclimatic stations and databases with a graphic interface, being the model detailed in chapter 3 the management centre of the platform.

3. Coupling irrigation scheduling with solar energy production in a smart irrigation management system

This chapter has been published entirely in the journal "Journal of Cleaner Production", A. Mérida García, I. Fernández García, E. Camacho Poyato, P. Montesinos Barrios, J.A. Rodríguez Díaz (2018)

Abstract. In recent years, pressurized pipe networks have improved the efficiency of irrigation systems while substantially increasing their energy demand. The progressive rise in energy costs makes it difficult to maintain the profitability of agricultural holdings. Moreover, global warming is a serious problem that threatens the environment worldwide and low CO_2 emission processes should be promoted. To address these issues, it is necessary to look for sustainable and more profitable alternatives for the agricultural sector. One of these new alternatives is the use of renewable energies for pumping irrigation water at farm level, particularly photovoltaic energy. Nevertheless, the instability of irradiation hinders its management for stand-alone photovoltaic installations. In this work, a real-time model called the Smart Photovoltaic Irrigation Manager (SPIM) is developed to synchronize the photovoltaic power availability with the energy required to pump the irrigation requirements of different sectors of irrigation networks. SPIM consists of different modules to calculate the key management variables of the photovoltaic irrigation system: the daily irrigation requirements, the hydraulic behaviour of the irrigation network, the instantaneous photovoltaic power production and the daily soil water balance. The lack of photovoltaic energy during daylight hours on any day of the irrigation season to supply the daily required amount of water is balanced with

either the water stored in the soil or by extending the duration of the irrigation events in the following days when necessary. SPIM has been applied to simulate the management of photovoltaic irrigation in a real olive orchard in Southern Spain during the 2013 irrigation season. The results showed that the proper management of the photovoltaic irrigation system provided enough water to satisfy crop irrigation requirements throughout the irrigation season and avoided the emission of 1.2 t CO_2 eq. using only the energy generated by solar panels.

Keywords: Precision irrigation; Energy availability; Sustainable irrigation.

3.1. Introduction

In some areas, the consequences of climate change on the availability of resources seem to be evident. Irregular and unpredictable precipitations or extended periods of drought and floods are some examples of such effects. These changes also favour the emergence of severe pests and crop diseases, which result in harvest losses and the need for higher agrochemical applications (Rosenzweig et al., 2001). In subsequent years, contamination and climate change will have negative impacts on agriculture, thus threatening world food security (Nelson et al., 2009). Against this backdrop, proper energy and water management is essential to reduce contaminant emissions and ensure world food production (Tubiello et al., 2014). Moreover, a growing population has resulted in a significant increase in global food demand that entails greater pressures on water resources. To address this problem, agriculture has undergone significant intensification, which has involved the development of new harvesting technologies and new irrigation systems, among others. In recent years, for example, open channel systems have been fully transformed into pressurized pipe systems and more efficient on-farm irrigation systems have been adopted in

Mediterranean countries, where irrigated agriculture is of major importance. Although this process of modernization has led to improved water use efficiencies, large amounts of energy are required for the abstraction, transportation and distribution of water (Corominas, 2010). Irrigation networks are usually powered by electric energy coming from the power grid. However, in the case of isolated areas where grids are not available, pumping systems mainly depend on diesel engines. Hence, agricultural modernization and its consequent dependence on electric energy and fuel motors have led to an exorbitant increase in carbon emissions. In the last fifty years, greenhouse gas (GHG) emissions generated by agriculture, forestry and fishing have doubled. In 2010, more than 785 million tonnes of CO_2 corresponded to emissions related to the use of energy in the agricultural sector. This figure represents nearly one fifth of the total world CO_2 emissions (Tubiello et al., 2014). Moreover, the increase in electrical rates and fuel prices linked to the large consumption of energy on farms has dramatically raised the annual operating costs of agricultural activities. To remediate this situation, it is essential to search for new management alternatives for agricultural systems that focus on reducing environmental impact, while enhancing farm profitability. In order to improve energy efficiency in pressurized irrigation systems, several methodologies have been developed. Fernández García et al. (2013) reduced energy consumption by network sectoring, achieving energy savings of between 20% and 29%. Another option to diminish energy demand is to control critical points (hydrants with high energy requirements due to their distance from the supply point or to their elevation) (Khadra and Lamaddalena, 2010; Díaz et al., 2012). The proper management of critical points improves the overall efficiency of the irrigation infrastructure with minimal costs, saving around 27% of the energy consumed previously in the peak month (González Perea et al., 2014). However,

these strategies were designed for networks powered by conventional energy sources (electricity grid or fuel). Due to global warming and environmental damage, renewable energies are being promoted as new, clean and sustainable alternatives to conventional energy sources. Photovoltaic and wind energy, for example, are being incorporated as reliable energy sources in the industrial and agricultural sectors. Hamidat et al. (2003) applied solar energy to small-scale irrigation, covering daily water needs in plots smaller than 2 ha in the Sahara region. Other works have shown that the use of hybrid (wind/solar) systems as an energy source can satisfy irrigation energy requirements and increase profitability by combining winter and summer crops (Vick, 2010). Other authors have estimated the real power production of photovoltaic panels and developed sizing and performance optimization methods for irrigation systems powered by solar energy (Jafar, 2000; Bakelli et al., 2011; López-Luque et al., 2015; Louazene et al., 2017). In this way, Chandel et al. (2017) and Li et al. (2017) analysed the different factors affecting the performance of the photovoltaic pumping system, considering also hybrid systems (photovoltaic-wind) as a solution to improve the overall efficiency of the energy production system. However, these previous works do not integrate irrigation management with solar energy production, which varies seasonally and during the day. Carrillo Cobo et al. (2014b) combined network sectoring with an energy supply based partially on solar energy. In their study, the authors defined the sector size to best match the variable production of photovoltaic energy and reduce dependence on the electricity grid. Based on this methodology, they estimated energy cost savings of up to 72%. A recent work (Yahyaoui et al., 2016) focused on the optimal management of energy sources (photovoltaic panels and batteries) aimed at storing the monthly crop irrigation requirements in the reservoir that supplies water to the irrigation system.

Ghavidel et al. (2016) studied the most economical option using a modified gravitational search algorithm for a system which also included a water tank for both drinking and domestic water and compared the use of photovoltaic energy and PATs (pump as turbine) with and without the use of combustion engines. Reges et al. (2016) presented a photovoltaic system which included batteries for the energy storage. Kabalci et al. (2016) worked also with a similar system, including a water storage tank remote controlled. The use of energy and water storage systems is justified due to the continuous variations in sun irradiation, which can drastically decrease the efficiency of the irrigation system (Closas and Rap, 2017). Maheshwari et al. (2017) designed a photovoltaic irrigation system which pumped the irrigation water into a storage tank, supplying water to the irrigation system by gravity. Bhosale et al. (2017) also worked on a smart scale model at lab level for a photovoltaic irrigation system, including batteries and soil moisture sensors to automatically control the water supply. In a similar line, Bhattacharjee et al. (2017) developed an optimized power management method in which a battery provided the required energy in the intervals with insufficient photovoltaic power. Ouachani et al. (2017) developed intelligent algorithms for the optimal management of renewable energy systems that combine wind turbines and photovoltaic panels and store energy in a battery bank. However, none of the cited works has studied the interaction among the variability of solar energy production, the hydraulic behaviour of the irrigation system and irrigation scheduling at farm level on a daily basis. These factors strongly affect the operation of the pumping system when water is supplied directly to the irrigation system without batteries or intermediate water tanks. In this work, we have developed a smart irrigation management model based on the use of solar energy to directly supply the irrigation water to the network, without intermediate storage

elements (water tanks and batteries). The innovation of this model relies on the integration in a single algorithm of the coordinated operation of the solar energy production, the pumping station, the irrigation network and a soil-water-plant model to satisfy the crop irrigation requirements. To use efficiently the available amount of water, the model synchronizes, in real time, the power requirements of the irrigation system (related to its location, size and hydraulic features) with the instantaneous solar irradiation. Smart irrigation management relies on the model's memory to compensate insufficient daily irrigation times by extending the duration of irrigation events in the following days, according to the availability of energy. The model was applied to establish the daily operation of the irrigation system in an olive orchard located in Cordoba (southern Spain) for the 2013 irrigation season.

3.2. Methodology

3.2.1. Case study

This study analyses the operation of an irrigation network that uses solar energy to supply water to olive trees grown on an intensive basis. The trial site is located on the experimental farm of the University of Cordoba (southern Spain) (Fig. 3.1).

The farm spans an area of 13.4 ha and has an average elevation of around 160 m above sea level and a maximum elevation difference of 24 m. The agro-climatic characteristics of the experimental site are typically Mediterranean, with an average annual temperature of 17.5 ºC and total annual rainfall of 500-600 mm, mainly in fall and spring. The annual daily average irradiance is 5.14 kWm^{-2}, with maximum values from 9:30 h to 15:30 h (local time). The highest values of irradiance

on the horizontal plane are generally recorded in July, with more than 900 Wm^{-2} at midday (CENSOLAR, 2007). Climate data were obtained from a weather station located within the university campus. Concerning the soil features, trees are cultivated in a clay-loamy soil with increasing clay content in deeper soil profiles.

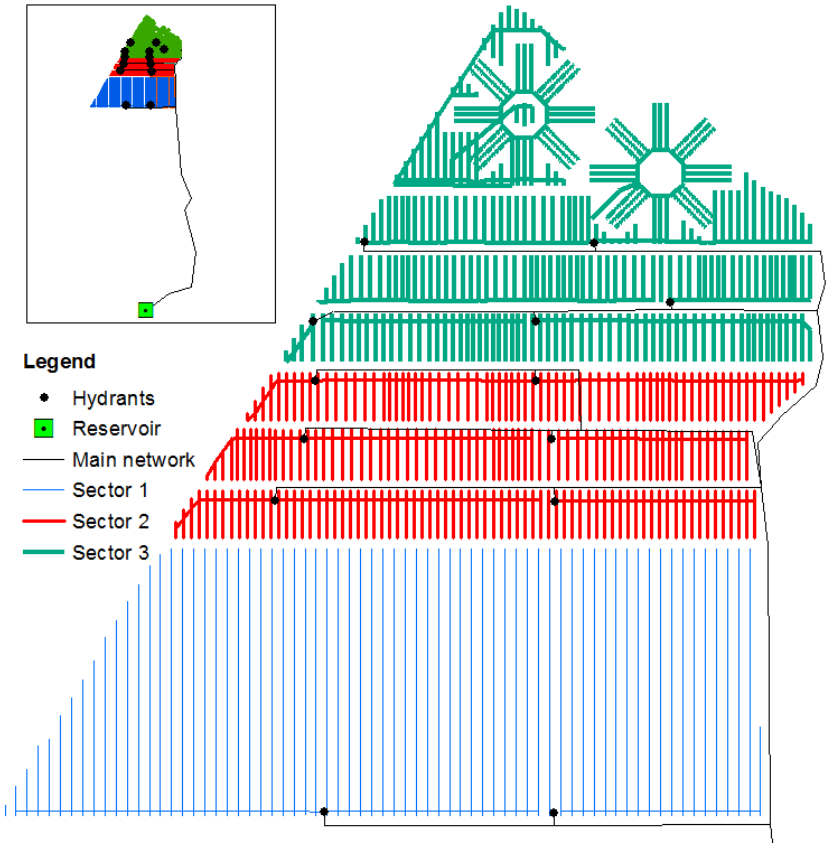

Fig. 3.1. Irrigation network of the experimental field at the University of Cordoba (Southern Spain)

A 13 kW submersible pump powers water from a reservoir into the irrigation network. The network feeds 13 hydrants grouped into 3 sectors, each of which is controlled by an electrovalve. The trees are watered by drip irrigation using pressure compensating emitters that work between 1 and 4 bar. The photovoltaic system is located on the roof of a storehouse located 200 m from the pump. The system provides a peak power of 15.4 kW by 120 photovoltaic panels that occupy 168 m^2 of surface area. The panels are south facing, with a fixed tilt angle of 15º. A solar irradiance sensor located near the solar panels provides information in real time. The pump operating point is controlled by a variable frequency drive, which matches pressure and flow according to the instantaneous solar irradiance.

3.2.2. Model description

The proposed model, which is called the Smart Photovoltaic Irrigation Manager (SPIM), was developed in MATLAB™. The aim of SPIM is to provide seasonal smart irrigation schedules on a daily basis for crops at plot scale using solar energy to pump water directly into the irrigation network. The duration of the daily irrigation events varies throughout the season depending on the crop requirements and the availability of energy. To facilitate the matching of energy availability and flow demand, the irrigation network is operated by sectors. The daily energy requirements of each sector are estimated according to the location, size, soil and crop parameters as well as the hydraulic features of the sector. The model matches the power demand of each sector in real time to satisfy the daily irrigation needs according to the available energy. Thus, the daily on-off sequence of sectors varies throughout the season depending on the instantaneous irradiance. The model's memory compares the accumulated values of the sectors' irrigation demands and the actual

accumulated volume of water applied as its aim is to reach the end of the irrigation campaign with the minimal difference between the values. The real operation time of each sector depends on the instantaneous photovoltaic power, $P_{pv\,n\,t}$, which in turn depends on the day of the year (n) and the time of day (t). It is also affected by reductions in irradiance due to adverse meteorological conditions (cloudy days). $P_{pv\,n\,t}$ is compared with the minimal power required to pump Q_i, $P_{min\,i}$ (W), and calculated as follows:

$$P_{\min i} = \frac{1}{\eta_p} \cdot \gamma \cdot Q_i \cdot H_i \tag{3.1}$$

where i is the sector index; H_i (m) is the minimum pressure head required for the proper operation of sector i, which depends on its elevation, size, hydraulic characteristics and type of emitters; Q_i (m^3s^{-1}) is the sector flow demand that depends on the sector's hydraulic characteristics; h_p is the pumping system efficiency for each pair of Q_i-H_i values and g (Nm^{-3}) is the water's specific weight. A daily irrigation time log is used to update the duration of the irrigation events of the different sectors on the following days, $t_{req\,i\,n+1}$ (min) (Eq. 3.2) according to the weather conditions, which affect both the crop irrigation requirements and solar energy availability.

$$t_{req\,i\,n+1} = t_{req\,i\,n} + \Delta t_{req\,i\,n} \tag{3.2}$$

where n is the day index; $t_{req\,i\,n}$ (min) is the required irrigation time to satisfy the daily irrigation needs of sector i on day n and $D_{treq\,i\,n}$ (min) is the time correction due to the non-satisfaction of the irrigation requirements for sector i on day n. After calculating the power requirements, the sectors are sorted in increasing order to compare their $P_{min\,i}$ values to the $P_{pv\,n\,t}$ values, which vary for the day of the year (n) and during the

daylight hours (t in min), while $P_{min\,i}$ values are constant for each sector. Any sector can operate when $P_{pv\,n\,t}$>1.1 $P_{min\,i}$ (Yahyaoui et al., 2016). The system will start to supply water consecutively to the lowest power demanding sectors (in increasing order) during their corresponding $t_{req\,i\,n}$ until $P_{pv\,n\,t}$ is sufficient to satisfy the highest power demanding sector that will be irrigated during its $t_{req\,i\,n}$. After irrigating this sector, the system irrigates the lower power demanding sectors in decreasing order until their corresponding $t_{req\,i\,n}$ are satisfied. Unexpected clouds can interrupt the operation of the system at any time. When this occurs, the total applied water for that day may be insufficient to satisfy the daily irrigation needs. If this is the case, the system will check the soil water balance and decide if the irrigation time for the following day should be corrected. A general overview of SPIM is given in Fig. 3.2, while details of the model are shown in Fig. 3.3. The main SPIM modules are described in what follows.

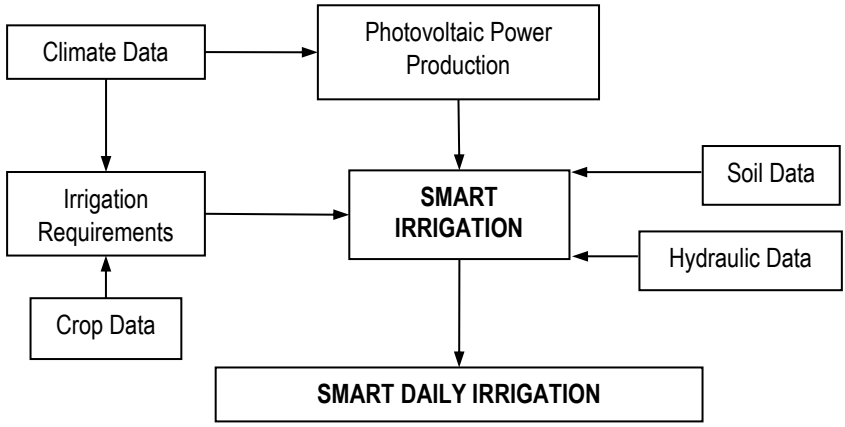

Fig. 3.2. SPIM Flow chart

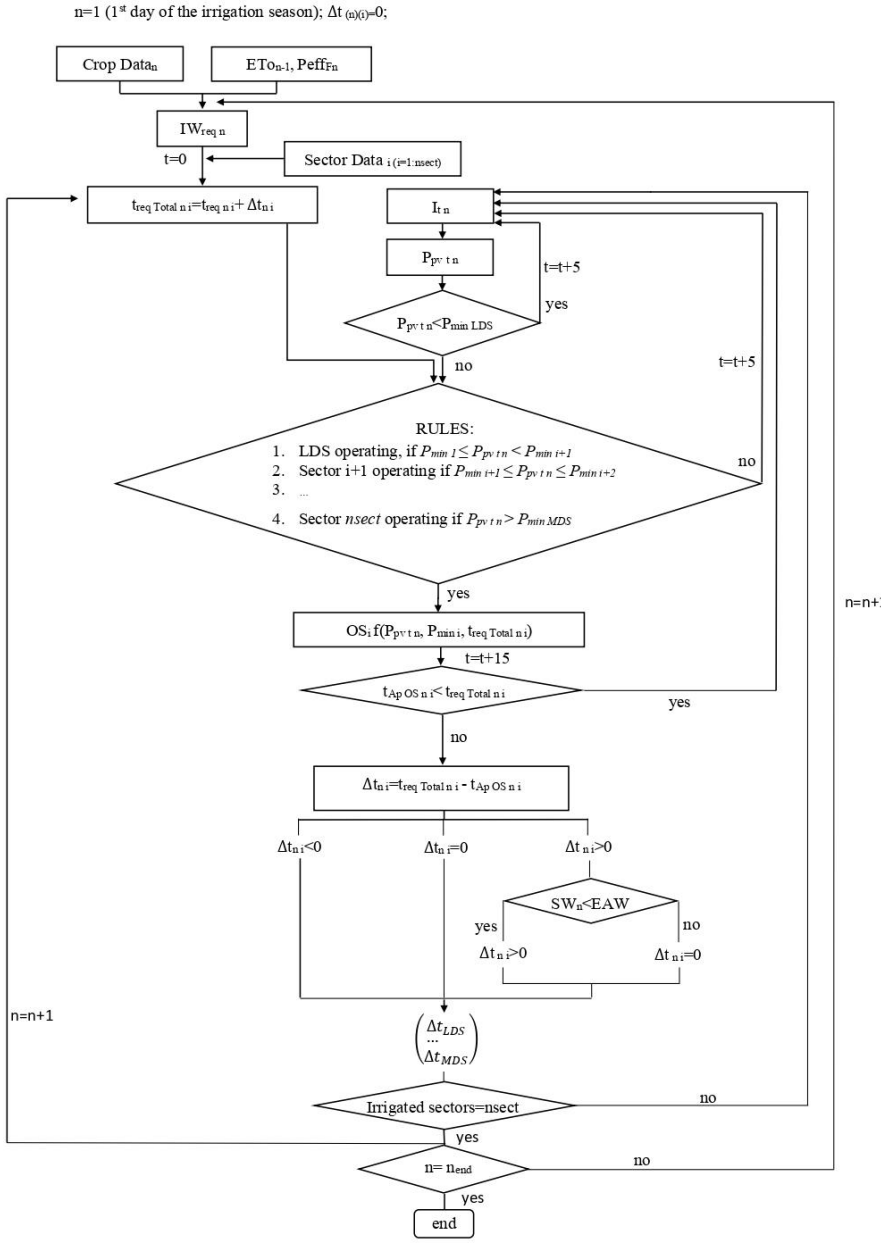

Fig. 3.3. Schematic representation of the operating mode of the model

3.2.3. Network hydraulic characterization module

In order to determine the net minimum power required for each sector, the entire irrigation network from pump to emitters is modeled in the hydraulic simulator EPANET (Rossman, 2000). The whole network is analyzed to determine the required pressure head in the pumping station that guarantees the minimum working pressure in the most unfavorable emitter. The different sectors are then simulated under a wide range of working conditions to determine their corresponding $P_{min\ i}$. To validate the simulation results, actual pump characteristic curves for the different pressure head settings of the variable speed drive should be determined from data recorded in the flowmeter and pressure gauge located at the pumping station.

3.2.4. Photovoltaic power controller

The available net instantaneous power, $P_{pv\ n\ t}$, provided by the photovoltaic system during the day was estimated using the following equation (López-Luque et al., 2015):

$$Ppv_{n\,t} = \frac{I_{n\,t}}{I_{stc}} * PP * [1 - \beta(T_{cell\ n\,t} - T_{stc})] \quad (3.3)$$

where t is the time index; I_{nt} is the irradiance on the collector plane (Wm^{-2}); I_{stc} is the irradiance under standard conditions ($1000Wm^{-2}$); PP is the peak power generated under standard conditions by the photovoltaic installation (W); b is the performance decay coefficient due to the rising temperature of the module cells (0.004 $ºC^{-1}$, for silicon cells); $T_{cell\ n\ t}$ is the cell temperature in the modules and T_{stc} is the cell module temperature under standard conditions (25 ºC). I_{nt} can be described as a function of the irradiance in the horizontal plane:

$$I_{n\,t} = rb \cdot I_{b\,n\,t} + \frac{1+cos\varphi}{2} \cdot I_{d\,n\,t} + \rho * \frac{1-cos\varphi}{2} * [I_{b\,n\,t} + I_{d\,n\,t}] \quad (3.4)$$

where rb is the geometric factor which relates beam irradiation on the tilted plane to that on a horizontal surface, $I_{bn\,t}$, φ is the tilt angle of the modules (degree), I_{dnt} is the diffuse irradiance (Wm^{-2}) and r is the albedo (Duffie et al., 2013). Finally, the net power transferred to the pump, P_{nt}, is affected by the converter (η_{fc}) and the asynchronous motor (η_{am}) efficiencies (Eq. 3.5).

$$P_{n\,t} = \eta_{am} * \eta_{fc} * P_{pv\,n\,t} \quad (3.5)$$

To evaluate the instantaneous photovoltaic power available to water each sector, conservative fixed values for the converter and asynchronous motor efficiencies of 0.95 and 0.8, respectively, were considered in this study.

3.2.5. Crop irrigation needs

Daily crop irrigation needs are equivalent to crop daily evapotranspiration. The selected irrigation strategy was to replenish daily the crop evapotranspiration of the previous day. Thus, the daily irrigation volume is determined from real daily ET_o values recorded at the nearest agroclimatic station, and from the crop coefficients according to the crop stage, K_{cn} (Doorenbos and Pruitt, 1997):

$$ET_{c\,i\,n-1} = ET_{o\,i\,n-1} \cdot K_{c\,i\,n-1} \cdot K_{r\,i} \quad (3.6)$$

where $ET_{c\,i\,n-1}$ is the crop evapotranspiration for day n-1 and sector i (if a different crop is cultivated in each sector) and K_{ri} is the coefficient of soil evaporation reduction, which varies during the year in a range of 0-1 for crops with less than 60% of soil cover, and equals 1 otherwise.

Daily irrigation depth was calculated as the difference between ET_c on the previous day and the effective precipitation on the current day, P_{eff}, which represents the precipitation fraction that infiltrates into the soil and is available for the crop. This irrigation depth is affected by the regulated deficit irrigation coefficient, RDI_n, which usually ranges from 0.4 to 1 depending on the crop tolerance to the lack of water in the different phenological phases. This coefficient permits different irrigation managements according to the crop production conditions. When RDI_n equals 1, the crop will be watered to satisfy its full irrigation requirements. Values below 1 indicate that the irrigation target is to partially satisfy the crop irrigation needs according to water availability. This irrigation management practice is known as deficit irrigation, and is very common in water scarce regions. Controlled deficit irrigation allows maintaining crop production by reducing water consumption in those periods when the lack of water does not affect harvest, while small reductions or even no reductions in the irrigation needs are applied in the most critical periods (Pérez-Rodríguez and Parras-Cintero, 2014). Hence, this daily irrigation volume is calculated by:

$$V_{req_{i\,n}} = [(ET_{c\,i\,n-1} - P_{eff\,n}) \cdot IE \cdot RDI_{i\,n-1}] \cdot A_i \cdot 10 \qquad (3.7)$$

where A_i is the irrigated area (ha) associated to sector i, the value of 10 is the unit conversion factor and IE is the irrigation efficiency.

Once $V_{req\,i\,n}$ is determined, the estimated value of the required daily irrigation time $t_{req\,i\,n}$ is calculated using the hydraulic information of each sector (number of emitters). These values are updated according to equation 2 during the irrigation season.

3.2.6. Daily soil water balance

The soil water balance is calculated on a daily basis to evaluate the correction term $D_{treq\,i\,n}$ in Eq. (2). This correction adjusts the initial value of the required daily irrigation time $t_{req\ i\ n}$ according to real climate data (effective precipitation and irradiance) and the real irrigation depth applied. During the irrigation season, soil water content, $SW_{i\,n}$, in sector i is calculated at the end of each day according to the following soil water balance equation:

$$SW_{i\,n} = SW_{i\,n-1} + P_{effR\,n} + I_{Ap\,i\,n} - ET_{c\,adj\,i\,n} - R_{i\,n} - D_{i\,n} \quad (3.8)$$

where $SW_{i\,n-1}$ is the soil water content (mm) at the end of day n-1, $P_{effR\,n}$ is the real effective rainfall (mm), $R_{i\,n}$ is runoff (mm) and $D_{i\,n}$ is deep percolation (mm). $I_{Ap\,i\,n}$ is the applied irrigation depth (mm), which is calculated from water meter records and $ET_{c\ adj\ i\ n}$ is the real crop adjusted evapotranspiration of the current day, which is calculated by Eq. (3.9) (FAO, 2006):

$$ET_{c\,adj\,i\,n} = \left(\frac{TAW - Dr_{i\,n}}{TAW - EEW_i}\right) \cdot ET_{c\,i\,n} \quad (3.9)$$

where TAW is the total available soil water, Dr is the soil moisture depletion in the root area (mm) and EAW is the easily accessible water, estimated as a percentage of TAW. In cloudy days, if $SW_{i\,n}$ values are greater than a threshold based on EAW, then $D_{treq\,i\,n}$ is 0. Otherwise, its value is calculated by:

$$\Delta t_{req\,i\,n} = \frac{Vreq\,i\,n - I_{Ap\,i\,n} \cdot A_i}{\sum q_{e\,i}\, n_{e\,i}} \quad (3.10)$$

where $q_{e\,i}$ is the emitter's flow (l h^{-1}) for sector i and $n_{e\,i}$ the number of emitters of the sector i. The duration of the irrigation season can be previously defined, being subsequently adjusted depending on the water allocation and the precipitation distribution in the year.

3.3. Results and discussion

3.3.1. Hydraulic network analysis

SPIM has been applied to schedule the irrigation season of the olive orchard described in section 2.1. The irrigation system consisted of 3 sectors (S1, S2 and S3), whose $P_{min\,i}$, were determined by hydraulic analysis. These values increased by 10%, resulting in threshold powers of 5.94 kW, 12.39 kW and 9.6 kW for S1, S2 and S3, respectively. The pump provided pressure head values ranging from 35 to 55 m, with a corresponding range of power requirements between 2 and 11.5 kW depending on the sector and the flow. Fig. 3.4 shows the experimental flow-power curves for each sector at different pressure heads.

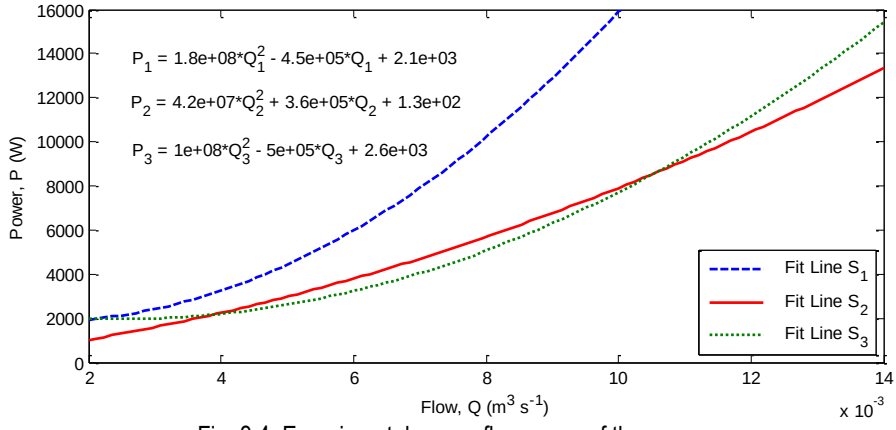

Fig. 3.4. Experimental power-flow curve of the pump

As a threshold was established for the operation of each sector, each sector provides the flow corresponding to this power threshold most of the time, with only small fluctuations (5.7 l s^{-1}, 12.6 l s^{-1}, and 11 l s^{-1} for sector 1, 2 and 3, respectively).

3.3.2. Photovoltaic energy production

The production of photovoltaic energy during the day was estimated according to the irradiance on the horizontal plane, which was measured by an irradiance sensor in 5-min intervals. The highest monthly irradiance within the annual energy production of the photovoltaic system coincides with the irrigation season in the region for woody crops (from April to September) (Fig. 3.5).

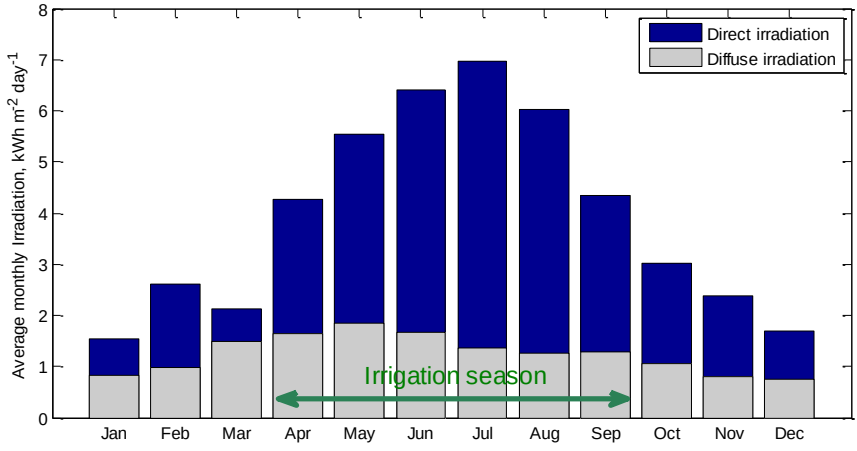

Fig. 3.5. Average monthly irradiation for 2013 and duration of the olive tree irrigation season

In general, on clear days, the distribution of the irradiance follows a Gaussian curve with a progressive increase in the produced energy until noon when the maximum value is reached. Fig. 3.6a shows the evolution of the power generated

(blue line) by the photovoltaic system on 30th June (clear day) in which the maximum power provided by the system was 15.62 kW, corresponding to an irradiance value of 1419 Wm^{-2} on the inclined collector plane. In partially cloudy days, such as 25th April (Fig. 3.6b), the energy production of the photovoltaic system (blue line) showed large fluctuations. On these days, the number of available hours with sufficient solar power was lower.

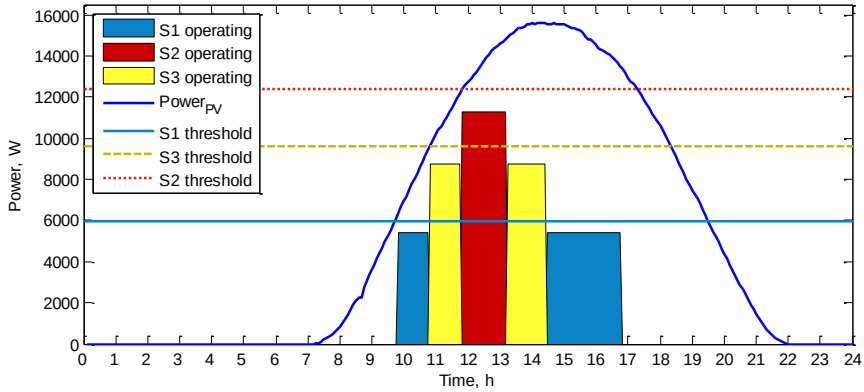

Fig. 3.6.a. Photovoltaic power generation on 30th June 2013, power threshold and operation sequence of sectors S1, S2 and S3 of the irrigation network.

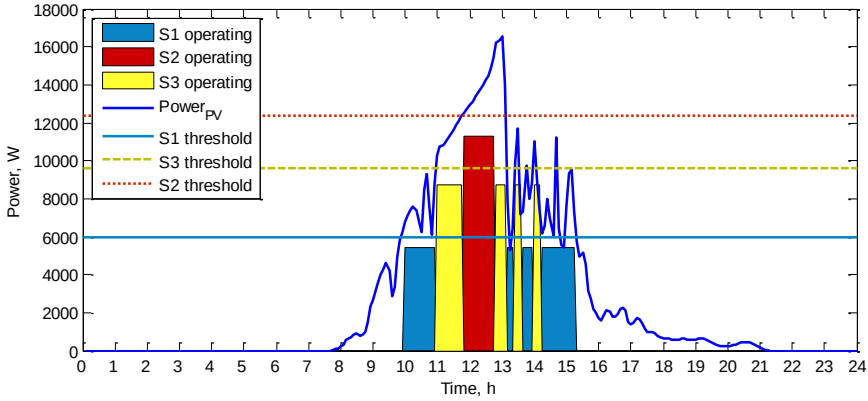

Fig. 3.6.b. Photovoltaic power generation on 25th April 2013, power threshold and operation sequence of sectors S1, S2 and S3 of the irrigation network.

Table 3.1 shows the highest, medium and lowest values of the daily energy produced each month of the 2013-irrigation season and the monthly energy produced by the photovoltaic installation. In some cases, months with a higher expected energy production (August) have a lower maximum daily energy production compared to other months, such as May. This is due to the negative effect of high temperatures on the modules' performance (Binshad et al., 2016). Additionally, the monthly absolute energy requirements and their fraction over the generated energy are also included in the table. The range of energy demand over energy production varied between 16 and 35.5%, thus indicating that the photovoltaic station assuring the application of the full water allocation during the irrigation season. The remaining energy that is not used in irrigation could be employed in other activities or even be delivered to the grid if permitted under national electrical regulations.

Table 3.1. Maximum (E_{max}), minimum (E_{min}) and mean (E_{mean}) daily energy production, total monthly energy production (E_{gen}), total monthly energy required (E_{req}) and total monthly energy required to produced energy ratio (%) at the experimental site for 2013.

	E_{max} (kWh/d)	E_{mean} (kWh/d)	E_{min} (kWh/d)	E_{gen} (kWh)	E_{req} (kWh)	%
April	125.10	90.15	26.45	2,704.54	459.78	17.00
May	146.88	113.19	47.37	3,508.77	910.91	26.00
June	147.69	122.39	57.01	3,671.77	1301.87	35.50
July	136.03	126.04	95.52	3,907.24	690.96	17.70
August	127.67	109.22	52.24	3,385.97	541.81	16.00
September	117.11	84.90	24.94	2,547.05	646.70	25.40

3.3.3. Irrigation requirements and daily soil water balance

The model was used to manage irrigation from 15th April to 30th September 2013. The experimental site is located in a water scarce region where deficit irrigation is a common practice for most crops. The water allocation for irrigating the trial field ranged from 1000 to 2000 m^3 ha^{-1} depending on the sector. The daily irrigation volume was calculated by Eqs. (3.6) and (3.7), and is related to ET_o of the previous day, the estimated effective precipitation and several coefficients. The soil coefficient K_r was 1 (60% of soil cover) and Kc, the crop coefficient, varied from 0.45 (July and August) to 0.65 (for autumn and spring months) for olive trees within the province of Cordoba (Pastor and Orgaz, 1994). The coefficient that controlled deficit irrigation, RDI, varied over the season (0.75 April-June, 0.4 July-August and 0.64 September) (Pérez-Rodríguez and Parras-Cintero, 2014). Additionally, following the proportion established by the RDI coefficients, daily irrigation volumes were adjusted to the water allocation corresponding to each sector. Daily soil water balances were carried out to update $t_{req\ i\ n}$. As the trial field was drip irrigated, runoff and deep percolation were deemed null. Based on the soil characteristics, the threshold value of soil water content to update the irrigation time was 25% of the total available water (TAW), since the value of the easily accessible water considered in this study for olive tree was 75% of TAW (Orgaz and Fereres, 1999). The daily irrigation requirements for the 2013 irrigation season are shown in Fig. 3.7a, b and c for sectors 1, 2 and 3, respectively. Peak irrigation demand occurred in May and June, whereas the irrigation needs were lower in July and August consistent with the RDI_n values. For the whole season, the irrigation needs were 1413 m^3 ha^{-1}, which is the average value of irrigation demand in each sector (1000 m^3 ha^{-1}; 1714 m^3 ha^{-1} and 1795 m^3 ha^{-1}, for

sector 1, sector 2 and sector 3, respectively). As for the soil water content, it generally decreased throughout the irrigation season due to the deficit irrigation scheduling.

3.3.4. Smart irrigation scheduling

Considering the minimum required power for each sector, the less power demanding sector, S1, was irrigated when the produced photovoltaic power was between 5.94 kW and 9.60 kW. The next sector in increasing order of demanded power, S3, was irrigated when the power ranged from 9.60 kW to 12.39 kW. Finally, S2, which is the most power demanding sector, was irrigated when the power was higher than 12.39 kW. Table 3.2 presents these values together with the daily peak and medium power produced during the 2013 irrigation season, which show the capability of the photovoltaic system to supply the irrigation requirements of the crop.

Table 3.2. Monthly peak (P_{max}) and mean (P_{mean}) of the instantaneous power produced by the photovoltaic installation at the experimental site in 2013 and the minimum power required by each sector for their proper operation.

	P_{max} (kW)	P_{mean} (kW)	$Pmin_{S1}$ (kW)	$Pmin_{S2}$ (kW)	$Pmin_{S3}$ (kW)
April	19.09	3.76	5,94	12,39	9,60
May	20.81	4.72	5,94	12,39	9,60
June	20.38	5.10	5,94	12,39	9,60
July	17.79	5.25	5,94	12,39	9,60
August	16.61	4.55	5,94	12,39	9,60
September	16.69	3.54	5,94	12,39	9,60

The smart irrigation system operated at 5 min intervals. When the photovoltaic power reached the threshold for supplying water to the less demanding sector, the operational rule was to remain on standby for 5 min to prevent system instabilities

due to irradiance fluctuations. After that time, if the irradiance level remained above the lowest threshold, the irrigation of the lowest energy demanding sector (S1) commenced. Once S1 was activated, this sector was irrigated for at least 15 min in order to avoid system instability although irradiance fluctuations occurred. This occurs whenever a new sector starts to irrigate. In this case study, the pump characteristics allow the system to work as long as the power provided by the photovoltaic installation exceeds 2 kW, even though the corresponding flow is lower. Thus, if irradiance fluctuations drastically reduced the generated power (lower than 2 kW) while any sector was operating, the pump would switch off. Once these 15 min elapsed, the system evaluated the power availability at 5-min intervals, as well as the remaining time needed to satisfy the irrigation requirements of the sector. If the remaining time was between 5 and 15 min, the working sector would continue to be irrigated although the generated photovoltaic power was sufficient to activate other sectors with higher power requirements (S2 or S3). In contrast, if the remaining irrigation time was greater than 15 min and the available photovoltaic power was higher than the minimum required power to operate S2 or S3, the most power demanding sector would be activated. This process continued until the irrigation time of the 3 sectors was satisfied or until the irradiance was insufficient to provide the minimum power required in any sector. Days on which irrigation needs entailed an irrigation time below 15 min for any sector (irrigation requirements were smaller than the pumped water volume for 15 min) the system would not operate. At the end of the day, SPIM evaluated the soil water content to check if the irrigation time of the following day should be updated or not to compensate the lack of irrigation. The irrigation time of the following day was only updated in the event that the soil water content was below the established threshold. Moreover, if the estimated effective

precipitation was greater than the crop irrigation requirements on rainy days, the system would not operate (Fig. 3.7). As an example, Fig. 3.6a mentioned above shows the scheduling of the 3 sectors on 30th June, a typical sunny day. S1 started to water at 9:50 h (local time) and irrigated for 60 min. S3 was then activated for 60 min, after which S2 started to irrigate until 13:15 h. Once the most power demanding sector finished, S3 began to irrigate again for 75 min (14:30 h) until the irrigation requirements of the sector were satisfied. Finally, S1 operated for a further 140 min until 16:50 h. On this day, the total irrigation time was 7 h; one of the longest irrigation times of the season. As is shown in Fig. 3.6a, on clear days, the total available hours with enough photovoltaic power were generally higher than the required hours, so the installation did not use its full potential on these particular days. In contrast, 25th April is a good example of a cloudy day with large irradiance fluctuations. The operation of the photovoltaic irrigation system is shown in Fig. 3.6b, in which the sector activation sequence matched the available power during the daytime. On this day, irrigation started with the operation of S1 at 10:00 h (local time) and lasted for 60 min. S3 then started to irrigate until 11:50 h, after which S2 operated for 1 h (12:50 h). At 12:50 h, S3 began irrigating again for 1 h and 20 min (13:10 h), after which S1 irrigated for an additional 15 min (13:25 h). As S3 had not finished, the sector began to irrigate again for 15 min since the power provided by the photovoltaic installation reached it threshold. This was followed by 20 min of irrigation in S1 as the photovoltaic power decreased again. At 14:00 h, S3 restarted irrigation for 15 min until completing its irrigation time. Finally, S1 finished with 65 more minutes of irrigation. In this case, the total irrigation time was 5 h and 20 min. However, due to the irradiance fluctuations described above, there were too many changes in the

operating sector. In contrast to Fig. 3.6a, b shows that both the available and required hours were much more similar on cloudy days.

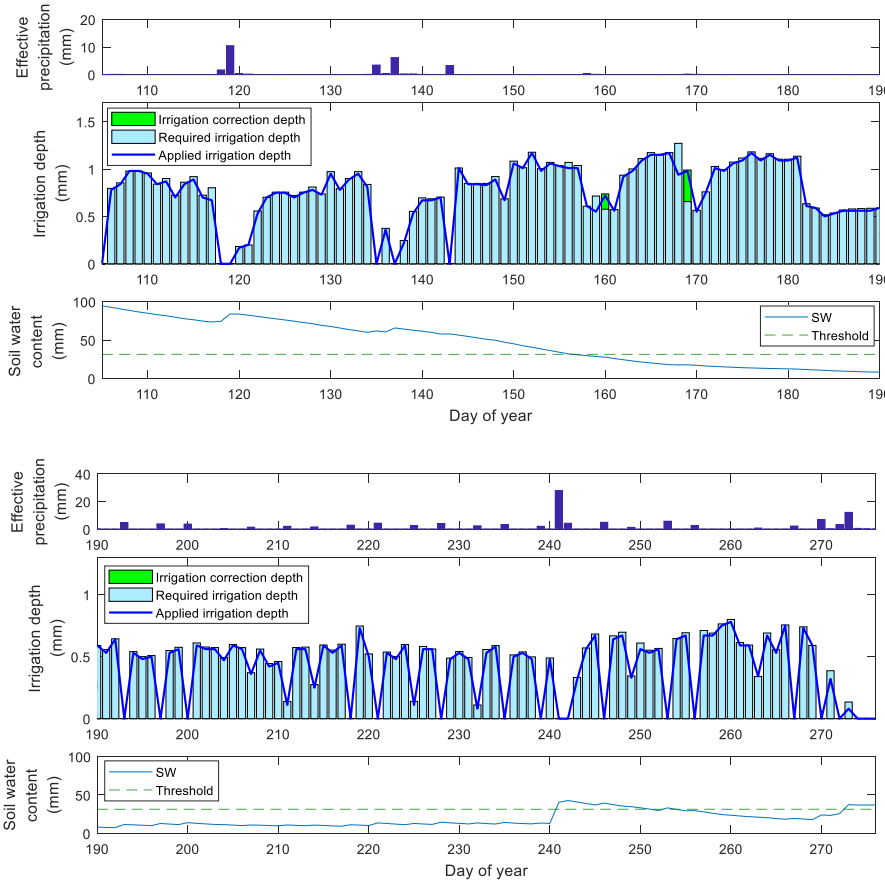

Fig. 3.7.a. Seasonal distribution of daily effective precipitation, soil water content (SW), soil water content threshold for corrections, required and applied irrigation depth and irrigation correction depth in S1 for the 2013 irrigation season.

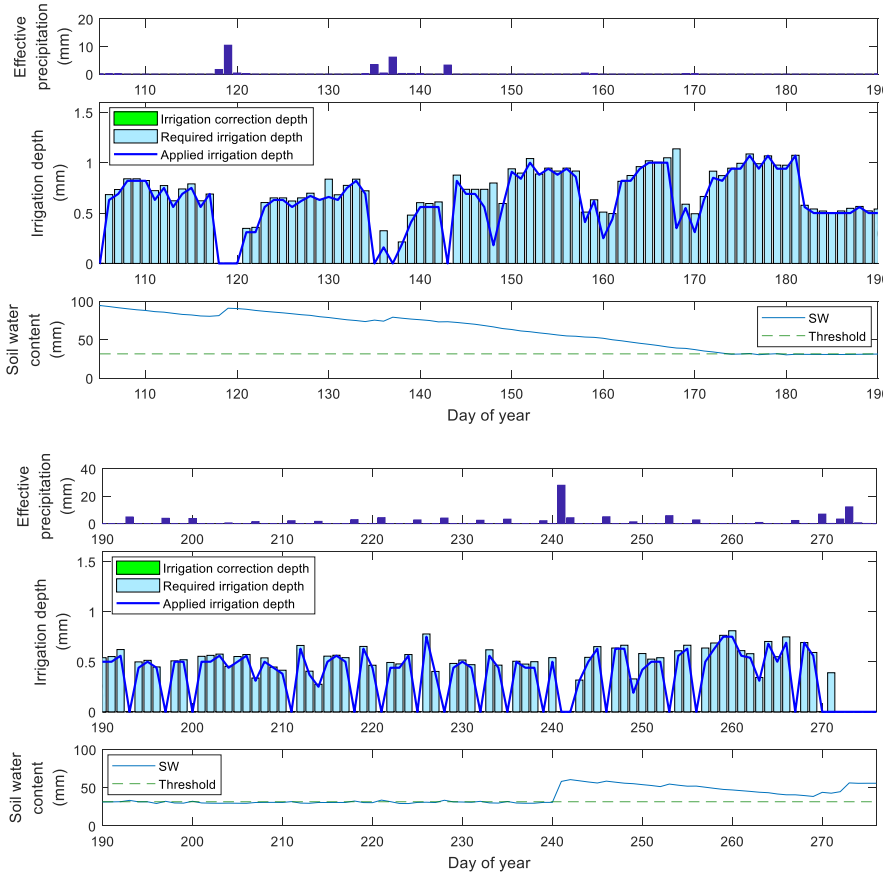

Fig. 3.7.b. Seasonal distribution of daily effective precipitation, soil water content (SW), soil water content threshold for corrections, required and applied irrigation depth and irrigation correction depth in S2 for the 2013 irrigation season.

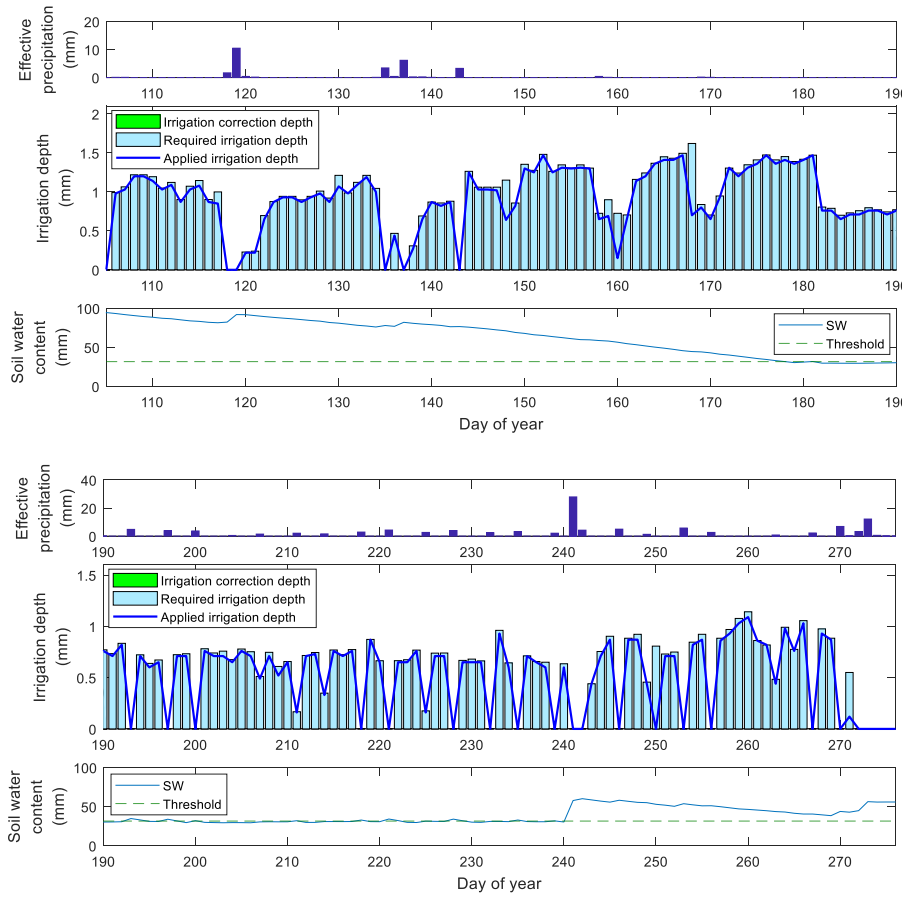

Fig. 3.7.c. Seasonal distribution of daily effective precipitation, soil water content (SW), soil water content threshold for corrections, required and applied irrigation depth and irrigation correction depth in S3 for the 2013 irrigation season.

The smart irrigation scheduling of the whole irrigation season for the 3 sectors is shown in Fig. 3.7a, b and c. Required and applied water volumes are given, as well as the correction of the required water volume when necessary. Generally, days with low solar energy production coincided with periods in which crop irrigation needs

were low. Most of the days, the system could provide enough energy to satisfy the irrigation requirements. Nevertheless, when the system was unable to apply the scheduled amount of water due to weather conditions, this water deficit was considered in the soil water balance to check if the irrigation time of the following day should be modified or not, as explained above.

As can be observed in Fig. 3.7a, b and c, the irrigation requirements could not be satisfied due to a lack of energy on only 7 days of the irrigation season in certain sectors. This is also shown in Table 3 where both the water volume and operation times (required and applied) are given. On 17th June, for example, the photovoltaic power was higher than the threshold for only 30 min in S2. However, S2 required 90 min, so the irrigation needs of this sector, as well as those of the other sectors, could not be satisfied. In the case of S1, the operation time was 15 min less than the required irrigation time on 27th April, 8th June and 17th June, while the same thing occurred for S2 (the most demanding sector) on 28th May, 9th and 17th June and 28th September. Finally, in the case of S3, irrigation could not be satisfied on 28th May, 8th, 9th and 17th June, 7th and 28th September. Table 3.3 also shows the percentage deficit of water and operation time for each sector, with the maximum deficit occurring on 7th and 28th September (100% in S3 and S2, respectively) and the minimum deficit on 27th April (16.63% in S1). As shown in Fig. 3.7a, b and c, it was only necessary to update the irrigation schedule on 2 days of the irrigation season for S1 (8th and 17th June) in order to increase the irrigation time programmed for the following days. For the rest of the cases (5 days), although the irrigation requirements were higher than the applied irrigation, the soil water content was sufficient to satisfy the difference, and no correction was needed.

Table 3.3. List of days on which irrigation was not fully satisfied in the different sectors (OS), irrigation volume required ($Vreq_{Total}$ (l)), irrigation volume applied (V_{Ap} (l)) and irrigation deficit during the 2013 irrigation season in percentage and time units (min).

DAY	OS	$Vreq_{Total}$	V_{Ap}	Deficit	t_{def}
27th Apr	.	49,093	40,927	16.63 %	24
28th May	S2	48,862	10,790	77.92 %	50
	S3	70,416	38,918	44.73 %	48
8th June	S1	43,769	33,891	22.57 %	29
	S3	55,017	42,350	23.02 %	19
9th June	S2	31,182	15,360	50.74 %	20
	S3	44,369	9,311	79.01 %	53
17th June	S1	77,780	57,417	26.18 %	60
	S2	69,609	21,165	69.59 %	63
	S3	99,197	43,018	56.63 %	85
7th Sep	S3	49,386	0	100 %	75
28th Sep	S2	23,872	0	100 %	31
	S3	33,671	7,440	77.90 %	40

The rest of the days of the season the system was able to satisfy the irrigation requirements, so the differences between the required and the applied irrigation volume were due to the fact that the system operated at 5-min intervals. Therefore, when the difference between the required and operation times was less than 5 min, the system considered that daily irrigation was complete. On days when the real irrigation times were 15 min less than the required times, the soil water balance was the tool used to update the irrigation time of the following day (for example 18th June for S1) when the soil water content was below 31.5 mm, which was the established threshold corresponding to 25% of TAW for the soil of this plot.

The integration of solar energy in irrigation does not only eliminate electricity costs, which are leading farmers to question the viability of irrigation (Córcoles et al., 2015), but also reduces CO_2 emissions (Carrillo-Cobo et al., 2014). Taking into account that each kWh of conventional electric energy emits 0.264 kg of CO_2 equivalent (Iberdrola, 2012), the photovoltaic installation of the irrigation network studied here avoided the emission of 1.2 t CO_2 eq during the 2013 irrigation season corresponding to a total pumping time of 602 h and 20 min from 16th April to 30th September.

3.4. Conclusions

The use of solar energy to power irrigation systems involves the reduction or even the removal of energy costs for farmers. It is also a feasible option to supply energy in isolated areas. Moreover, the use of renewable energies is a low GHG emissions alternative to conventional electric energy or diesel engines, although the operation of the irrigation systems must be adapted to a variable energy supply.

The algorithm Smart Photovoltaic Irrigation Manager, SPIM, has been develop to schedule irrigation using solar energy. SPIM operates, in real time, the sectors of the irrigation networks synchronizing the photovoltaic energy production with the pumping power demand. The main feature of this algorithm is its ability to use jointly climatic, crop, hydraulic and soil data to operate efficiently the solar irrigation system, satisfying the crop irrigation needs throughout the irrigation season. Also, SPIM compensates occasional water supply lacks, due to irradiance fluctuations, in the following days with adequate weather conditions.

The proposed model has been evaluated in a real case study. SPIM was used to schedule the daily operation of a photovoltaic irrigation system in an olive orchard in Southern Spain during the 2013 irrigation season. The photovoltaic system operated for a period of 168 days and was able to supply the full water allocation to the experimental field (1000 m^3 ha^{-1}; 1714 m^3 ha^{-1} and 1795 m^3 ha^{-1}, for sector 1, sector 2 and sector 3, respectively) and provide the power requirements to each sector (5.94 kW, 12.39 kW and 9.6 kW for S1, S2 and S3, respectively). In 7 days, the irradiation level was insufficient to satisfy crop irrigation requirements. However, on the irrigation schedule was updated on only 2 of these days, thus increasing the irrigation time programmed for the following days since the soil water content was not sufficient to fulfil the non-satisfied irrigation volume. These results indicate that the system behaved very satisfactorily. Moreover, the substitution of the electricity grid for a 15.4 kW peak power photovoltaic installation during the entire irrigation season (602 h and 20 min) avoided the emission of 1.2 t CO_2 eq.

The main finding of this work is that solar irrigation in areas with appropriate irradiance levels is a feasible alternative to use renewable energy sources, when tools like SPIM are available, increasing the sustainability and profitability of irrigated agriculture.

3.5. References

Bakelli, Y., Hadj Arab, A., Azoui, B., 2011. Optimal sizing of photovoltaic pumping system with water tank storage using LPSP concept. Sol. Energy 85, 288–294. https://doi.org/10.1016/j.solener.2010.11.023

Bhattacharjee, A., Mandal, D.K., Saha, H., 2017. Design of an optimized battery energy storage enabled Solar PV Pump for rural irrigation. 1st IEEE Int. Conf.

Power Electron. Intell. Control Energy Syst. ICPEICES 2016 1–6. https://doi.org/10.1109/ICPEICES.2016.7853237

Bhosale, S.B., Ghumare, K.S., Phad, S.M., Sharmila, M., 2017. Automatic Solar Power for Feeding System for. J. Electr. Electron. Eng. Natl. Conf. Emerg. Trends Eng. Technol. 11–14.

Binshad, T.A., Vijayakumar, K., Kaleeswari, M., 2016. PV based water pumping system for agricultural irrigation. Front. Energy 10, 319–328. https://doi.org/10.1007/s11708-016-0409-7

Carrillo-Cobo, M.T., Camacho-Poyato, E., Montesinos, P., Rodriguez-Diaz, J.A., 2014. Assessing the potential of solar energy in pressurized irrigation networks. The case of Bembézar MI irrigation district (Spain). Spanish J. Agric. Res. 12, 838–849. https://doi.org/10.5424/sjar/2014123-5327

Carrillo Cobo, M.T., Camacho Poyato, E., Montesinos, P., Rodríguez Díaz, J.A., 2014. New model for sustainable management of pressurized irrigation networks. Application to Bembézar MD irrigation district (Spain). Sci. Total Environ. 473–474, 1–8. https://doi.org/10.1016/j.scitotenv.2013.11.093

CENSOLAR, 2007. Distribución horaria de la irradiación solar global incidente sobre superficie horizontal en las cinco zonas climáticas definidas en el Código Técnico de la Edificación de España.

Chandel, S.S., Naik, M.N., Chandel, R., 2017. Review of performance studies of direct coupled photovoltaic water pumping systems and case study. Renew. Sustain. Energy Rev. 76, 163–175. https://doi.org/10.1016/j.rser.2017.03.019

Closas, A., Rap, E., 2017. Solar-based groundwater pumping for irrigation : Sustainability , policies , and limitations. Energy Policy 104, 33–37. https://doi.org/10.1016/j.enpol.2017.01.035

Córcoles, J.I., Tarjuelo, J.M., Carrión, P.A., Moreno, M.Á., 2015. Methodology to minimize energy costs in an on-demand irrigation network based on arranged opening of hydrants. Water Resour. Manag. 29, 3697–3710. https://doi.org/10.1007/s11269-015-1024-9

Corominas, J., 2010. Agua y energía en el riego en la época de la sostenibilidad. Ing. del agua 17, 219–233.

Díaz, J.A.R., Montesinos, P., Poyato, E.C., 2012. Detecting Critical Points in On-Demand Irrigation Pressurized Networks - A New Methodology. Water Resour. Manag. 26, 1693–1713. https://doi.org/10.1007/s11269-012-9981-8

Doorenbos, J., Pruitt, W., 1997. Crop water requirements. Food and Agricultural Organization of the United Nations, Rome.

Duffie, J. a., Beckman, W. a., Worek, W.M., 2013. Solar Engineering of Thermal Processes, 4nd ed., Wiley, John Wiley & Sons. Wiley, John Wiley & Sons , Inc., Hoboken, New Jersey. https://doi.org/10.1115/1.2930068

FAO, 2006. Guidelines for predicting crop water requirements, Irrigation and Drainage Paper 24 (Rev. 1). Food Agric. Organ. United Nationes, Roma, 144 p.

Fernández García, I., Rodríguez Díaz, J.A., Camacho Poyato, E., Montesinos, P., 2013. Optimal Operation of Pressurized Irrigation Networks with Several Supply Sources. Water Resour. Manag. 27, 2855–2869. https://doi.org/10.1007/s11269-013-0319-y

Ghavidel, S., Aghaei, J., Muttaqi, K.M., Heidari, A., 2016. Renewable energy management in a remote area using Modified Gravitational Search Algorithm. Energy 97, 391–399. https://doi.org/10.1016/j.energy.2015.12.132

González Perea, R., Camacho Poyato, E., Montesinos, P., Rodríguez Díaz, J.A.,

2014. Critical points: Interactions between on-farm irrigation systems and water distribution network. Irrig. Sci. 32, 255–265. https://doi.org/10.1007/s00271-014-0428-2

Hamidat, A., Benyoucef, B., Hartani, T., 2003. Small-scale irrigation with photovoltaic water pumping system in Sahara regions. Renew. Energy 28, 1081–1096. https://doi.org/10.1016/S0960-1481(02)00058-7

Jafar, M., 2000. Model for small-scale photovoltaic solar water pumping. Renew. Energy 19, 85–90.

Kabalci, Y., Kabalci, E., Canbaz, R., Calpbinici, A., 2016. Design and implementation of a solar plant and irrigation system with remote monitoring and remote control infrastructures. Sol. Energy 139, 506–517. https://doi.org/10.1016/j.solener.2016.10.026

Khadra, R., Lamaddalena, N., 2010. Development of a Decision Support System for Irrigation Systems Analysis. Water Resour. Manag. 24, 3279–3297. https://doi.org/10.1007/s11269-010-9606-z

Li, T., Roskilly, A.P., Wang, Y., 2017. Life cycle sustainability assessment of grid-connected photovoltaic power generation: A case study of Northeast England. Appl. Energy 227, 465–479. https://doi.org/10.1016/j.apenergy.2017.07.021

López-Luque, R., Reca, J., Martínez, J., 2015. Optimal design of a standalone direct pumping photovoltaic system for deficit irrigation of olive orchards. Appl. Energy 149, 13–23. https://doi.org/10.1016/j.apenergy.2015.03.107

Louazene, M.L., Garcia, M.C.A., Korichi, D., 2017. Efficiency optimization of a photovoltaic water pumping system for irrigation in Ouargla, Algeria. AIP Conf. Proc. 1814. https://doi.org/10.1063/1.4976258

Maheshwari, T.K., Kumar, D., Kumar, M., 2017. Solar Photovoltaic Irrigation

Pumping System 6, 1884–1889.

Nelson, G.C., Rosegrant, M.W., Koo, J., Robertson, R., Sulser, T., Zhu, T., Ringler, C., Msangi, S., Palazzo, A., Batka, M., Magalhaes, M., Valmonte-Santos, R., Ewing, M., Lee, D., 2009. Cambio Climático: El impacto en la agricultura y los costos de adaptación. Instituto Internacional de Investigación sobre políticas Alimentarias, Washington. https://doi.org/10.2499/0896295370

Orgaz, F., Fereres, E., 1999. Riego, in: El Cultivo Del Olivo, 6ª Edición. Barranco, D., Fernández-Escobar, R. Y Rallo, L. (Eds.) Junta de Andalucía Y Ediciones Mundi-Prensa, Madrid. pp. 269–288.

Ouachani, I., Rabhi, A., Yahyaoui, I., Tidhaf, B., Tadeo, T.F., 2017. Renewable Energy Management Algorithm for a Water Pumping System. Energy Procedia 111, 1030–1039. https://doi.org/10.1016/j.egypro.2017.03.266

Pastor, M., Orgaz, F., 1994. Riego deficitario del olivar. Revista Agricultura, nº746, páginas 768 a 776.

Pérez-Rodríguez, J.M., Parras-Cintero, J., 2014. Manual práctico de riego del olivar de almazara. Centro de Investigaciones Científicas y Tecnológicas de Extremadura. CICYTEX., Badajoz.

Reges, J.P., Braga, E.J., Dos, L.C., De, A.R., 2016. Inserting Photovoltaic Solar Energy to an Automated Irrigation System. Int. J. Comput. Appl. 134, 1–7. https://doi.org/10.5120/ijca2016907751

Rosenzweig, C., Iglesius, A., Yang, X.B., Epstein, P.R., Chivian, E., 2001. Climate change and extreme weather events - Implications for food production, plant diseases, and pests. Glob. Chang. Hum. Heal. 2, 90–104. https://doi.org/10.1023/A:1015086831467

Rossman, L., 2000. EPANET 2. Users manual. US Environmental Protection Agency

(EPA), USA.

Tubiello, F.N., Salvatore, M., Cóndor-Golec, R.D., Ferraca, A., Rossi, S., Biancalani, R., Federici, S., Jacobs, H., Flammini, A., 2014. Agriculture, Forestry and Other Land Use Emissions by Sources and Removals by Sinks. Climate, Energy and Tenure Division, FAO.

Vick, B.D., 2010. Developing a Hybrid Solar / Wind Powered Irrigation System for Crops in the Great Plains. Am. Sol. Energy Soc.

Yahyaoui, I., Tadeo, F., Segatto, M.V., 2016. Energy and water management for drip-irrigation of tomatoes in a semi- arid district. Agric. Water Manag. 183, 4–15. https://doi.org/10.1016/j.agwat.2016.08.003

4. Comparing the environmental and economic impacts of on- or off- grid solar photovoltaics with traditional energy sources for rural irrigation systems

This chapter has been published entirely in the journal "Renewable Energy", A. Mérida García, J. Gallagher, A. McNabola, E. Camacho Poyato, P. Montesinos Barrios, J.A. Rodríguez Díaz (2019)

Abstract. This study quantifies the environmental and economic life cycle impacts of solar photovoltaics (PV), grid electricity and a diesel generator as power sources for pumping water in an irrigation network in Spain. It compares these energy sources in the context of on-grid or off-grid scenarios, where the PV energy is consumed solely by the irrigation pumping system (off-grid) or distributed between the pump and grid (on-grid). Overall, the results show the PV as the option with lower burdens for most environmental impact categories in both, an off- and on-grid scenario, over a 30-year lifespan. However, solar PV demonstrated a higher abiotic resource depletion burden, due to the high material demands from its manufacturing. The on-grid PV option allowed for the export of excess energy, having environmental impacts six times lower than the off-grid option. From an economic perspective, solar PV option was the cheapest energy source, despite higher initial investment. Finally, extending the grid connection to the isolated location ensures grid exports from the solar PV installation, reducing the associated impacts by between 54 and 77% for the different burden categories. Based on a 30-year lifespan, solar PV is the most

economically- and environmentally-viable energy source for pumping in irrigation networks.

Keywords: Pumping; Renewable energy; Grid electricity; Diesel generator; Life cycle assessment

4.1. Introduction

Global warming and its direct consequence, climatic change, is a problem that is affecting all corners of the planet (FAO, 2016). In parallel, the growing stress on the water-energy nexus and related interdependencies is more evident than ever (IEA, 2016). In 2014, the carbon intensity of electricity generation was 36% lower than 1990 levels in the EU-28 states. This is despite a 0.9% increase per annum observed in recent years, while the carbon intensity of electricity followed a continuous decreasing trend between 1990 and 2010 due to the increasing contribution of low carbon energy sources and improvement in efficiency (EEA, 2015). The European Union (EU) have set out to reduce greenhouse gas (GHG) emissions by 20% in comparison to 1990 levels (EC, 2017). Governments have outlined a range of actions to address this challenge, such as a transition to low carbon transportation, promoting energy efficiency and the growth of the renewable energy (RE) sector, which will play a vital role in achieving energy security and a low carbon future. In Spain, other cross-cutting activities include the voluntary registration of carbon footprints and the promotion of environmentally-driven actions and projects which help to support this reduction in national GHG emissions (MAPAMA, 2017).

In many countries, the agricultural sector has undergone a significant modernization process in recent years. As a consequence of the incorporation of

pressurized irrigation in a wide variety of crops, due to water scarcity, electric and diesel engines have been integrated into these systems to pump water to the required pressure and flow, thus increasing energy demands (Corominas, 2010). In parallel, a rise in annual oil and electricity prices has led to the uptake of alternative sources of energy, with RE technologies offering a cost effective and low carbon energy source for the agricultural sector. Recent projects have focused on solar photovoltaic (PV) pumping for irrigation, reducing the reliance of farms on grid electricity or diesel generation (Carrillo-Cobo et al., 2014; López-Luque et al., 2015; Reca et al., 2016). However, the biggest drawback for many RE technologies comes from its dependence on meteorological conditions. To overcome this problem some studies evaluated the use of energy storage, using batteries and intermediate water storage facilities, to ensure the availability of energy despite unfavourable climatic conditions (Bhattacharjee et al., 2017; Ouachani et al., 2017; Yahyaoui et al., 2016). Recently, Mérida García et al. (2018) developed a direct pumping model to synchronise solar PV energy production with the power requirements of an irrigation network on a real-time basis. It was demonstrated that an olive orchard in southern Spain could be sustained for an entire irrigation season using solar PV energy, avoiding 1.2 tonnes of carbon dioxide equivalent (t CO_2 eq.). Thus, solar PV energy presents a feasible alternative to reduce energy dependency on diesel and grid electricity for the irrigation sector.

However, despite solar PV not generating GHG emissions during its operation, there is a recognised environmental impact associated with its production (manufacturing, transport to site and installation) which should be considered (Desideri et al., 2012). Life cycle assessment (LCA) studies have presented not only the associated GHG emissions of solar PV technology, as global warming potential

(GWP), but also evaluate other environmental impact categories that relate to fossil resource depletion potential (FRDP), abiotic resource depletion potential (ARDP) and other polluting impacts (human toxicity potential e HTP, and acidification potential - AP) (Berger et al., 2010; Evans et al., 2009; Gerbinet et al., 2014; IEA, 2011). Most recently, Gallagher et al. (2017) examined the LCA of different RE technologies, including solar PV, and found high ARDP contributions over its life cycle. It was concluded that there is a need for adopting circular economy measures (EC, 2015), e.g. recycling and the adoption of eco-design initiatives, to further reduce the environmental impact of solar PV and other RE technologies in the future. Furthermore, in the case of solar PV as an energy source for seasonal irrigation (Mérida García et al., 2018), there is a need to consider the intermittent energy requirements for pumping and how the maximum generation potential of particular sites may not be fully utilised for this application of PV systems. Previous investigations have not considered that, the life cycle impact of solar PV systems in irrigation systems where the full power potential is not used, may be higher than previously published assessments of this form of RE.

4.2. Methodology

4.2.1. Goal and scope definition

This study evaluates the environmental impacts derived from the use of solar PV technology as an energy supply source in the irrigation sector, in comparison with the use of traditional energy supply options i.e. grid electricity or a diesel generator. Details of the materials used, manufacturing processes and installation demands for these three energy sources were collated and analysed. The LCA considered the manufacturing process, installation and operational stages of the life cycle of each

energy supply option. The environmental burdens associated with maintenance were omitted for all options, as it was negligible in the context of production related impacts.

Due to the case study focus on solar PV technology, and considering that the useful lifespan of PV modules is around 25-30 years (Knapp and Jester, 2001; Fthenakis and Alsema, 2006; Berger et al., 2010; IEA, 2011; De Wild-Scholten, 2013; Fu et al., 2015; Akinyele et al., 2017), a 30-year period was selected for the operational life cycle boundary conditions. The functional unit of 1 kWh of energy produced was considered suitable for comparing the different energy systems examined in this study. For the impact analysis, the CML method was chosen (CML, 2010), as it is a common impact assessment methodology which contains a wide variety of flows to evaluate the environmental burden of a process (Smith et al., 2015; Chen et al., 2016). Five impact categories were selected (Table 4.1) as the most representative and relevant for this case study (Goedkoop et al., 2008; Gallagher et al., 2015).

An analysis of two different scenarios was conducted, to consider the environmental impacts of an off-grid (Scenario 1) and on-grid (Scenario 2) installation. The life cycle cost (LCC) was also calculated, to determine the cost effectiveness and compare it with the environmental payback period.

Table 4.1. Impact categories to be evaluated in the LCA of PV, diesel and grid electricity systems.

Impact Category		Description
GWP	Global Warming Potential (kg CO_2 eq.)	Related to GHG emissions that contribute to climate change and its effects.
ARDP	Abiotic Resource Depletion Potential (kg Sb eq.)	Protection of human welfare, human and ecosystem health. Related with the extraction of minerals and fossil fuels, based on the global reserves.
AP	Acidification Potential (kg SO_2 eq.)	Acidifying substances impacts on soil, groundwater, surface water, organisms, ecosystems and materials. Calculated with the adapted RAINS 10 model.
HTP	Human Toxicity Potential (kg 1.4-DCBe eq.)	Effects of toxic substances on the human environment. Health risks of exposure in the working environment are not included. Expressed as 1,4-dichlorobenzene equivalents kg^{-1} emission. Calculated with USES-LCA.
FRDP	Fossil Resource Depletion Potential (kJ eq.)	Depletion of energy as fossil fuel deposits used to generate electricity (measured in equivalent kilojoules).

4.2.2. Case study: photovoltaic irrigation system, Córdoba (Spain)

The case study selected for this investigation was a solar PV powered irrigation system, providing the crop water needs for a 13.4-ha olive orchard in Córdoba in Southern Spain. A 168 m^2 solar PV plant was installed on the south facing roof of a storehouse, located 200 m from the pumping station and 1 km from the irrigated field (Fig. 4.1). The peak power from the 120-thin film module PV plant was calculated as 15.36 kW, to meet the energy requirements of the pump installation. The irrigation water was directly pumped from a reservoir into the irrigation network,

which was organised into three irrigation sectors, using a 13-kW submergible pump and without energy storage elements.

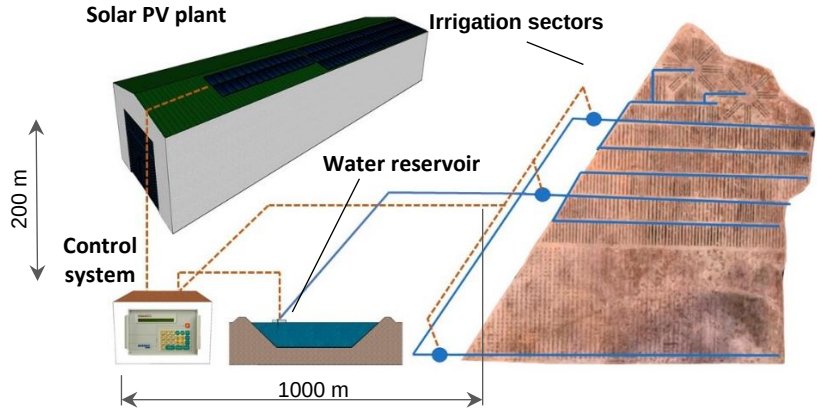

Fig. 4.1. Schematic representation of the PV irrigation installation in Cordoba (South Spain).

The power requirements of the sector and the daily irrigation demands were previously calculated. This work is based on the methodology and results explained in detail in Mérida García et al. (2018); in which a real-time model, the Smart Photovoltaic Irrigation Manager (SPIM), was developed to synchronise PV power production and irrigation requirements in an irrigation network. Moreover, in this same work, detailed calculations for the estimation of the power production of the PV plant is also provided, based on equations described on López-Luque et al. (2015). The estimation was based on the irradiance levels, as well as the PV plant peak power and the temperature. The crop was frequently irrigated in the drier months, April to September, each year. As such, irrigation was not necessary for the remaining six months of the year as there was sufficient rainfall and water storage in the soil.

Grid electricity and diesel generators are common sources of energy for pressurized irrigation systems (Mérida García et al., 2018). Diesel generators are commonly used where farms have energy requirements in isolated rural locations and do not have access to a grid connection. This study will undertake an environmental and economic assessment for each of these energy options considered to determine the life cycle performance of solar PV in comparison to traditional energy systems.

4.2.3. Inventory analysis

A database was generated in Microsoft Excel, including the raw materials, manufacturing, installation and transport processes for each technology. The data is provided in the supplementary information (S.I.) section (Table S.4.6.1). OpenLCA software and the Ecoinvent database were used to collect the data (Ecoinvent, 2014). ISO 14040 standards for LCA were followed to ensure that at least 95% of the total mass and 90% of the total energy inputs for each energy source were accounted for (ISO, 2006).

The environmental burden associated with each impact category was calculated as the sum of all materials and processes involved in each option, as it is expressed in Eq. (4.1):

$$EB_{s,i} = \sum_{x=1}^{X} K_{x,i} \cdot U_x \quad (4.1)$$

where EB is the environmental burden associated to the option s (off-grid solar PV, diesel generator, on-grid solar PV, grid electricity) and the impact category i; K is the environmental burden associated to each material or process; X is the total number

of different materials and processes; and U is the total units for the material or process involved in each option.

4.2.3.1. Photovoltaic energy

The solar panels installed in this plant were Sharp thin-film solar PV modules, model No. NS-F128G6, with a nominal peak power of 128 W and a total weight of 26 kg per module. The rest of the components of the PV installation were the inverter, the cable for connecting the solar PV plant and the pump, and the metallic frame connecting the panels to the storehouse roof. In addition, the transportation of these components, installation of the panel frames on the rooftop and site works (excavation for the installation of the power cable) were also accounted for in the calculations. Each PV module consisted of several few-microns thick semiconductors layers, which reduced the overall material demands and costs of the modules (Edoff, 2012). The manufacturing process of thin-film solar PV modules represents most of the energy requirements, due to the material deposition processes (Chatzisideris et al., 2016). In this study, it was assumed that the operational environmental impacts associated with maintenance would be negligible for the solar PV installation.

4.2.3.2. Diesel generator

The diesel generator considered for this study was a 15 kW Cummins Power Generation generator, model C15 D6, with a Kubota engine, and a total weight of 481 kg. The diesel generator system was composed of several elements: engine, alternator, radiator, electronic controls, skid, air filter and turbo charger. As it was considered in Benton et al. (2017), the first five components were estimated to represent approximately 87% of the materials involved. Due to the complexity of the

materials composition, the breakdown was synthesized based on Jiang et al. (2014), in which the material list was generated based on requirements for the manufacturing process of the diesel generator (e.g. steel, cast iron, aluminium, rubber, copper and polyethylene), including the energy requirements of the process. In addition, the cumulative diesel consumption required by the generator over the operational lifetime to irrigate the olive orchard was estimated. Diesel consumption was estimated from hourly fuel requirements of the generator and the annual irrigation hours required for the crop determined in Mérida García et al. (2018). The materials and energy requirements for the diesel storage tank were also included (sufficient to store all the fuel required for an entire irrigation season). Lastly, the transport of the generator, tank and fuel to the pumping station location were also accounted for in the assessment.

4.2.3.3. Electricity grid

The environmental impact of grid electricity was derived from national inventory data relating to energy sources in Spain for 2017, as well as accounting for the embodied burdens of the distribution network. In Spain, RE contributes to 34.4% of the total energy generation, with nuclear (21.7%) and coal (14.5%) representing other key sources of energy (REE, 2016). The mix of these sources for a specific country varies over time, therefore these calculations show an approximation based on the most recent information. To account for the changing energy mix likely to occur over the next 30 years, with a continued increase of RE contributions, the operational energy demands accounted for the dynamic environmental impacts of grid electricity over time (Gallagher et al., 2017), as is shown in the S.I. (Fig. S.4.6.2). In this study, it was assumed that the grid connection existed for the system and therefore the

default scenario only accounted for operational impacts of the supply of grid electricity.

4.2.4. Life cycle cost and payback period

Following the methodology described by Wu et al. (2018); which accounted for the life cycle cost (LCC) as the sum of the equipment, consumables and maintenance costs, considering a range of fuel cost variations, this study calculated the LCC for (i) the construction stage only, or (ii) the combined construction and operational stages. Thus, the LCC was estimated for each option (off-grid solar PV, diesel generator, on-grid solar PV and grid electricity) by applying the following Eq. (4.2):

$$LCC_s = LCC_{inst} + LCC_{ope} \quad (4.2)$$

where LCCs represents the life cycle cost of the option s; and LCC_{inst} and LCC_{ope} relate to the total life cycle cost associated to the installation and operation stages, respectively. From this, the payback period for the investment of these off and on-grid scenarios of the solar PV installation could be compared. To do so, the future annual operational costs related to diesel and electricity for the irrigation network were estimated. This allows for a comparison of the economic and environmental impacts of the solar PV installation with these traditional energy sources for irrigation systems over time.

4.2.4.1. Future diesel and electricity costs

Diesel and electricity prices are continuously varying, and it is difficult to predict the future cost of the energy consumed by the irrigation installation. The

energy price in the EU depends on a range of different supply and demand conditions, such as the national energy mix, the geographical situation or the network costs (Eurostat, 2017). A sensitivity analysis was included to incorporate changes in fuel and electricity prices (Wu et al., 2018). A range of prices for diesel, between € 0.80 and € 1.30 l^{-1}, and for electricity, between € 0.14 and € 0.24 kWh^{-1}, were considered. In the final case, a fixed cost due to the peak power contracted was also included to account for fixed costs by the electricity supplier.

4.2.5. Scenario and sensitivity analysis

Scenario 1 compared the off-grid energy options of a standalone solar PV installation and a diesel generator. For this solar PV installation, the energy demand for pumping during the irrigation season was only accounted for, and any surplus energy generated could not be used or stored. In Scenario 2, which had an available grid-connection, the solar PV installation was compared with grid electricity. In this situation, the total energy generated by the solar PV installation was accounted for, as surplus energy was assumed to be fed back into the grid.

For the sensitivity analysis of the environmental impacts of these energy scenarios, different lifespan lengths of between 5 and 30 years were considered. The impact of adding grid connection to a specific location in which the grid was not available, as well as the analysis of different prices for fuel and electricity, for the economic evaluation, were also included.

4.3. Results & discussion

4.3.1. Energy balance

The irrigation demand of the field of the case study was concentrated in the period comprised between April to September, as previously explained. This period entailed a total irrigation time of about 603 h, with an average of 4 h day^{-1}, corresponding to the three sectors. The power demanded by the sectors varied between 5.4 and 11.3 kW, depending on the size, topography and flow demand. Thus, the total energy required by the network was about 4620 kWh $year^{-1}$. This information was obtained from the SPIM model in the case study network for an irrigation season, as it was previously detailed (Mérida García et al., 2018).

In the case of the diesel engine and grid electricity options, the environmental burden associated to its installation and operation stages was related to the energy consumed in the total operation hours. Nevertheless, in the case of the PV plant, the total energy generated (around 28,700 kWh $year^{-1}$) greatly exceeded the energy demand of the irrigation network, which only represented a 16% of the total, and a 25% of the energy generated during the irrigation season. That was the key point in the difference between the environmental burden per kWh associated to the on- and off-grid PV plants. Thus, for the on-grid PV plant option, the environmental burden was associated to the total energy generated by the PV modules, due to the surplus of energy (28,700 -4,618 kWh $year^{-1}$) was considered to be injected into the grid. On the other hand, for the off-grid PV plant, the environmental burden was associated only to the energy requirements of the irrigation network (4,618 kWh $year^{-1}$), as the surplus of energy could not be used nor stored.

4.3.2. Contribution analysis

4.3.2.1. Component contributions

The cumulative environmental impacts per kWh for each method of energy generation to support pumping in the irrigation network, in a 30 years lifespan analysis, are presented in Fig. 4.2.

Firstly, the differences in the environmental impact values are evident for the solar PV installation in Scenario 1 (off-grid connection) and Scenario 2 (grid connection). The total energy produced in Scenario 1 was not fully consumed through the process of pumping in the irrigation network, and there is no grid connection availability for exporting the excess electricity generated. Furthermore, the solar PV installation generated surplus daily electricity due to a 4-h average pumping regime and irrigation is only required for six months of the year, April to September (the irrigation season for olive tree in the Mediterranean region). As Fig. 4.2 shows, the environmental impacts for the off-grid solar PV installation was approximately six times higher than the on-grid solar PV plant for each environmental burden category. Most of this impact was associated with the installation stage (due to manufacturing) of the solar PV's life cycle, corresponding to previous findings by Peng et al. (2013); while the replacement of the inverter was the only factor affecting the operational environmental impacts for both the on- and off-grid scenarios.

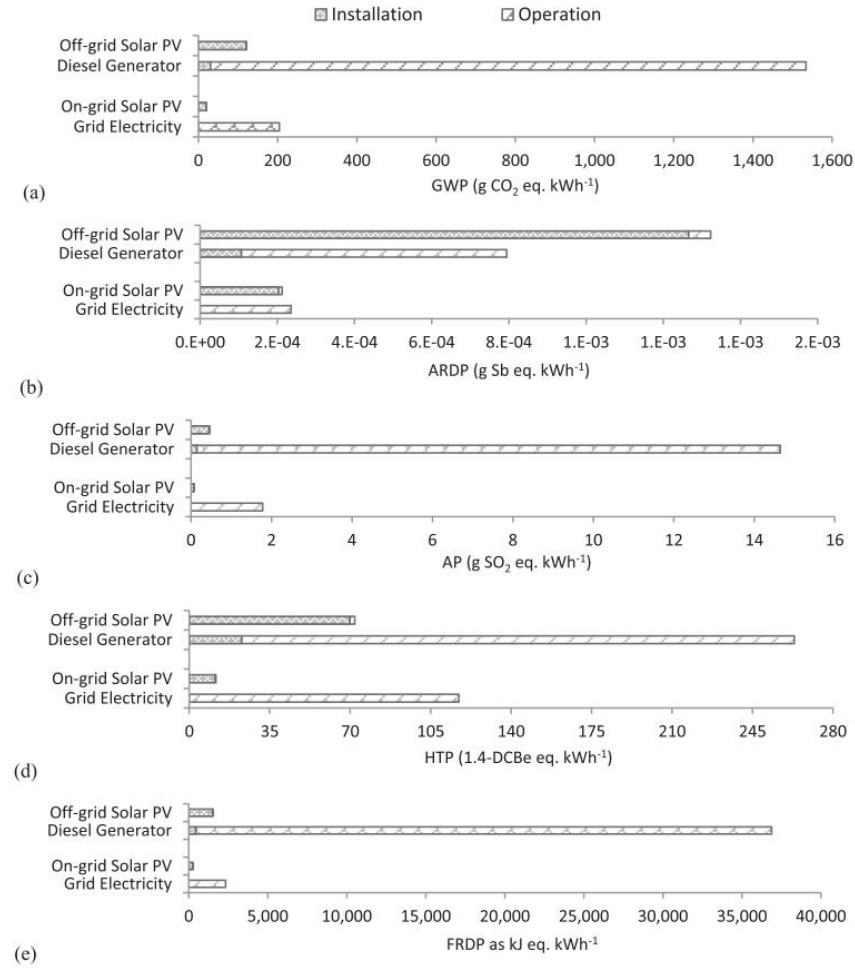

Fig. 4.2. Environmental burdens associated with the installation and operation of the different energy generation options assessed.

In Scenario 1, in which a grid connection was not available, the GWP burden for the solar PV plant was 121 g CO_2 eq. kWh^{-1}, compared to a value of 20 g CO_2 eq. kWh^{-1} for Scenario 2. The results for Scenario 2 were comparable with that of

previous LCA studies of solar PV (Kim et al., 2012; Irvine and Rowlands-Jones, 2016; Gallagher et al., 2017; Luo et al., 2018). The evidence suggests that thin film panels have lower cumulative energy requirements in manufacturing than crystalline panels (Sumper et al., 2011; Kittner et al., 2013), suggesting there is scope to reduce the GWP burden of these solar PV panels through lean design and more sustainable manufacturing processes.

On the other hand, the ARDP burden for the on-grid PV plant was estimated at $2.1 \cdot 10^{-4}$ g Sb eq. kWh^{-1}, slightly lower than the previously obtained by Gallagher et al. (2017). This difference could be explained by the lower material use of thin film modules compared with polycrystalline. Nevertheless, Lunardi et al. (2018) estimated significantly lower values for tandem solar modules. This difference could be due to the contribution of aluminium, copper, zinc and tin dioxide. These materials showed a high burden associated to this category, although they appeared as minority components of the panels and inverter, being not included this list in the Lunardi et al. (2018) study. In the case of the AP, its burden showed a value of $7.3 \cdot 10^{-2}$ g SO_2 eq. kWh^{-1}, again below the results obtained by Gallagher et al. (2017) and Corona et al. (2017).

The largest contribution was related to the use of solar glass, because the module did not include metal frame, but it included nonetheless two glass layers, and the manufacturing process. Probably, the manufacturing was the main difference in the results, which could be related to the lower energy demand of thin film technology manufacturing process. In a similar line, the HTP burden estimated for the on-grid PV plant was 11.6 g 1.4 DCBe eq. kWh^{-1}, lower than the values showed in previous studies (Corona et al. 2017; Gallagher et al., 2017). This burden was mostly related

to the manufacturing process (55%) of the modules studied in this work, so the difference was again related to the lower energy requirements. In the same way, the FRDP burden (240 kJ eq. kWh^{-1}) was lower than the determined by Corona et al. (2017). In addition to the difference in the energy requirements, for the FRDP, the energy mix also played an important role. Thus, the high contribution of coal to the grid electricity in Morocco, where Corona et al. (2017) developed their work, could also explain this difference.

The alternative option for off-grid electricity in Scenario 1 was the diesel generator, while direct grid electricity provided the second option in Scenario 2. Both options provided the precise quantity of energy required during the operational stage of the systems life cycle. However, the diesel generator had associated burdens during the installation (generator and diesel storage tank) and operational (diesel supply and generator replacements) stages. An extension of the electricity grid was considered in the sensitivity analysis, and the environmental impacts were compared to the savings associated with the allowance of excess energy feeding into the grid.

The diesel generator presented the largest contribution for GWP, AP, HTP and FRDP burdens. In that way, Smith et al. (2015) and Amante-García et al. (2017) also compared a range of energy sources and showed that the diesel generator had the highest impact for most categories. In relation to carbon emissions, provided as the GWP results, the diesel generator showed a burden 13 times higher than an off-grid solar PV plant, while in the on-grid scenario, the solar PV plant burden represented a 10% of the grid electricity GWP. In the case of the AP, the off-grid solar PV plant represented only a 3% of the burden associated to the diesel engine, while the grid electricity showed a burden 24 times higher than the on-grid PV plant. In a

similar way, the HTP and FRDP burden for grid electricity were 10 times higher than the burden associated to the on-grid PV plant. Nevertheless, the diesel generator showed a HTP that was four times higher than the burden associated to the off-grid PV plant. For FRDP, the off-grid PV plant represented the 4% of the burden associated to the diesel generator, the option with the greatest value for this category, due to the fuel consumption. Finally, for the ARDP burden category, the off-grid PV installation provided the highest impact (Fig. 4.2b). The ARDP burden was two times higher than the diesel generator, which was due to the use of metals and glass for the different components of the PV plant. Nevertheless, for Scenario 2, in which all the energy generated by the PV plant was considered, both options (on-grid solar PV and grid electricity) provided very similar results, with grid electricity presenting a burden 10% higher than the on-grid PV plant.

4.3.2.2. Material contributions

In this study, all environmental burdens for the solar PV system included were associated not only to the panels, but also to the materials, energy requirements, transport and installation of the rest of the components (inverter, metal support structure and cable for the connection between the PV plant and the pump station). Thus, the materials and processes percentage contribution for Scenarios 1 and 2 is represented in Fig. 4.3.

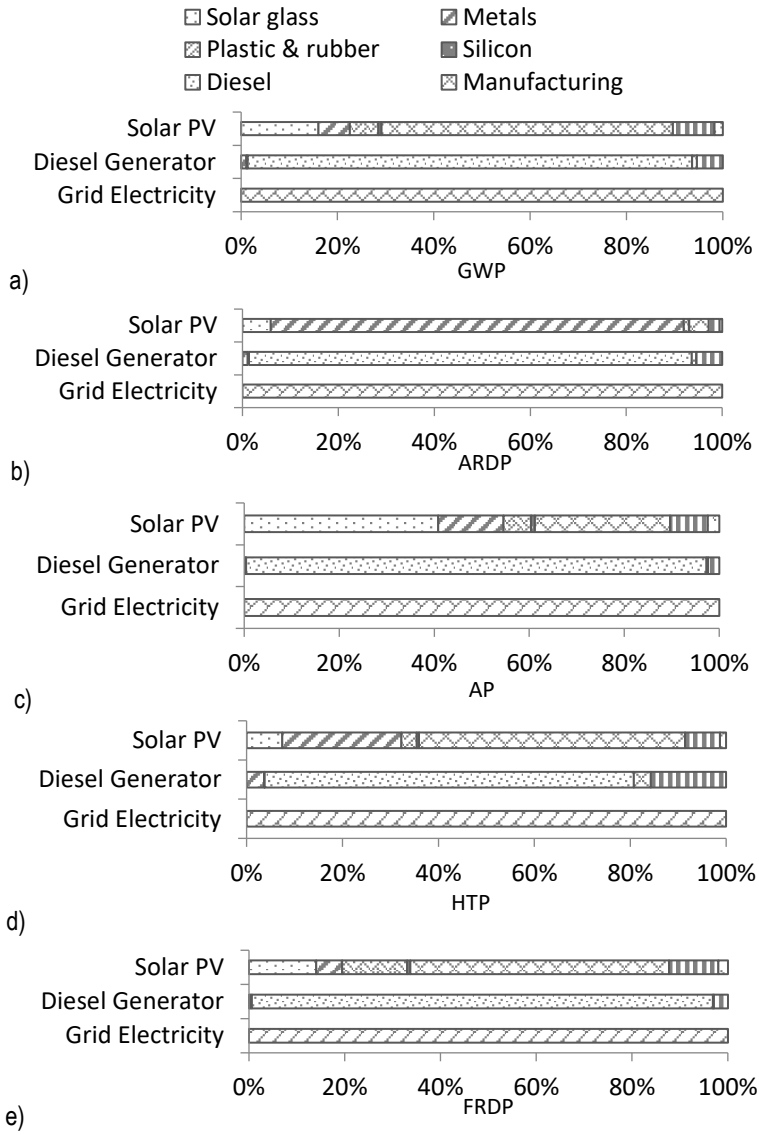

Fig. 4.3. Materials percentage contribution towards the installation of each energy generation option.

It can be noted that, in the PV installation, the materials implied a 29% of the total CO_2 emissions against a 60% for the energy requirements (manufacturing, mainly for the PV panels) (Fig. 4.3a). Similarly, for HTP and FRDP, the manufacturing process represented the highest burden, with 56% (Fig. 4.2d) and 54% (Fig. 4.2e), respectively. Nevertheless, for the ARDP burden, the metals represented 80%, against a 13% for the rest of the materials involved (Fig. 4.3b), while for the AP, solar glass and the manufacturing process represented the highest impact, with 41% and 29%, respectively (Fig. 4.3c). On the other hand, for the diesel generator option, the fuel represented the highest burden for all the impact categories, equating to 77% of the HTP burden and between 92 and 97% for all other impact categories. This was due to the annual consumption of more than 1,500 l of fuel, and the estimated 15-year generator lifespan, resulting in the material requirements of two generators over a 30-year period. The percentage contribution for the components for Scenarios 1 & 2 and impact categories are presented in plots in the S.I. (Fig. S.4.6.1).

4.3.3. Life cycle cost and energy payback period

The economic analysis was carried out following the energy prices for the last years in Spain, where the case study was placed, and assuming this as a mean value for the next 30 years. This assumption was considered sufficient to make an approximation to the comparison between the different options.

Firstly, the real investment cost of the solar PV plant was used and included an estimated cost for the replacement of the inverter after a 15-year period. For the diesel generator option, an average cost for the generator and tank was considered, provided by different commercial sources. The generator was replaced every 15 years. Moreover, for the fuel, the average price of the last 3 years was determined,

and applied as an assumed mean value (MINETAD, 2017a). Finally, for the electricity grid option, the fixed monthly cost per contracted kWh and the average price for the last 5 years for the kWh consumed were estimated (IDAE, 2017; MINETAD, 2017b). Fig. 4.4 shows the costs for the installation and operational costs for the different options over the lifespan of the project (30-year period).

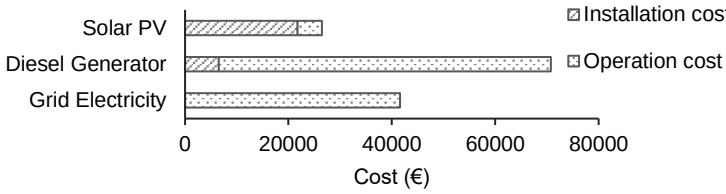

Fig. 4.4. Installation and operation costs (in Euros) for the different options for a 30-year lifespan.

Despite presenting the largest installation cost, the results showed that the lowest life cycle cost of € 26,444 was for solar PV. In the case of irrigation installations with the possibility of connecting to the grid electricity, the LCC took a value of € 41,593, for that period, while the high operational costs for the diesel generator led to a total of € 70,748. Nevertheless, although the difference between the LCC of the solar PV and grid electricity options was not very large, if the state legislation allowed selling the surplus of energy, profits for the farmer could also be considered. Thus, the solar PV plant represented 37% of the LCC of the diesel generator, while it represented 64% of the LCC of the grid electricity option, over a 30-years period.

Based on the location of the solar PV plant and its irradiation conditions, the energy payback time (EPBT) was estimated as 0.5 and 3.1 years for the on-grid and off-grid scenarios respectively. These EBPT result falls in the range of previous studies: 0.3 years for thin film modules by Peng et al. (2013); 0.9-1.1 years for multi-

and mono-crystalline silicon by Wetzel and Borchers (2015); and 3.5-5.0 years for a polycrystalline silicon PV plant by Sumper et al. (2011). Moreover, the economic payback time was estimated as 8.6 years for the off-grid PV installation, while for an on-grid solar PV plant, the selling of the surplus of energy should be considered, and this will depend on the legislation of each country. Finally, the environmental/carbon payback time estimated for the off-grid solar PV installation was 2.4 years, when it was compared to diesel engine, while in a comparison with the grid electricity, this value was almost 18 years. However, if all the energy generated by the PV plant is considered, this ratio takes a significantly lower value, slightly lower than 3 years. Despite of the fact that with a grid connected PV plant all the energy generated by the solar panels could be used, the lower total carbon emissions linked to the grid electricity made this ratio higher than the obtained for the PV-diesel comparison. This was due to the energy consumed by the irrigation representing a sixth part of the total energy generated, while the GWP per kilowatt-hour attributed to the grid electricity was 7.5 times lower than the estimated for the diesel engine.

4.3.4. Sensitivity analysis

4.3.4.1. Lifespan duration of each energy source

The influence of adopting shorter operational lifespans of 5, 10 and 20 years were examined, to determine the impact of this and the environmental impacts per kWh generated for the different energy supply options. By doing so, the shorter lifespan durations of 5 and 10 years only included one diesel generator and one inverter for the solar PV plant, as the useful life for both components was considered to be 15 years. Fig. 4.5 presents the results of the sensitivity analysis for the lifespan duration assessment.

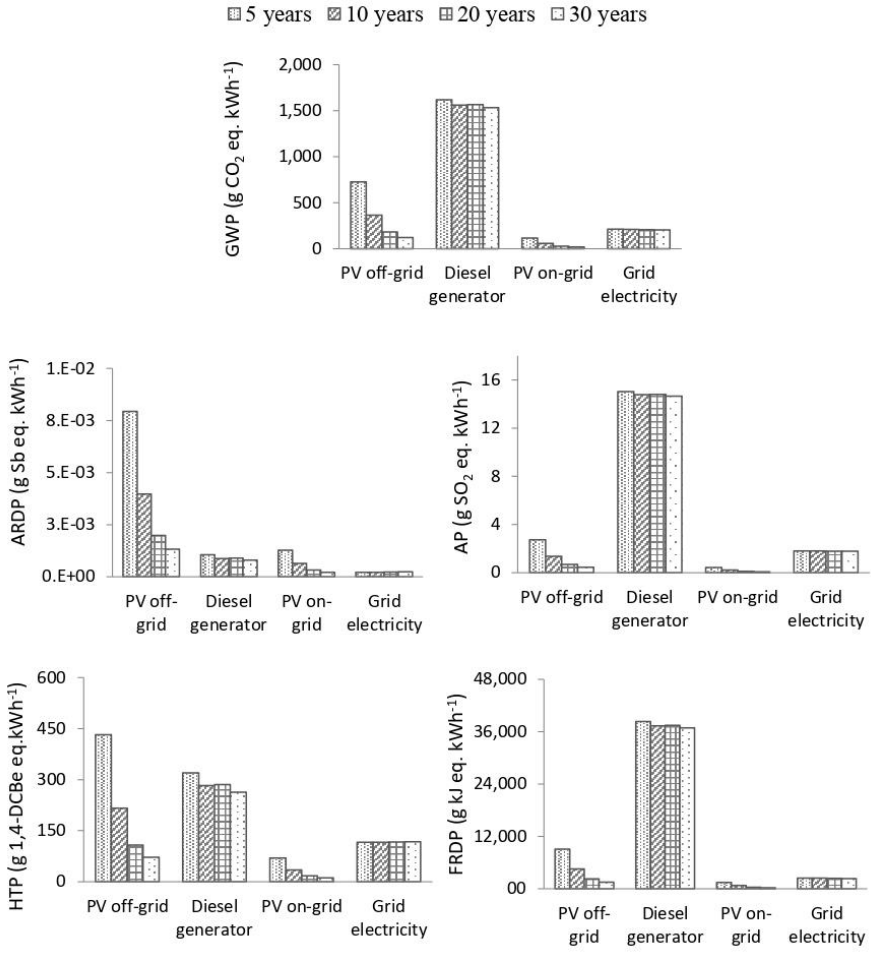

Fig. 4.5. Environmental impact (a) GWP, (b) ARDP, (c) AP, (d) HTP and € FRDP burden categories for each energy supply option for a range of different lifespan durations.

It can be noted that, for the diesel generator option, the different environmental burdens did not experience significant variations for the lifespan lengths between 10 and 30 years, the difference for the 5 years lifespan being slightly

higher. It was due to most of the burden being linked to the operation stage and the results were expressed per kWh. Thus, a longer period implied a higher fuel consumption but also a higher amount of energy in which this burden was distributed. In a same way, the grid electricity only experienced very small variations, imperceptible in most of the plots. These variations were due to the evolution of the electricity mix over the years, which represented an increase of 11% in the ARDP, while GWP and FRDP decreased by 4% and 5%, respectively. However, for the PV plant, the longer the period is, the lower the burden results, due to fact that the impact of the PV installation is mostly associated to the preoperational time, and the same modules can work for a 30-year period.

In a comparison between Scenarios 1 and 2, it can be noted that the PV option without grid connection had a higher GWP impact than the electricity grid option for a lifespan period below 20 years. Nevertheless, for a longer lifespan, the PV plant presented a lower GWP burden for both, grid and no grid connected installations, than grid electricity (Fig. 4.5a). For the ARDP burden, the PV plant presented the highest values, but for a grid connected installation, the ARDP burden received a lower burden than the diesel generator option when the lifespan length overcame 10 years (Fig. 4.5b). For the HTP category, the grid connected PV plant showed a lower burden than the traditional options. Nevertheless, for the off-grid PV plant, the HTP burden also achieved lower values than diesel engine and grid electricity for a 10- and 20-years lifespan and beyond, respectively (Fig. 4.5d). Finally, the FRDP always showed the greatest values for the diesel generator option.

4.3.4.2. Adding a grid connection for the off-grid solar PV installation

The additional impact of adding an extra cable and electric poles to reach the grid connection for an isolated irrigation network, for relatively short distances, was considered. The results are shown in Table 4.2. It can be noted that the addition of 1 km of cable and the corresponding poles (placed at 50 m intervals) increased the GWP, ARDP, AP, HTP and FRDP by 52%, 47%, 64% 185% and 38% respectively, in comparison with the on-grid PV plant, in which the connection to the grid was already available. Nevertheless, if these results are compared with the off-grid PV plant, all the impact categories experienced a reduction of between 73 and 77%, except for the HTP, which showed a decrease of 54%. Thus, the incorporation of the grid connection to the off-grid PV plant resulted in a substantial decrease in all the impact categories. Despite the additional materials and energy required for the cable and poles, this decrease was because the surplus of energy generated could be exported. In that way, the environmental burden was distributed to the total energy generation of the PV plant, so the impact was lower than the off-grid PV plant solution, for all the impact categories.

Table 4.2. Effects of adding the extension of the grid –cable and poles- to reach the grid in an isolated farm for the different impact categories.

	GWP	ARDP	AP	HTP	FRDP
Off-grid solar PV	121	$1.3 \cdot 10^{-3}$	$4.6 \cdot 10^{-1}$	72	1,509
Solar PV with existing grid connection	19	$2.1 \cdot 10^{-4}$	$7.3 \cdot 10^{-2}$	12	242
Solar PV with new grid connection*	29	$3.1 \cdot 10^{-4}$	$1.2 \cdot 10^{-1}$	33	336

* New grid connection includes additional 1 km of cable and poles.

** GWP (g CO2 eq. kWh^{-1}), ARDP (Sb eq. kWh^{-1}), AP (g SO_2 eq. kWh^{-1}), HTP (1.4-DCBe eq. kWh^{-1}), FRDP (kJ eq. kWh^{-1})

4.3.4.3. Effect of different energy prices

To evaluate the impact of the oscillation in the fuel and electricity costs, due to the difficulty in predicting their evolution, a range of different prices were evaluated. Thus, the LCC for the diesel engine option, with a range of prices between € 0.80 and € 1.30 per lite (l^{-1}) for the off-grid scenario, was recalculated. Similarly, a range of prices for electricity, between € 0.14 and € 0.24 per kilowatt hour (kWh^{-1}) were recalculated for the on-grid scenario. These values are shown in Table 4.3.

Table 4.3. Effect of fuel and electricity cost variation on the LCC for the solar PV plant.

Diesel Generator		**Electricity**	
Unit Cost (€ l^{-1})	Diesel generator (€)	Unit cost (€ kWh^{-1})	Grid electricity (€)
0.80	55,795	0.14	36,245
0.90	61,255	0.16	39,016
1.07	70,748	0.18	41,593
1.20	77,633	0.20	44,558
1.30	83,092	0.24	50,100

It can be noted that, despite the oscillation in the energy prices, for both, the traditional on-grid and off-grid options, the LCC determined was always higher than that estimated for the PV plant (€ 26,444). Although the probability of cheaper prices in the following years is not very high, these values were included to show a wider variety of possibilities, showing both diesel engine and grid electricity options, even for those, a higher LCC than the PV plant.

4.4. Conclusions

The PV technology is being widely integrated in the agriculture sector, as a cleaner and profitable alternative to traditional energy sources. This technology has no significant environmental impacts during its operational time, but the manufacturing process must be evaluated. Thus, in this work, the LCA of a PV irrigation system was analysed and compared with the most common energy supply options in the irrigation sector (diesel engine and grid electricity) for off-grid and on-grid scenarios. In that way, the PV option offered the lowest GWP burden, for both, on-grid and off-grid plants. For the rest of the impact categories, the PV plant showed the best option, except for the ARDP, in which the off-grid PV plant showed the highest value. Moreover, it should be noted that the off-grid PV plant impact per kWh was 6 times higher than the on-grid PV option, as the plant operates the whole year using part of the energy generated for irrigation and the excess energy could be exported.

Economically, the initial cost for the PV plant showed the highest value of the three options, although in the operation stage, both, the diesel generator and grid electricity option presented higher values. Consequently, the total cost for a 30 years lifespan showed the PV plant as the cheapest option, for all the diesel and grid electricity price range evaluated. Finally, the energy payback time for the PV plant was estimated in 0.5 and 3.1 years, when all its energy production was the required by the irrigation network, for on-grid and off-grid installations, respectively. The lifespan length sensitivity analysis showed that the PV plant gradually decreased its environmental burden from 5 to 30 years, due to the major impact was linked to the installation stage. Nevertheless, for the diesel generator and grid electricity option, the magnitude of the environmental impact per kWh did not experience significant

differences, due to most of the impacts being linked to the operational time. The evaluation of adding a grid connection to an isolated PV plant showed the possibility of using the remaining 80% of the energy generated by the PV plant. Thus, despite of the additional environmental impact of the cable and poles, the possibility of connecting the PV plant to the grid, for relatively close locations, allowed to reduce between 54 and 77% the environmental impact per kWh for the different categories. In a final overview, it can be noted that the characteristics of the irrigation installation can play an important role to determine the best option to satisfy the energy requirements from an environmental and economic point of view. So that, depending on the length of the lifespan of the project, as well as the availably of grid electricity connection, the possibility to sell the surplus of energy, and the annual energy requirements of the irrigation installation, the PV plant environmental burden and economic impact will show it convenience. For the case study analysed, it was demonstrated that the PV plant offers a lower environmental impact for most of the categories. Moreover, for a 30 years lifespan, it also showed the best option from an economic point of view, even if the surplus of energy cannot be sold.

4.5. References

Akinyele, D.O., Rayudu, R.K., Nair, N.K.C., 2017. Life cycle impact assessment of photovoltaic power generation from crystalline silicon-based solar modules in Nigeria. Renew. Energy 101, 537–549. doi:10.1016/j.renene.2016.09.017

Amante-García, B., Grimau, V.L., Casals, L.C., 2017. LCA of different energy sources for a water purification plant in Burkina Fasso. Desalin. Water Treat. 76, 375–381. doi:10.5004/dwt.2017.20462

Benton, K., Yang, X., Wang, Z., 2017. Life cycle energy assessment of a standby diesel generator set. J. Clean. Prod. 149, 265–274.

doi:10.1016/j.jclepro.2017.02.082

Berger, W., Simon, F.G., Weimann, K., Alsema, E.A., 2010. A novel approach for the recycling of thin film photovoltaic modules. Resour. Conserv. Recycl. 54, 711–718. doi:10.1016/j.resconrec.2009.12.001

Bhattacharjee, A., Mandal, D.K., Saha, H., 2017. Design of an optimized battery energy storage enabled Solar PV Pump for rural irrigation. 1st IEEE Int. Conf. Power Electron. Intell. Control Energy Syst. ICPEICES 2016 1–6. doi:10.1109/ICPEICES.2016.7853237

Carrillo-Cobo, M.T., Camacho-Poyato, E., Montesinos, P., Rodriguez-Diaz, J.A., 2014. Assessing the potential of solar energy in pressurized irrigation networks. The case of Bembézar MI irrigation district (Spain). Spanish J. Agric. Res. 12, 838–849. doi:10.5424/sjar/2014123-5327

Chatzisideris, M.D., Espinosa, N., Laurent, A., Krebs, F.C., 2016. Ecodesign perspectives of thin-film photovoltaic technologies: A review of life cycle assessment studies. Sol. Energy Mater. Sol. Cells 156, 2–10. doi:10.1016/j.solmat.2016.05.048

Chen, W., Hong, J., Yuan, X., Liu, J., 2016. Environmental impact assessment of monocrystalline silicon solar photovoltaic cell production: A case study in China. J. Clean. Prod. 112, 1025–1032. doi:10.1016/j.jclepro.2015.08.024

CML, 2010. Characterization Factors database available online from Institute of Environmental Sciences (CML).

Corominas, J., 2010. Agua y energía en el riego en la época de la sostenibilidad. Ing. del agua 17, 219–233.

Corona, B., Escudero, L., Quéméré, G., Luque-Heredia, I., San Miguel, G., 2017. Energy and environmental life cycle assessment of a high concentration

photovoltaic power plant in Morocco. Int. J. Life Cycle Assess. 22, 364–373. doi:10.1007/s11367-016-1157-y

De Wild-Scholten, M.J., 2013. Energy payback time and carbon footprint of commercial photovoltaic systems. Sol. Energy Mater. Sol. Cells 119, 296–305. doi:10.1016/j.solmat.2013.08.037

Desideri, U., Proietti, S., Zepparelli, F., Sdringola, P., Bini, S., 2012. Life Cycle Assessment of a ground-mounted 1778kWp photovoltaic plant and comparison with traditional energy production systems. Appl. Energy 97, 930–943. doi:10.1016/j.apenergy.2012.01.055

EC, 2017. 2020 climate & energy package. European Commission [WWW Document]. URL https://ec.europa.eu (accessed 10.2.17).

EC, 2015. Roadmap - Circular Economy - Closing the loop. European Commission.

Ecoinvent, 2014. In:SimaPro, a.v (Ed.). Ecoinvent Database Version 3.

Edoff, M., 2012. Thin film solar cells: Research in an industrial perspective. Ambio 41, 112–118. doi:10.1007/s13280-012-0265-6

EEA, 2015. Overview of electricity production and use in Europe. European Environment Agency 15.

Eurostat, 2017. Electricity price statistics [WWW Document]. Eurostat. URL http://ec.europa.eu/eurostat/statistics-explained/index.php/Electricity_price_statistics (accessed 3.27.18).

Evans, A., Strezov, V., Evans, T.J., 2009. Assessment of sustainability indicators for renewable energy technologies. Renew. Sustain. Energy Rev. 13, 1082–1088. doi:10.1016/j.rser.2008.03.008

FAO, 2016. Climate change and food security: Risks and responses.

Fthenakis, V., Alsema, E., 2006. Photovoltaics Energy Payback Times, Greenhouse

Gas Emissions and External Costs: 2004–early 2005 Status. Prog. Photovolt Res. Appl. 14, 275–280. doi:10.1002/pip

Fu, Y., Liu, X., Yuan, Z., 2015. Life-cycle assessment of multi-crystalline photovoltaic (PV) systems in China. J. Clean. Prod. 86, 180–190. doi:10.1016/j.jclepro.2014.07.057

Gallagher, J., Basu, B., Browne, M., Kenna, A., McCormack, S., Pilla, F., Styles, D., 2017. Adapting Stand-Alone Renewable Energy Technologies for the Circular Economy through Eco-Design and Recycling 0, 1–8. doi:10.1111/jiec.12703

Gallagher, J., Styles, D., McNabola, A., Williams, A.P., 2015. Life cycle environmental balance and greenhouse gas mitigation potential of micro-hydropower energy recovery in the water industry. J. Clean. Prod. 99, 152–159. doi:10.1016/j.jclepro.2015.03.011

Gerbinet, S., Belboom, S., Léonard, A., 2014. Life Cycle Analysis (LCA) of photovoltaic panels: A review. Renew. Sustain. Energy Rev. 38, 747–753. doi:10.1016/j.rser.2014.07.043

Goedkoop, M., Oele, M., de Schryver, A., Vieira, M., 2008. SimaPro Database Manual - Methods Library. Pré Consultants, The Netherlands.

IDAE, 2017. Informe precios energéticos regulados [WWW Document]. URL http://www.idae.es/ (accessed 1.15.18).

IEA, 2016. World Energy Outlook. Int. Energy Agency. Fr.

IEA, 2011. Methodology Guidelines on Life Cycle Assessment of Photovoltaic Electricity. Int. Energy Agency. Photovolt. power Syst. Program.

Irvine, S.J.C., Rowlands-Jones, R.L., 2016. Potential for further reduction in the embodied carbon in PV solar energy systems. IET Renew. Power Gener. 10, 428–433. doi:10.1049/iet-rpg.2015.0374

ISO, 2006. ISO 14040: Environmental Management e Life Cycle Assessment e Principles and Framework. ISO, Geneva.

Jiang, Q., Liu, Z., Li, T., Zhang, H., Iqbal, A., 2014. Life cycle assessment of a diesel engine based on an integrated hybrid inventory analysis model. Procedia CIRP 15, 496–501. doi:10.1016/j.procir.2014.06.091

Kim, H.C., Fthenakis, V., Choi, J.K., Turney, D.E., 2012. Life Cycle Greenhouse Gas Emissions of Thin-film Photovoltaic Electricity Generation: Systematic Review and Harmonization. J. Ind. Ecol. 16. doi:10.1111/j.1530-9290.2011.00423.x

Kittner, N., Gheewala, S.H., Kamens, R.M., 2013. An environmental life cycle comparison of single-crystalline and amorphous-silicon thin-film photovoltaic systems in Thailand. Energy Sustain. Dev. 17, 605–614. doi:10.1016/j.esd.2013.09.003

Knapp, K., Jester, T., 2001. Empirical investigation of the energy payback time for photovoltaic modules. Sol. Energy 71, 165–172. doi:10.1016/S0038-092X(01)00033-0

López-Luque, R., Reca, J., Martínez, J., 2015. Optimal design of a standalone direct pumping photovoltaic system for deficit irrigation of olive orchards. Appl. Energy 149, 13–23. doi:10.1016/j.apenergy.2015.03.107

Lunardi, M.M., Moore, S., Alvarez-Gaitan, J.P., Yan, C., Hao, X., Corkish, R., 2018. A comparative life cycle assessment of chalcogenide/Si tandem solar modules. Energy 145, 700–709. doi:10.1016/j.energy.2017.12.130

Luo, W., Khoo, Y.S., Kumar, A., Low, J.S.C., Li, Y., Tan, Y.S., Wang, Y., Aberle, A.G., Ramakrishna, S., 2018. A comparative life-cycle assessment of photovoltaic electricity generation in Singapore by multicrystalline silicon technologies. Sol. Energy Mater. Sol. Cells 174, 157–162. doi:10.1016/j.solmat.2017.08.040

MAPAMA, 2017. Actuaciones de reducción de emisiones [WWW Document]. URL http://www.mapama.gob.es (accessed 10.2.17).

Mérida García, A., Fernández García, I., Camacho Poyato, E., Montesinos Barrios, P., Rodríguez Díaz, J.A., 2018. Coupling irrigation scheduling with solar energy production in a smart irrigation management system. J. Clean. Prod. 175, 670–682. doi:10.1016/j.jclepro.2017.12.093

MINETAD, 2017a. Precios medios nacionales de carburantes y componentes energéticos del IPC [WWW Document]. URL http://www.minetad.gob.es (accessed 11.17.17).

MINETAD, 2017b. Precio neto de la electricidad para uso doméstico y uso industrial [WWW Document]. URL http://www.minetad.gob.es (accessed 11.17.17).

Ouachani, I., Rabhi, A., Yahyaoui, I., Tidhaf, B., Tadeo, T.F., 2017. Renewable Energy Management Algorithm for a Water Pumping System. Energy Procedia 111, 1030–1039. doi:10.1016/j.egypro.2017.03.266

Peng, J., Lu, L., Yang, H., 2013. Review on life cycle assessment of energy payback and greenhouse gas emission of solar photovoltaic systems. Renew. Sustain. Energy Rev. 19, 255–274. doi:10.1016/j.rser.2012.11.035

Reca, J., Torrente, C., López-Luque, R., Martínez, J., 2016. Feasibility analysis of a standalone direct pumping photovoltaic system for irrigation in Mediterranean greenhouses. Renew. Energy 85, 1143–1154. doi:10.1016/j.renene.2015.07.056

REE, 2016. Estructura de Generación de Energía Anual Nacional. Red Eléctrica España.

Smith, C., Burrows, J., Scheier, E., Young, A., Smith, J., Young, T., Gheewala, S.H., 2015. Comparative Life Cycle Assessment of a Thai Island's diesel/PV/wind

hybrid microgrid. Renew. Energy 80, 85–100. doi:10.1016/j.renene.2015.01.003

Sumper, A., Robledo-García, M., Villafáfila-Robles, R., Bergas-Jané, J., Andrés-Peiró, J., 2011. Life-cycle assessment of a photovoltaic system in Catalonia (Spain). Renew. Sustain. Energy Rev. 15, 3888–3896. doi:10.1016/j.rser.2011.07.023

Wetzel, T., Borchers, S., 2015. Update of energy payback time and greenhouse gas emissions data for crystalline silicon photovoltaic modules. Prog. photovoltaics Res. Appl. 23, 1429–1435.

Wu, B., Maleki, A., Pourfayaz, F., Rosen, M.A., 2018. Optimal design of stand-alone reverse osmosis desalination driven by a photovoltaic and diesel generator hybrid system. Sol. Energy 163, 91–103. doi:10.1016/j.solener.2018.01.016

Yahyaoui, I., Tadeo, F., Segatto, M.V., 2016. Energy and water management for drip-irrigation of tomatoes in a semi- arid district. Agric. Water Manag. 183, 4–15. doi:10.1016/j.agwat.2016.08.003

4.6. Supplementary information

Table S.4.6.1. Raw material and processes included in the LCA of the different energy sources examined for the irrigation network.

Material / Process	Scenario 1		Scenario 2	
	Off-grid Solar PV	Diesel Generator	On-grid Solar PV	Grid Electricity**
Solar glass	●		●	
Metals	●	●	●	
Plastic & rubber	●	●	●	
Silicon	●		●	
Diesel		●		
Manufacturing	●	●	●	
Transport	●	●	●	
Installation	●		●	
Grid Electricity				●*

*The analysis of the grid electricity was based on the information about its generation structure (REE, 2016) (Hydraulics 16.2%, wind 21.6%, photovoltaic 3.6%, nuclear 25.4%, coal 17%, fuel + gas 3%, combined cycle 13.2%).

**It considered the embodied and operational burdens associated to each electricity contributor (renewable and non-renewable).

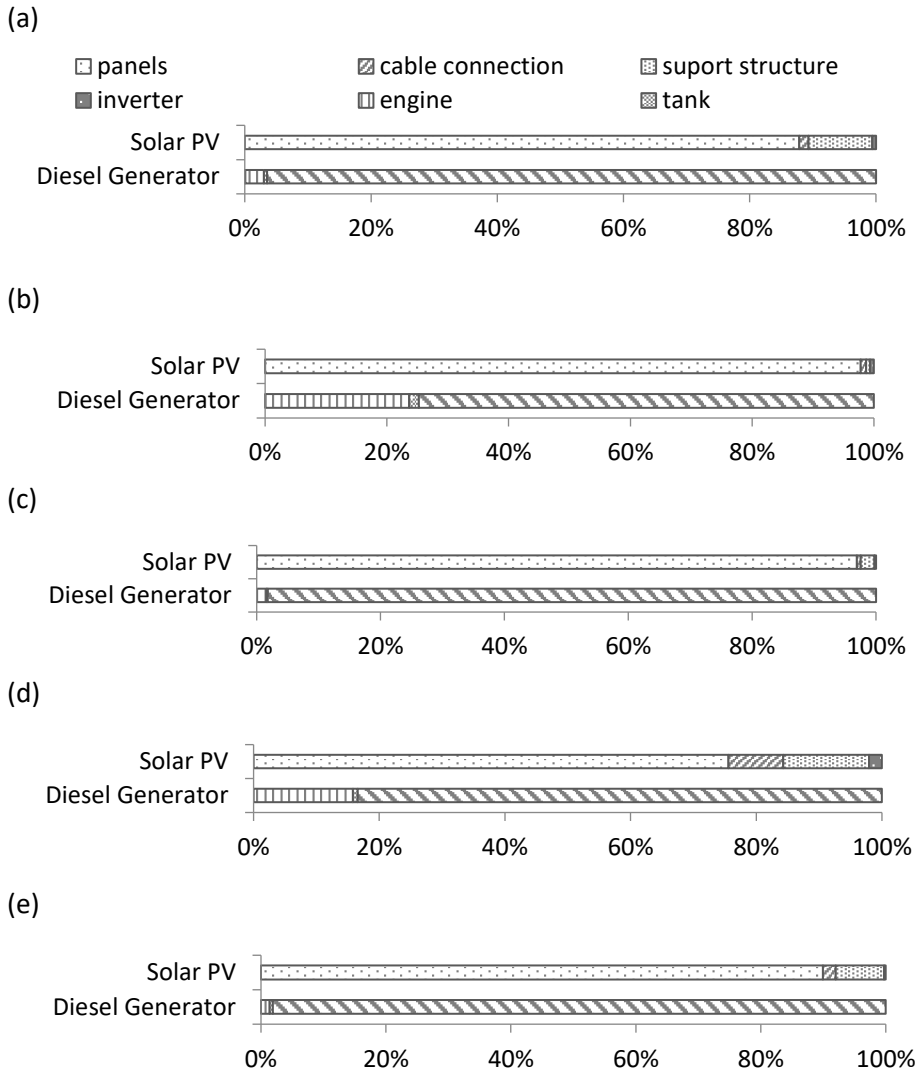

Fig. S.4.6.1. Percentage contribution of components in Scenarios 1 and 2, comparing the solar PV and diesel generator, for the five impact categories examined: (a) GWP, (b) ARDP, (c) AP (d) HTP and (e) FRDP burdens.

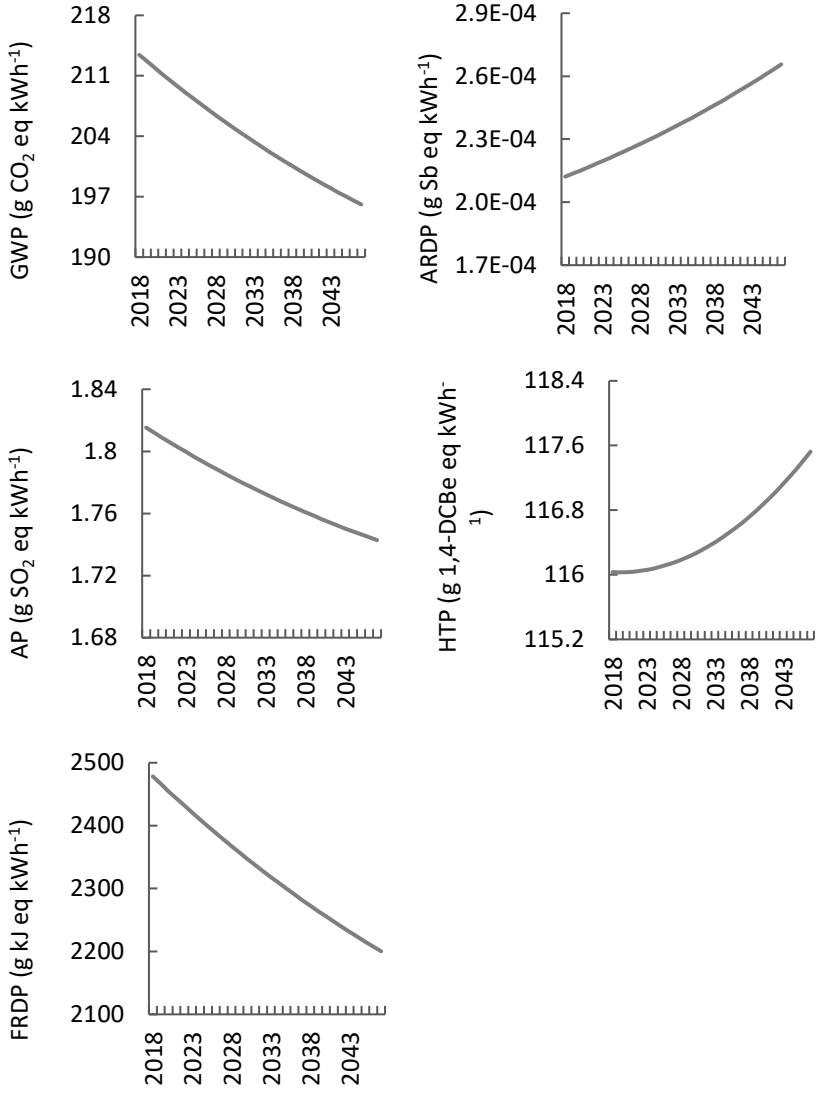

Fig. S.4.6.2. Dynamic environmental impact of the grid electricity for each of the five impact categories investigated, which is based on increased renewable energy contributions to the grid over the next 30-years.

5. Comprehensive sizing methodology of smart photovoltaic irrigation systems

This chapter has been published entirely in the journal "Agricultural Water Management", A. Mérida García, R. González Perea, E. Camacho Poyato, P. Montesinos Barrios, J.A. Rodríguez Díaz (2020)

Abstract. The use of photovoltaic (PV) energy in irrigation is increasing its relevance as energy source in irrigated agriculture. The main reason relays on its economic and environmental benefits, compared to traditional options. To reduce economic, materials and energy requirements of PV irrigation systems, its design and dimensioning should be optimal. In this work, we developed the model MOPISS (Model for Optimal Photovoltaic Irrigation System Sizing) focussed on the selection of pipe diameters and PV plant dimensioning, optimizing jointly the investment cost and operation of the system. MOPISS, developed in MATLAB™, integrated a customized version of the Non-dominated Sorting Genetic Algorithm (NSGA-II) with two objective functions, aimed at searching the optimal sizing of the irrigation network and PV plant. The results showed a series of solutions with optimal hydrants grouping in sectors, pipe diameters and PV plant size. MOPISS was applied to a real case study obtaining solutions which satisfied 96% of the irrigation requirements while saved cost between 22.9 and 38.2% over the total investment cost, compared with the original design. MOPISS is a useful tool to produce optimal designs of sizing new PV irrigation system under a comprehensive approach that considers crop, water and energy availability and network layout.

Keywords: MOPISS, photovoltaic irrigation, optimization, pipe diameters dimensioning, PV peak power, NSGAII, genetic algorithm

5.1. Introduction

Nowadays, the remarkable increase in energy consumption and the general concern about global warming has promoted the use of renewable energies in the irrigation agriculture sector. Related to this, photovoltaic (PV) technology offers a more sustainable alternative for the energy supply compared to traditional options, such as diesel generators and grid electricity (GIZ, 2016). This technology has a lower environmental burden due to the virtually zero environmental impacts associated to its operation (Mérida García et al., 2019). Furthermore, the period with the highest PV energy production usually coincides with the irrigation season for a wide variety of crops. Nevertheless, as the energy production levels rely on the instant irradiation (López-Luque et al., 2015) that is affected by the occurrence of clouds, the management of an irrigation network just powered by PV energy results much more complex. Thus, the variable power availability must be properly managed to fully satisfy the daily irrigation requirements of the different sectors of a network. For the optimal dimensioning of the PV irrigation system it should be considered the variability of the solar radiation throughout the irrigation season and during the day. Moreover, the hydrants location and the layout of the irrigation network determine the power demand of each sector of the irrigation network, conditioning the pumping power and the size of the PV plant. For that reason, the sizes of the pipes of the irrigation network and the size of the PV plant should be determined jointly.

The search for optimal design solutions in the water distribution network sector has been widely studied by numerous authors. Tayfur (2017) summarized the

main characteristics of the most popular optimization methods used in water resources planning, engineering and management. Among them, the Genetic Algorithms (GA), Ant Colony (AC), Differential Evolution (DE), Particle Swarm (PS), Harmony Search (HS), Genetic Programming (GP) and Genetic Programming Expression (GPE) can be highlighted. Creaco and Franchini (2014) presented a procedure to find optimal solutions in the cost-reliability space for multi-objective design of looped water distribution systems. This work pointed out the computational and numerical efficiency of low-level hybrid optimization procedures for multi-objective water network design. Most recently, Fernández García et al. (2017) presented an optimization methodology for the design and operational costs of pressurized irrigation networks, using the NGSA-II algorithm. Lapo et al. (2017) combined linear programming (LP) and GA in a hybrid model to optimize the pipe design, operating pressure at the head of the network, total investment cost and working shifts assigned to each hydrant. All these works focussed on the optimal design of the irrigation network, while none of them questions the availability and characteristics of the energy source. On the other hand, related to the adoption of PV technology in the irrigation sector, several works focused on the development of optimal sizing methods. The aim of these works was to determine the optimal peak power for the PV plant to satisfy crop irrigation requirements using the existing irrigation network (Bakelli et al., 2011; López-Luque et al., 2015). In order to reduce the dependence on climate factors, other works also focused on the optimal management of installations which incorporated some water/energy storage elements, as well as auxiliary support systems (e.g. diesel generator). In that way, Wissem et al. (2012), Reges et al. (2016) and Yahyaoui et al. (2016), studied the inclusion of batteries in the system. Later, Rodríguez-Gallegos et al. (2017) studied

the combination of the PV modules with both, a battery and a diesel generator. This PV-battery-diesel combination allowed reducing the overall system cost and control of the grid voltage, based on PS methods. In a similar way, the hybridization of the PV plant with other renewable energy supply systems, as wind or water turbines, was also evaluated by Ouachani et al. (2017); and Ramli et al. (2018). Another common application of PV technology in irrigation is the use of an intermediate water storage tank. This tank is located at a higher level to feed the irrigation system by gravity (Olcan, 2015; Kabalci et al., 2016; Ghavidel et al., 2016; Muhsen et al., 2018). This option is possible for relatively small plots, with a suitable height difference. These actions generally offer more flexibility to the system operation but have higher economic and, in some cases, higher environmental cost, due to material requirements. Nevertheless, Mérida García et al. (2018) proved that some crops, as olive orchard in Southern Spain, could be irrigated with a PV plant by a direct injection irrigation system, without storage elements. This was possible using a real time synchronization model, which searched for the best fit between the power production and irrigation requirements. Even so, most of the operating solar PV plants were designed to power existing irrigation systems that previously were powered by the grid. Thus, the design of these irrigation systems (pumps, pipes and irrigation sectoring) was developed to use the grid power and not the power from a solar energy source. Moreover, nowadays, the price of the PV technology is dropping and fostering the transformation of rain-fed farms to irrigated lands, allowing the use of pressurized irrigation in isolated areas.

In this context, the objective of this work was to develop a methodology for the optimal sizing of the hydraulic network and the PV plant of an irrigation system with smart management, from a techno-economic point of view. Thus, the sizing

process considers both hydraulic and energy criteria, in a comprehensive model, developed in MATLAB^{TB} (Pratap, 2010). The search of optimal solutions, based on economical and operational criteria, was carried out using a customized version of the Non-dominated Sorting Genetic Algorithm (NSGA-II) (Deb et al., 2002). This model includes a modified version of SPIM (Mérida García et al., 2018), a smart photovoltaic irrigation manager to operate PV irrigation systems. Therefore, the novelty of this work relies on the joint sizing of the network pipes and the PV plant, so the irrigation system will work using efficiently the available water and solar energy. Finally, the developed model was applied to a real case study, placed in South Spain, comparing the original and optimized design solutions.

5.2. Methodology

5.2.1. Case study

The case study is an experimental PV irrigation system that waters a 13.4-ha olive orchard in the University of Córdoba (South Spain). The trial plot is divided into different subplots according to the olive tree variety and water allocation (ranging from 1000 to 2000 m^3ha^{-1}), conditioning the layout of the irrigation network (Figure 5.1). The irrigation system is composed of a 13-hydrants irrigation network grouped in 3 sectors, a submergible pump, directly powered by a PV plant, an inverter and the control system. The material of pipes was polyethylene (PE). The pump was located 1.35 km away from the irrigated field. The irrigation network was originally designed for conventional energy supply and the PV plant was installed afterwards, not considering simultaneously the joint design of the irrigation system and the PV plant. The total installation cost was € 80,309.

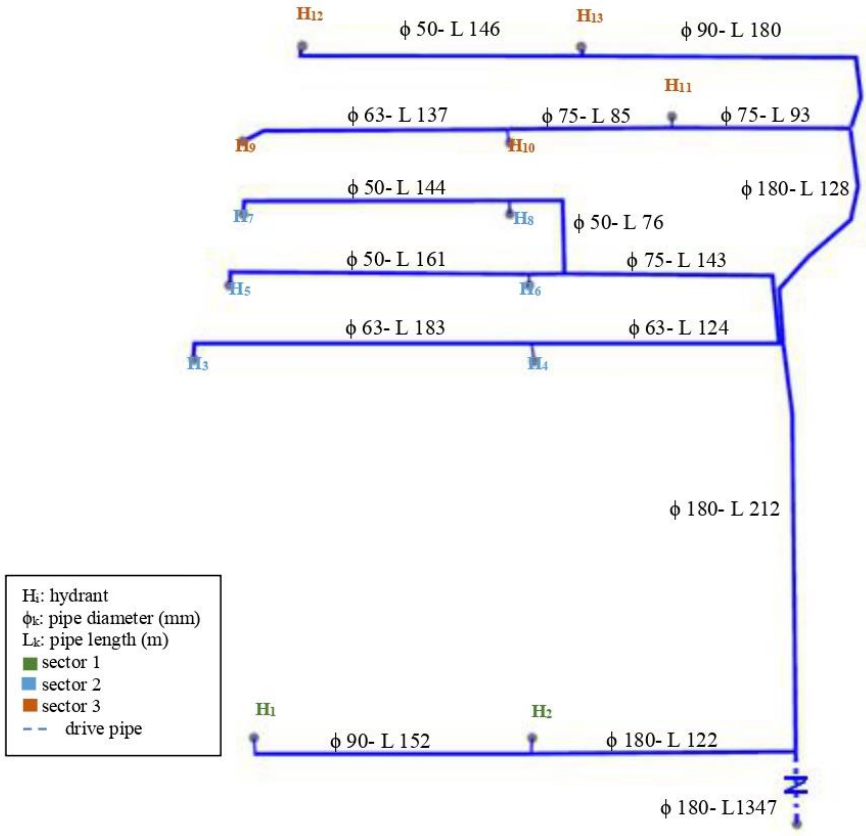

Fig. 5.1. Layout of the PV irrigation system of the University of Córdoba

5.2.2. Problem definition

The objective of this work was to develop a procedure to determine the diameters of the network pipes and the required PV peak power (PVPP) to minimize the investment cost of a PV irrigation system, ensuring its proper operation. The developed methodology was integrated in the algorithm MOPISS (Model for Optimal Photovoltaic Irrigation System Sizing). The model assumes the crop distribution on

the field as an initial constraint that conditions hydrants locations and the layout of the irrigation network that will not be modified through the optimization process. Moreover, hydrants operation is controled by individual electrovalves that could be operated remotely.

The problem was defined as a multi-objective optimization issue, with two objective functions OF1 and OF2. These functions quantify the investment and operational cost of the irrigation system, including the hydraulic network and the PV plant. The use of PV energy does not entail operating cost and its maintenance cost are very small. For this reason, operation and maintenance cost have not been included in the problem statement. The first objective function (OF1) focused on the minimization of the investment cost of the irrigation system (pipes and pumps) (Eq. 5.1):

$$OF1 = \left[\sum_{p=1}^{p=n}(PC_{\emptyset} \cdot L_p) + C_p\right]_{norm} \quad (5.1)$$

where PC_{φ} is the unit cost of the commercial pipe diameters, L_p is the total length of each pipe type included in the network and C_p represents the pumping system cost, based on commercial information. This last cost was included after the pump power selection, defined after the sectors power demand calculation. OF1 values were then normalized, between 0 to 1, in order to be comparable with OF2 values.

The second objective function (OF2) evaluated the PV plant cost and its capacity to provide enough energy to the irrigation network (Eq. 2):

$$OF2 = \rho \cdot [PVPP \cdot UC]_{norm} + \omega\left[\frac{\sum_{s=1}^{s=S}\sum_{d=1}^{d=IS}(RWV_{s,d} - AWV_{s,d})}{\sum_{s=1}^{s=S} WA}\right]_{norm} + \gamma\left[\frac{S_{pv}}{S_c} \cdot 100\right]_{norm} \quad (5.2)$$

In that way, the first term of OF2 quantified the PV plant cost as the product between the PVPP (expressed in W) and a unit cost (UC), expressed in € per W of peak power. The PVPP depends on the system operation, and it is then traduced into the required number of PV modules and inverter dimensioning. To reduce its value, the network will be operated by sectors. The maximal number of operating sectors, S, will be described later. Thus, PVPP was estimated as a function of the sectors power demand, previously determined for each sectoring network alternative. This estimation was carried out using the hydraulic simulator Epanet (Rossman, 2000), evaluating the pressure requirements for the most restrictive hydrant in each sector. The UC included the cost associated to the modules, the wiring, the inverter and the installation of all the elements of the PV plant. The second term evaluated the pumping capacity of the PV plant during the irrigation season (being IS its duration in days) to satisfy the irrigation requirements. This capacity is expressed as the ratio between the sum of the required and the applied water volumes difference (RWV and AWV, respectively) throughout the irrigation season and the total water allocation assigned to the sectors. All these values are expressed in m^3. This evaluation was carried out using SPIM (Smart Photovoltaic Irrigation Manager) (Mérida García et al., 2018). SPIM defined the daily operation sequence of the network sectors according to their power demand, daily crop irrigation requirements and the instant radiation levels. Thus, at the end of the irrigation season, the model provides the total water volume applied to each sector and compares it with their water allocations. Finally, the third term of the equation represents the ratio between the PV modules surface (S_{pv}) and the cultivated area (S_c). The value of OF2 was then also normalized, weighting each term with ρ, ω and γ coefficients. These weighting factors allowed the study of the influence of each term in the selection of the best

solutions. The model can be easily adapted to the specific characteristics of each project and user preferences.

5.2.3. Hydrants sectoring

As hydrants can operate independently, the maximal number of groups of hydrants that can work simultaneously, number of sectors, S, must be calculated before starting the optimization process. This figure depends on the available daily solar peak hours, for a specific location, and the daily average irrigation time for a specific crop (Eq. 5.3):

$$S = \left[\frac{\sum_{d=1}^{Dm} SPH_d \, / Dm}{\frac{WA/CD}{ID} / DF \cdot NE} \cdot 10^{-3} \right]_{min} \tag{5.3}$$

were SPH is the solar peak hours for day d, expressed as $h \cdot day^{-1}$; D is the total days for month m; WA is the monthly water allocation, in $m^3 ha^{-1}$; CD is the crop density, expressed as $plants \cdot ha^{-1}$; ID represents the irrigation days of the month; DF is the emitter flow rate, in $l \cdot h^{-1}$; NE represents the number of emitters per plant and 10^{-3} an unit conversion factor.

The SPH, which represents the daily number of hours with irradiance over 1 kWm^{-2}, was obtained as an average of historical irradiation records of agroclimatic stations. These solar peak hours determine the total hours in which the PV plant power production is equal or over its set peak power. Moreover, the average daily irrigation time was estimated considering the water allocation assigned to each sector, the irrigation scheduling strategy, the emitter flow (drip irrigation, in the case study), crop density, the number of emitters per plant and the total irrigation days per month. Once the daily available hours with enough irradiance and the average

irrigation time were evaluated for each month, the most restrictive results defined S value.

Once S value was defined, hydrants, with its respective flow demand, were randomly assigned to each sector to stablish the different network operation configurations, represented in each chromosome.

5.2.4. Multi-Objective Solution Algorithm

The search procedure of optimal irrigation network and PV plant was based on the multi-objective genetic algorithm NSGA-II. The NSGA-II generates a series of chromosomes (population of possible problem solutions). The fitness of these solutions (combination of possible network sectoring, pipe diameters and PV plant size) is evaluated by the objective functions, OF. Once the initial population is generated, as will be described in section “Initial population”, and evaluated, chromosomes are sorted based on the OF values, and those with highest fitness are selected to be combined by the crossover genetic operator or to be muted by the mutation operator (Deb et al., 2002) aimed at expanding the solutions search space. This process is repeated until the model complete the pre-fixed generations (gen). The last generation presents a set of possible optimal solutions, that minimize the OF values constituting the Pareto front (Deb et al., 2002). In this work, a customized version of the NSGA-II algorithm was applied to minimize OF1 and OF2, which flow chart is shown in Fig. 5.2. The modifications made on the genetic operators are detailed below.

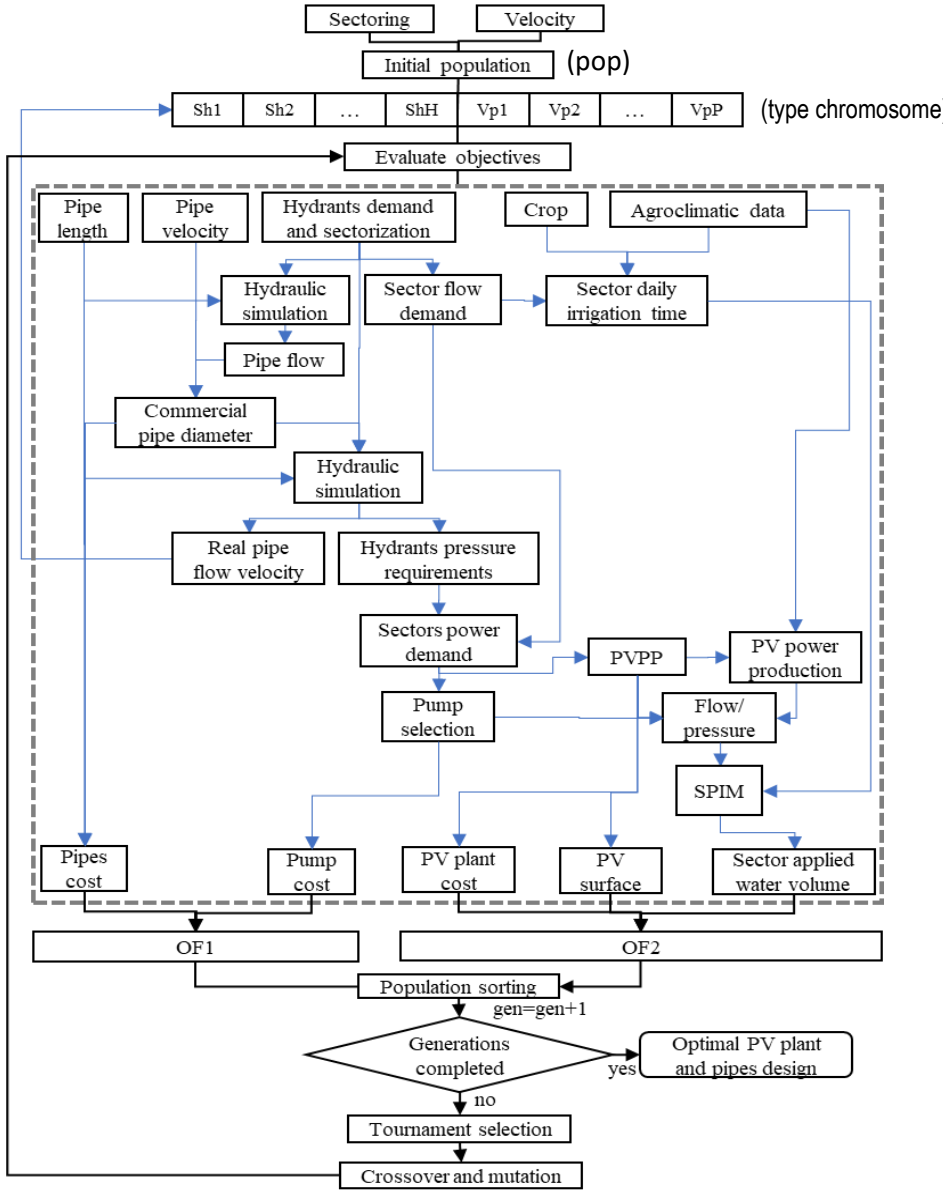

Fig. 5.2. Flow chart for MOPISS algorithm.

5.2.4.1. Initial population:

The initial population was integrated by a set of chromosomes (pop) with v variables, which value was randomly assigned responding to specific ranges, which must be previously defined. The number of variables v was H+P, the sum of the number of hydrants and pipes, respectively, that composed the network, represented in a type chromosome in Fig. 5.2. The value of the first H variables represents the sector of each hydrant (S_{h_H}), ranging from 1 to S. On the other hand, the following P variables corresponded to each pipe flow velocity in the network (V_{p_P}). In this case, the pipe velocity values were randomly assigned between a maximum (V_{max}) and minimum (V_{min}) velocity rates, which must be defined beforehand. These V_{max} and V_{min} are stablished according to the desired operating conditions in the water distribution network for each particular case, based on its size. Then, these velocity values are adjusted in the chromosome in the optimization process described below. The first H variables are discrete variables and the remaining P variables are continuous ones.

5.2.4.2. Evaluation of the objective functions:

The value for the previously detailed OF1 and OF2 were calculated for each chromosome. A first simulation of the network, including hydrants grouping in sectors, fixed in the chromosome, and hydrants flow, provided pipes flow rates. Pipes velocity, also fixed in the chromosome, and pipe flow rates data determined pipe diameters. These diameters were then adapted to the closest commercial ones, ensuring a logical progression. These logical progression entails that larger diameters are located closer to the pumping station while consecutive pipes must have equal or smaller diameters. After this adjustment, the irrigation network was

again simulated. This hydraulic analysis provided the real velocity rates for each pipe and nodes pressures, after the diameters adjustment. The chromosome is then updated, with the real velocity rates. The main steps of this process are represented in Fig. 5.3. Based on nodes pressure data, the sectors power demand is determined, as a function of the most pressure demanding hydrant in each sector. The sectors' power demand was used in the calculation of OF1 (pump selection) and OF2, for PVPP calculation, operation of the PV plant during the irrigation season and size of the photovoltaic panels surface area. The PVPP was calculated based on the most power demanding sector of each chromosome, considering the corresponding engine and inverter efficiencies.

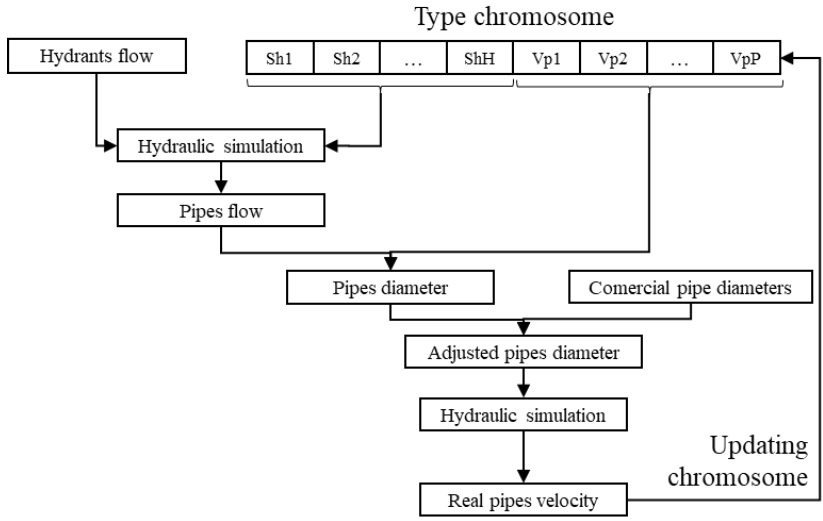

Fig. 5.3. Schematic representation of the process for pipes diameter sizing and real pipes velocity determination.

For the calculation of the second term of OF2, the daily irrigation requirements of the crop were previously estimated, based on the difference between the effective

precipitation and crop evapotranspiration. Finally, the daily crop irrigation requirements were calculated for each irrigation sector, based on the hydrants organization, as well as the sectors' water allocation.

5.2.4.3. Modified genetic operators

The genetic operators, crossover and mutation, of the NSGA-II were modified in order to ensure the generation of new child solutions different from parent solutions, keeping discrete and continuous variables in the right positions in the chromosomes. A specific coefficient determines the probability of being applied crossover/mutation processes over the set of parent chromosomes. Thus, for crossover operator, a two-point crossover procedure was applied to each pair of parents, randomly selected. Crossover points were also randomly chosen, one in each section of the chromosome (corresponding to hydrants and pipes) (Fig. 5.4):

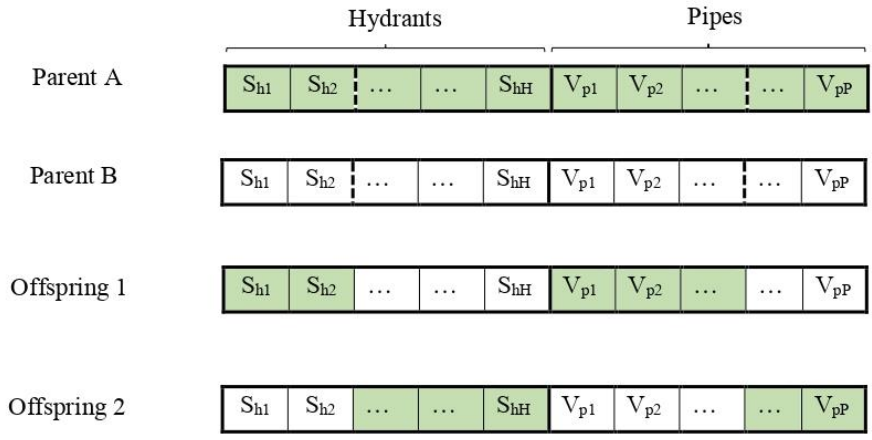

Fig. 5.4. Schematic representation of the two-point crossover operator.

The mutation process was applied to a randomly selected parent, acting over a small portion of its variables, which position was randomly selected. Once the mutation positions were chosen, a new random value for the corresponding variable was assigned within the stablished ranges.

5.3. Results and Discussion

The developed methodology was applied to optimize the irrigation network and PV plant sizing for the case study irrigation system. In the current design of the network, hydrants are grouped according to their location: hydrants 1 and 2 in sector 1 (S1), hydrants 3 to 8 in sector 2 (S2), while sector 3 (S3) was composed by the 5 remaining hydrants (9 to 13). Thus, the sectors power and flow requirements were 7.07, 6.77 and 13.35 kW and 9.67, 9.60 and 12.40 ls^{-1}, for S1, S2 and S3, respectively. The pump power was 15 kW, so the dimension of the PV plant was 17.7 kW. The optimization of pipes size, based on diameter selection, must consider the material of pipes. The selected material for this irrigation network was polyethylene (PE). Thus, commercial diameters, roughness and pipe thickness were selected according to the material and specific characteristics of the network. Finally, precipitation and reference evapotranspiration, for crop irrigation needs calculation, as well as irradiance data, for the evaluation of the PV system, of an average year were used to perform the simulation of the case study irrigation system. Moreover, in the crop irrigation needs calculations, the irrigation scheduling strategy, which in the case study was focussed on a controlled deficit irrigation, was also considered.

5.3.1. Sectoring alternatives.

The estimation of the possible maximum number of sectors (S) that permits the satisfaction of the daily irrigation requirements was 3 in June, the most restrictive month for the case study analised. The average total solar peak hours were 6.75 h per day, and the average daily irrigation time was 2.08 h perday. The S value was fixed for the subsequent network designing process, matching the current number of network sectors in the case study. Thus the 13 hydrants, with their corresponding flow demand and elevation, were randomly grouped into 1 to 3 sectors in each chromsome of the initial population. Nevertheless, after the optimization process all solutions in the Pareto front had their hydrants grouped in 3 sectors.

5.3.2. Optimization process

The optimal sizing of the irrigation network and PV plant for the case study was performed with a population size of 200 individuals (pop) and 100 generations (gen), as no significative changes were observed for a larger number of generations. Moreover, crossover and mutation probabilities were fixed at 90% and 10%, respectively. Each chromosome was conformed by 60 decision variables corresponding to the 13 hydrants (H) and 47 pipes (P) of the case study irrigation network. The first 13 variables, which possible values ranged between 1 to 3 (maximum number of sectors), defined hydrants organization in sectors. On the other hand, the remaining 47 variables were the flow velocities of each pipe of the network. The flow velocity ranged between 0.5 and 1.85 ms^{-1}, following the process of generation of the initial population, described in section “Initial population”. Then, pipe diameters, calculated from velocity values, were aproximated to the closest commercial diameters among a set of 22 possibilities, ranging from 32 to 630 mm

(28 to 555.2 mm of internal diameter). Then, the network was simulated, using the software Epanet (Rossman, 2000). Once the real flow velocity rates for pipes after the diameters adjustement were obtained, the chromosome information updated. The simulation also provided the sectors power requirements and PVPP, considering engine and inverter efficiencies of 0.8 and 0.95, respectively. The values of OF1 and OF2 per chromosome were normalized, ranging between 0 to 1, to allow their comparison.

Two scenarios for OF2 were analysed: 80-10-10% and 45-10-45%, for ρ, ω and γ weighting coefficients, respectively. In both scenarios ω gives a small weight to the no satisfaction of the required irrigation depths. This was decided after testing that the synchronization model always achieved good results for the satisfaction of the irrigation needs of the case study analized, as the sectors power demand was managed properly. Scenario 1 gave the largest weight to the first term, referring to the economic cost of the irrigation system, while Scenario 2 distributed the highest weights between the economic term and the one related to the photovoltaic surface.

After the optimization process, the evolution of OF1 and OF2 values in each generation is shown in Fig. 5.5. Thus, it can be noted that depending on the weighting coefficients values, the evolution of the minimum values of both OF were slightly different. The most significative reduction was shown in the first 10 generations for both OF. Then, only small reductions were appreciated in OF1 and OF2 up to generations 18 and 41, and 66 and 58, for scenarios 1 and 2, respectively. These figures show a fast stabilization of the minimum values and consequently, the achivement of optimal results. It was due to the boundary conditions stablished to manage the individuals generation, as the flow velocity in pipes, which were

generated within an adequate range, or the control in the distribution of diameters in the network, eliminating unlogical solutions.

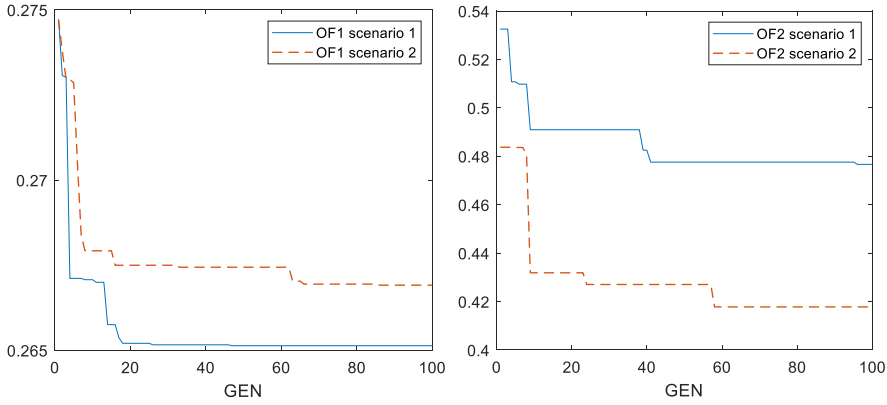

Fig. 5.5. Evolution of OF1 (left) and OF2 (right) throughout 100 generations for scenario 1 and 2.

On the other hand, the Pareto front for the last generation showed a series of possible optimal solutions, represented in Fig. 5.6 for both scenarios. In this particular optimization problem, a balance between the minimization of the two OF was essential, in order to achieve a solution with the lowest total cost of the system. Nevertheless, all solutions presented realistic designs from an hydraulic point of view because in the previous diameter selection the extreme values were avoided by constraining the pipe flow velocity within a fixed range. Thus, the OF results ranged from 0.27 to 0.32 and 0.27 to 0.37 for OF1 in scenario 1 and 2, respectively, while for OF2, these values ranged from 0.48 to 0.92 and 0.42 to 0.84 for scenario 1 and 2, respectively. In economical terms, these results corresponded to total costs values ranging between € 49,154 and € 61,402 for scenario 1, while solutions in scenario 2 showed a total investment cost between € 48,955 and € 58,917. All solutions had

total costs under the cost of the original installation, (€ 80,309) as it is shown in Table 5.1, which OF values were 0.60 for OF1 and 0.53-0.48 for OF2 in scenario 1 and 2, respectively.

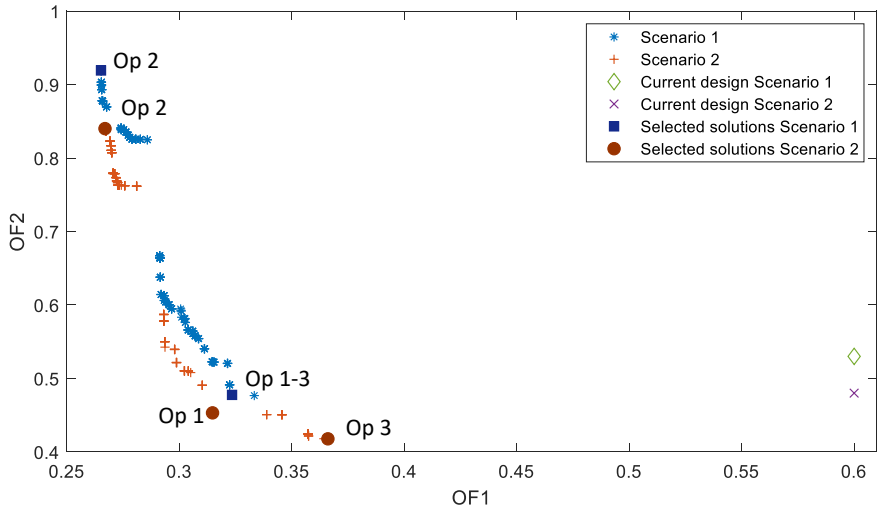

Fig. 5.6. Pareto front for OF1 and OF2 for generation 100

Table 5.1 shows the total/ irrigation network/ PV plant lowest cost option (Op1, Op2 and Op3 respectively), obtained for both OF2 scenarios desagregated into the total investments cost, the irrigation system cost and the PV plant cost. It must be highlighted that the propossed optimal sizings presented a cost reduction between 23.5% to 39.1% in relation to the investment cost of the current system. A fraction of this reduction was due to the drop in the investment cost of the irrigation network, which oscillated between 38.9% and 55.9%. Nevertheless, depending on the selected solution and its OF values, both the hydraulic and/or PV components of the investment cost, was a cheaper solution than the original design. This fact can be observed in Op 2, for both scenarios. In these cases, the total cost was lower than

the original one due to a significative decrease in the irrigation network cost. The reduction in pipes diameter size reduced the investment cost, although involved higher power demands and, consequently, a larger PV plant, which increased its cost by a 100% and 83.9% for scenario 1 and 2, respectively. Even then, the irrigation network was significlantly cheaper than the current irrigation system. On the other hand, the most economical PV plant, represented by Op 3, showed an investment cost of € 14,835 and € 14,227 for scenario 1 and 2, which supossed 10.9% and 14.6% cost reductions.

Table 5.1. Economical costs and total investment cost reductions associated to the best solutions obtained related to the original design of the case study system.

		Total investment cost (€)	Irrigation network cost (€)	PV plant cost (€)	Cost reductions** (%)
Original design		80,309	63,649	16,659	-
Scenario 1	**Op 1-3***	49,154	34,319	14,835	38.8
	Op 2*	61,402	28,084	33,318	23.5
Scenario 2	**Op 1***	48,955	33,391	15,564	39.1
	Op 2*	58,917	28,274	30,643	26.6
	Op 3*	53,107	38,880	14,227	33.9

*Options refer to: Op1 (the best solution related to total cost with both individual costs- irrigation network and PV plant cost- lower than the original system design), Op 2 (the best solution related to the irrigation network cost) and Op 3 (the best solution related to the PV plant cost).
**Total investment cost reductions related to the original installation total investment cost.

Table 5.2 collects information about the sectors power demand for the selected solutions, as well as the fullfilment of irrigation needs and required PV surface area. Thus, it can be observed that all these options grouped the 13 hydrants in three sectors, with power demands between 10.0 and 26.6 kW per sector and 14.9

and 35 kW of PVPP. Moreover, all selected designs satisfied the irrigation needs in more than a 96%, requiring a PV modules area between 163.8 and 383.6 m^2.

Table 5.2. Sector power demand, PVPP of the PV plant, % irrigation requirements and required PV area for the best solutions.

		PS1 (kW)	PS2 (kW)	PS3 (kW)	PVPP (kW)	Irrigation requirements (%)	PV area (m^2)
Scenario 1	**Op 1***	11.2	11.9	10.9	15.7	96.73	172.2
	Op 2*	21.3	18.9	26.6	35.0	96.67	383.6
	Op 3*	10.9	11.9	10.9	15.7	96.82	172.2
Scenario 2	**Op 1***	12.5	11.1	10.8	16.4	96.74	179.2
	Op 2*	22.4	19.0	24.6	32.3	96.53	354.2
	Op 3*	10.0	11.4	9.3	14.9	96.66	163.8

*Options refer to: Op1 (the best solution related to total cost with both individual costs- irrigation network and PV plant cost- lower than the original system design), Op 2 (the best solution related to the irrigation network cost) and Op 3 (the best solution related to the PV plant cost).

Finally, figure 5.7 represents the total pipe length per commercial diameter (internal) included in the irrigation network design for each selected solution. All these solutions combined between 5 to 6 different sizes of diameter. Moreover, it showed flow pipe velocity values in pipes between 0.96 and 2.34 ms^{-1}, which was within the recommended values for the correct operation of these pipes. Moreover, these selected diameters oscillated between 28 to 123.4 mm, which represented an important reduction in the irrigation network cost, compared with the original design of the network, with diameters from 44 to 158.6 mm. Moreover, this figure also shows that the highest length was always represented by the largest diameter. This fact was due to the length of the drive pipe, which covered the distance between the pumping station and the irrigation field.

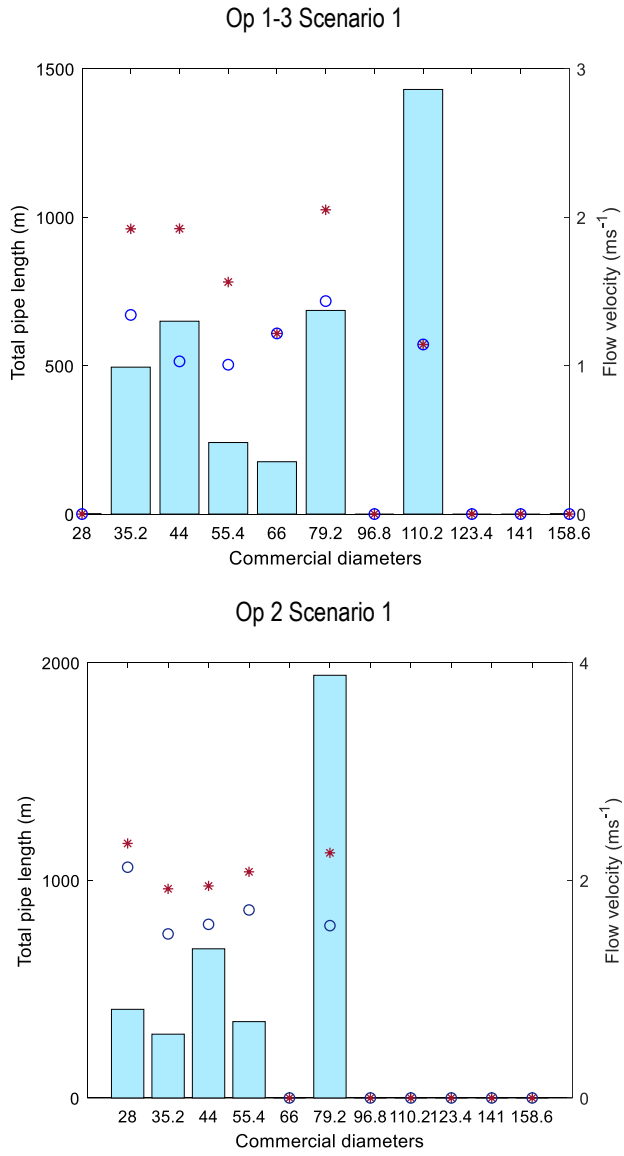

Fig. 5.7. Maximum and minimum flow velocities and total length for each pipe diameter (mm) in the network design for solutions for both scenarios.

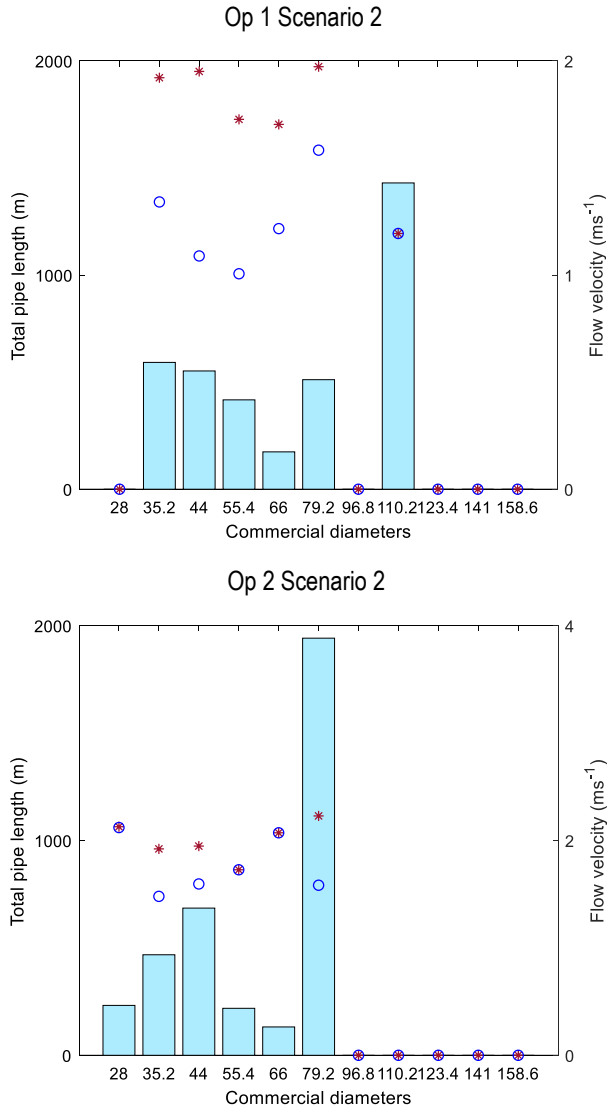

Fig. 5.7. Maximum and minimum flow velocities and total length for each pipe diameter (mm) in the network design for solutions for both scenarios.

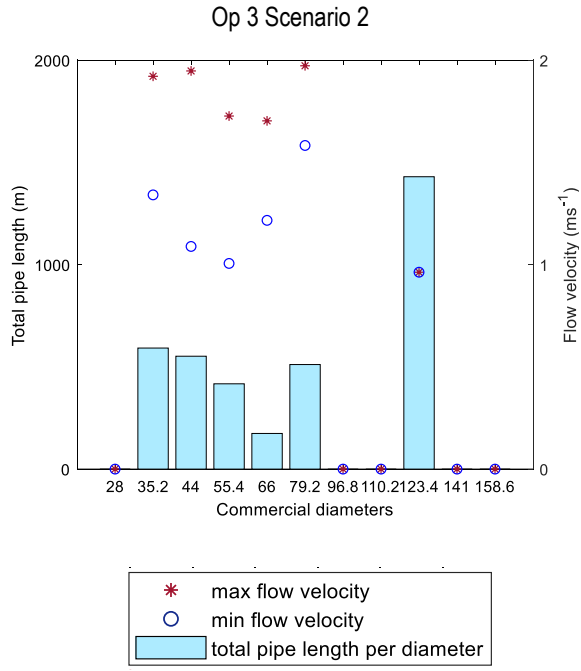

Fig. 5.7. Maximum and minimum flow velocities and total length for each pipe diameter (mm) in the network design for solutions for both scenarios.

5.4. Conclusions

The MOPISS model provides the optimal size of pipe diameters and the PV plant dimensioning of a PV irrigation system. It has been applied to a real case study. The model considers the reduction of the total investment cost and the right operation of the system. The optimization is based on the sectorization of hydrants operation, the determination of the pipe diameters, ensuring adequate flow pipe velocity, and the PV plant dimensioning that can pump enough water to satisfy the irrigation requirements.

The model was applied to an actual operating PV irrigation system, showing a series of solutions which presented important savings, between 22.9 and 38.2%, compared with the original system design. The cheapest solution, in relation to the total cost, offered a design in which both, the hydraulic and photovoltaic components had balanced costs, although separately, none of them was the cheapest option. On the other hand, the cheapest irrigation network involved a higher investment in the PV plant. This solution could suggest an interesting option under an energy net balance scenario, in which the excess of PV energy generated (when the irrigation system is not working) could be sold to the electricity grid. In contrast, the cheapest PV solution entailed the smallest PV plant, with the reduction on the required surface for the PV modules installation and the corresponding reduction of the environmental impact derived from the modules production. All solutions satisfied the irrigation requirements over a 96%, which together with the control of the flow velocity in pipes, allowed the generation of adequate and cheaper system designs options. The results showed several possible optimal solutions, that can be prioritised according to the minimization of the total investment- irrigation network- or PV plant costs, depending on the specific characteristics of the project.

5.5. References

Bakelli, Y., Hadj Arab, A., Azoui, B., 2011. Optimal sizing of photovoltaic pumping system with water tank storage using LPSP concept. Sol. Energy 85, 288–294. https://doi.org/10.1016/j.solener.2010.11.023

Creaco, E., Franchini, M., 2014. Low level hybrid procedure for the multi-objective design of water distribution networks. Procedia Eng. 70, 369–378. https://doi.org/10.1016/j.proeng.2014.02.042

Deb, K., Pratab, S., Agarwal, S., Meyarivan, T., 2002. A Fast and Elitist Multiobjective Genetic Algorithm: NGSA-II. IEEE Trans. Evol. Comput. 6, 182–197. https://doi.org/10.1109/4235.996017

Fernández García, I., Montesinos, P., Camacho Poyato, E., Rodríguez Díaz, J.A., 2017. Optimal Design of Pressurized Irrigation Networks to Minimize the Operational Cost under Different Management Scenarios. Water Resour. Manag. 31, 1995–2010. https://doi.org/10.1007/s11269-017-1629-2

Ghavidel, S., Aghaei, J., Muttaqi, K.M., Heidari, A., 2016. Renewable energy management in a remote area using Modified Gravitational Search Algorithm. Energy 97, 391–399. https://doi.org/10.1016/j.energy.2015.12.132

GIZ Deutsche Gesellschaft für Internationale Zusammenardbeit, 2016. Frequently asked questions on Solar Powered Irrigation Pumps.

Kabalci, Y., Kabalci, E., Canbaz, R., Calpbinici, A., 2016. Design and implementation of a solar plant and irrigation system with remote monitoring and remote control infrastructures. Sol. Energy 139, 506–517. https://doi.org/10.1016/j.solener.2016.10.026

Lapo, C.M., Pérez-García, R., Izquierdo, J., Ayala-Cabrera, D., 2017. Hybrid Optimization Proposal for the Design of Collective On-rotation Operating Irrigation Networks. Procedia Eng. 186, 530–536. https://doi.org/10.1016/j.proeng.2017.03.266

López-Luque, R., Reca, J., Martínez, J., 2015. Optimal design of a standalone direct pumping photovoltaic system for deficit irrigation of olive orchards. Appl. Energy 149, 13–23. https://doi.org/10.1016/j.apenergy.2015.03.107

Mérida García, A., Fernández García, I., Camacho Poyato, E., Montesinos Barrios, P., Rodríguez Díaz, J.A., 2018. Coupling irrigation scheduling with solar energy production in a smart irrigation management system. J. Clean. Prod. 175, 670–682. https://doi.org/10.1016/j.jclepro.2017.12.093

Mérida García, A., Gallagher, J., Mcnabola, A., Camacho Poyato, E., Montesinos Barrios, P., Rodríguez Díaz, J.A., 2019. Comparing the environmental and economic impacts of on- or off-grid solar photovoltaics with traditional energy sources for rural irrigation systems. Renew. Energy 140, 895–904. https://doi.org/10.1016/j.renene.2019.03.122

Muhsen, D.H., Khatib, T., Abdulabbas, T.E., 2018. Sizing of a standalone photovoltaic water pumping system using hybrid multi-criteria decision making methods. Sol. Energy 159, 1003–1015. https://doi.org/10.1016/j.solener.2017.11.044

Olcan, C., 2015. Multi-objective analytical model for optimal sizing of stand-alone photovoltaic water pumping systems. Energy Convers. Manag. 100, 358–369. https://doi.org/10.1016/j.enconman.2015.05.018

Ouachani, I., Rabhi, A., Yahyaoui, I., Tidhaf, B., Tadeo, T.F., 2017. Renewable Energy Management Algorithm for a Water Pumping System. Energy Procedia 111, 1030–1039. https://doi.org/10.1016/j.egypro.2017.03.266

Pratap, R., 2010. Getting started with Matlab. A quick introduction for scientist and engineers. Oxford University Press, USA.

Ramli, M.A.M., Bouchekara, H.R.E.H., Alghamdi, A.S., 2018. Optimal sizing of PV/wind/diesel hybrid microgrid system using multi-objective self-adaptive

differential evolution algorithm. Renew. Energy 121, 400–411. https://doi.org/10.1016/j.renene.2018.01.058

Reges, J.P., Braga, E.J., Dos, L.C., De, A.R., 2016. Inserting Photovoltaic Solar Energy to an Automated Irrigation System. Int. J. Comput. Appl. 134, 1–7. https://doi.org/10.5120/ijca2016907751

Rodríguez-Gallegos, C.D., Gandhi, O., Yang, D., Alvarez-Alvarado, M.S., Zhang, W., Reindl, T., Panda, S.K., 2017. A Siting and Sizing Optimization Approach for PV-Battery-Diesel Hybrid Systems. IEEE Trans. Ind. Appl. 9994, 1–1. https://doi.org/10.1109/TIA.2017.2787680

Rossman, L., 2000. EPANET 2. Users manual. US Environmental Protection Agency (EPA), USA.

Tayfur, G., 2017. Modern Optimization Methods in Water Resources Planning, Engineering and Management. Water Resour. Manag. 31, 3205–3233. https://doi.org/10.1007/s11269-017-1694-6

Wissem, Z., Gueorgui, K., Hédi, K., 2012. Modeling and technical-economic optimization of an autonomous photovoltaic system. Energy 37, 263–272. https://doi.org/10.1016/j.energy.2011.11.036

Yahyaoui, I., Tadeo, F., Segatto, M.V., 2016. Energy and water management for drip-irrigation of tomatoes in a semi- arid district. Agric. Water Manag. 183, 4–15. https://doi.org/10.1016/j.agwat.2016.08.003

6. Conclusions

- Photovoltaic energy is a very good alternative to traditional energy sources for energy supply in irrigation in areas with adequate solar radiation levels, offering a solution for isolated farms without electricity grid access. However, its high dependence on climatic variables requires new management tools.
- The development of intelligent models for real-time management of photovoltaic irrigation by synchronising the power generated and that demanded by the different sectors which make up the network made possible to satisfy more than 96% of the irrigation requirements of the crop, in the case study analysed. These results prove the efficiency and autonomy of the system, which also allowed reducing the emission of 1.2 tn of CO_2 eq. in an irrigation season.
- Photovoltaic energy has a virtually zero environmental impact during the period of operation. However, the manufacturing process of photovoltaic modules requires a significant demand for materials and energy. Even so, the potential for global warming, acidification, depletion of fossil fuel resources and human toxicity linked to 1kWh of energy, for the photovoltaic energy supply option was significantly lower than the showed by traditional supply options (electricity grid and diesel generator).
- The seasonality of irrigation notably affects the environmental impact linked to each kWh of useful photovoltaic energy. Thus, the possibility of exporting the surplus of photovoltaic energy produced and not consumed by the irrigation network to the electricity grid showed, for the case study analysed, an environmental burden for each kWh of energy used 6 times lower than

that determined for the irrigation option in which the photovoltaic plant is not connected to the electricity grid.

- Photovoltaic energy as a source of energy supply for irrigation entails a higher initial investment than that corresponding to the use of traditional energy sources. However, the total cost (investment and operating costs) linked to the photovoltaic irrigation option for the selected case study resulted in cost reductions of 63% and 36% compared to the use of a diesel generator and the electricity grid, respectively.
- The development of optimization tools for the dimensioning of the photovoltaic irrigation system integrating economic and operational aspects, as well as hydraulic and energetic variables, allows to obtain design solutions that contemplate the minimization of the total investment cost, assuring the correct operation of the system.

New avenues of research:

After the results obtained in this thesis, some of the possible future avenues of research are listed below:

- The integration of the environmental aspects in the optimization models for the dimensioning of photovoltaic irrigation systems, such as life cycle assessment.
- The adaptation of the dimensioning optimization for the photovoltaic irrigation system to crops with greater irrigation restrictions, evaluating a possible photovoltaic energy supply combined with other energy sources.

- The integration in the optimal dimensioning of photovoltaic irrigation system models of the assessment of the partial sale of the energy generated as a complementary economic activity to the agricultural farm.
- The study of the possibility of photovoltaic energy supply in more complex irrigation networks, such as irrigation districts with on demand irrigation, considering a possible net balance scenario.

6. Conclusiones

La energía fotovoltaica es una muy buena alternativa a las fuentes de energía tradicionales para el suministro energético en el riego en zonas con adecuados niveles de radiación solar, ofreciendo una solución para explotaciones aisladas de la red eléctrica. Sin embargo, su alta dependencia de las variables climáticas requiere nuevas herramientas de gestión.

 El desarrollo de modelos inteligentes para la gestión en tiempo real del riego fotovoltaico mediante la sincronización de la potencia generada y la demandada por los distintos sectores que componen la red ha permitido satisfacer en más de un 96% los requerimientos de riego del cultivo en el caso de estudio analizado. Estos resultados prueban la eficacia y autonomía del sistema, que además permitió reducir la emisión de CO2 eq. en 1.2 tn en una campaña de riego.

 La energía fotovoltaica presenta un impacto ambiental casi despreciable durante el periodo de funcionamiento. Sin embargo, la etapa de fabricación de los módulos fotovoltaicos requiere una importante demanda de materiales y energía. Aun así, el potencial de calentamiento global, de acidificación, de agotamiento de recursos fósiles y de toxicidad humana vinculado a 1kWh de energía, para la opción de suministro energético fotovoltaico fue significativamente menor al mostrado por las opciones de suministro tradicionales (red eléctrica y generador diésel).

 La estacionalidad del riego afecta notablemente al impacto ambiental vinculado a cada kWh de energía fotovoltaica útil. Así, la posibilidad de exportar a la red eléctrica el excedente de energía fotovoltaica producida y no consumida por la red de riego mostró, para el caso de estudio analizado, una carga ambiental para

cada kWh de energía aprovechado 6 veces inferior a la determinada para la opción de riego en la que la planta fotovoltaica permanece aislada de la red.

 La energía fotovoltaica como fuente de suministro energético en el riego conlleva una mayor inversión inicial que la correspondiente al uso de fuentes de energía tradicionales. Sin embargo, el coste total (costes de inversión y funcionamiento) vinculado a la opción de riego fotovoltaico para el caso de estudio seleccionado resultó en un ahorro del 63% y 36% en comparación con el uso de un generador diésel y la red eléctrica, respectivamente.

 El desarrollo de herramientas de optimización para el dimensionamiento del sistema de riego fotovoltaico que integran aspectos económicos y de operatividad, así como variables hidráulicas y energéticas, permite obtener soluciones de diseño que contemplan la minimización del coste total de inversión, asegurando un correcto funcionamiento del sistema.

Nuevas vías de investigación:

Tras los resultados obtenidos en esta tesis, a continuación, se recogen algunas de las posibles futuras vías de investigación:

 Integrar los aspectos ambientales en los modelos de optimización del dimensionamiento de sistemas de riego fotovoltaico, como la evaluación del ciclo de vida.

- Adaptar la optimización del dimensionamiento del sistema de riego fotovoltaico a cultivos con mayores restricciones de riego, evaluando un posible suministro energético fotovoltaico combinado con otras fuentes de energía.

- Integrar en los modelos de optimización del dimensionamiento del sistema de riego fotovoltaico la valoración de la venta parcial de la energía producida como actividad económica complementaria a la explotación agrícola.

- Estudiar el posible abastecimiento energético fotovoltaico en redes de riego más complejas, como comunidades de regantes con organización del riego a la demanda, considerando un posible escenario de balance neto.

Appendix A. Middleware to operate Smart photovoltaic irrigation systems in real time.

This chapter has been published entirely in the journal "Water", R. González Perea, A. Mérida García, I. Fernández García, E. Camacho Poyato, P. Montesinos Barrios, J.A. Rodríguez Díaz (2019)

Abstract. Climate change, water scarcity and higher energy requirements and electric tariff compromises the continuity of the irrigated agriculture. Precision agriculture (PA) or renewable energy sources which are based on communication and information technologies and a large amount of data are key to ensuring this economic activity and guaranteeing food security at the global level. Several works which are based on the use of PA and renewable energy sources have been developed in order to optimize different variables of irrigated agriculture such as irrigation scheduling. However, the large amount of technologies and sensors that these models need to be implemented are still far from being easily accessible and usable by farmers. In this way, a middleware called Real time Smart Solar Irrigation Manager (RESSIM) has been developed in this work and implemented in MATLAB™ with the aim to provide to farmers a user-friendly tool for the daily making decision process of irrigation scheduling using a smart photovoltaic irrigation management module. RESSIM middleware was successfully tested in a real field during a full irrigation season of olive trees using a real smart photovoltaic irrigation system.

Keywords: irrigation scheduling; precision agriculture; sustainable

irrigation; software; ICTs; hydraulic modelling.

A.1. Introduction

The increase in energy requirements and water scarcity, has led to a rise in the operating costs of irrigated agriculture (Corominas, 2010), aggravated by higher electricity tariff and fuel prices. Likewise, pressurized irrigation systems have greater environmental impact than gravity irrigation systems due to the use of energy (Fernández García et al., 2014; García Morillo et al., 2015). To minimise these adverse impacts, the use of precision agriculture (González Perea et al., 2017) and renewable energy sources is being promoted to improve the sustainability of irrigation agriculture. Both precision agriculture and the use of renewable energy sources require the use of a large amount of data from highly heterogeneous sensors as well as the use of information and communication technologies (ICTs) for their communication. In this way, several works have been developed, such as Reference (Hamidat et al., 2003), in which solar energy was applied to small-scale irrigation, covering daily water needs. The hybrid use of several renewable energy sources (wind/solar) have also been developed to meet irrigation energy needs and to increase the crop profitability (Vick and Almas, 2011; Mérida García et al., 2018) developed a Smart Photovoltaic Irrigation Manager (SPIM), which provides a daily irrigation scheduling for crops at plot scale, using photovoltaic (PV) solar energy to pump water to the irrigation network to meet crop irrigation requirements according to the available solar energy. This model developed in MATLAB™ synchronizes the photovoltaic solar energy to optimize the daily irrigation scheduling computing the daily irrigation requirements, the hydraulic behaviour of the irrigation network

establishing the optimum irradiance threshold per irrigation sector, the instantaneous photovoltaic power production from pyranometer sensor and the daily soil water balance. Bhattacharjee et al. (2019) developed a model to collect underground water using a submersible pump by a solar photovoltaic system in remote areas. The model included a solar charge controller connected to an inverter for the pump motor operation. Bouchakour et al. (2019) developed an algorithm based on fuzzy logic to improve photovoltaic water pumping system performance. All these models are based on data from a wide range of sensors, various web platforms such as climatic web platforms and commercial irrigation controllers (Mérida García et al., 2018). However, the volume and nature of the data used by these models introduces a significant challenge in the implementation of solar irrigation management tools in commercial fields which must operate in real time. In addition, a development trend in precision agriculture is standardisation (Wang et al., 2006), in order to achieve software sharing and interoperability of computer programs (Marakami et al., 2007) and provide to farmers a robust, scalable and adaptable tool to help the daily making decision process. Peres et al. (2011) worked in this context developing an autonomous intelligent gateway infrastructure for in-field processing in precision viticulture. However, this model implements only the hardware, communication capabilities and software architecture of an intelligent autonomous gateway, designed to provide the necessary middleware between locally deployed sensor networks and a remote location within the whole farm without considering the implementations of smart photovoltaic irrigation models developed by other researchers.

In this work, a new middleware called Real time Smart Solar Irrigation

Manager (RESSIM) has been developed to control the operation of a smart photovoltaic irrigation system in real time. The core of this middleware is a smart photovoltaic irrigation management module, developed in MATLAB™, that handles the information received from the irrigation controller and climate web platforms. RESSIM has been developed under a user-friendly graphical user interface (GUI) with MATLAB™ GUIDE and was applied for irrigation management of a commercial olive grove in southern Spain.

A.2. RESSIM Design

A.2.1. Model Description

RESSIM is a platform which connect software modules, graphical user interface (GUI), databases (building and management) and remote connections with different data sources (irrigation controller and its linked sensors and web platforms).

RESSIM links six modules (Fig. A.1): smart PV irrigation management, database, irrigation control, field sensing, agroclimatic information and GUI to make RESSIM a user-friendly middleware. These modules are described next.

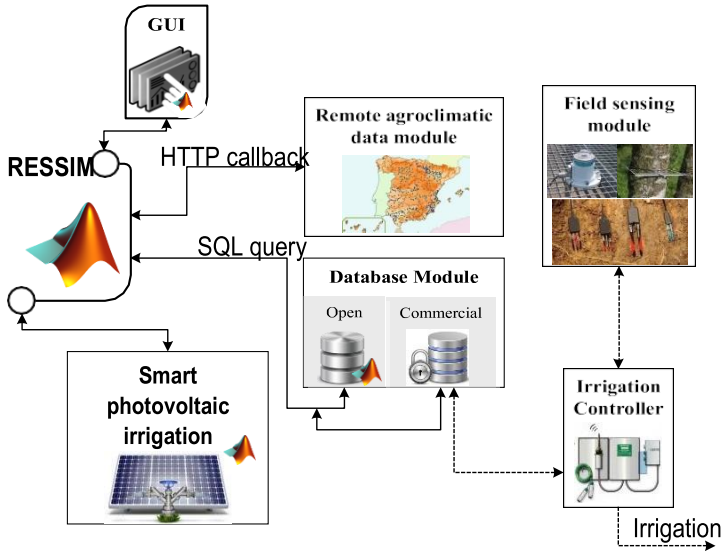

Fig. A.1. Architecture of Real time Smart Solar Irrigation Manager (RESSIM).

A.2. 1.1. Smart PV Irrigation Management Module

The core of RESSIM is the smart photovoltaic irrigation management module known as Smart Photovoltaic Irrigation Manager (SPIM) (Mérida García et al., 2018). This model synchronizes the availability of photovoltaic energy with the energy demand of the different irrigation sectors to meet the daily crop irrigation needs. SPIM integrates several calculation modules to obtain the decision variables required for irrigation management. One of these variables is the daily crop irrigation needs, calculated from evapotranspiration and precipitation data and crop water requirements. The irrigation system is operated in sectors, thus hydraulic modelling techniques are used to estimate the power requirements of each one. The supplied

electric power depends on the energy production of the photovoltaic plant, estimated according to Reference (López-Luque et al., 2015).

Additionally, in the SPIM model the soil is considered as a water storage tank, so the soil water balance is computed daily. Using this information and daily priority rules, the optimum operating sequence of the irrigation sectors can be established in real time. As only photovoltaic energy is used to power the system, the presence of clouds may prevent the system from operating long enough to meet the daily crop irrigation needs. When this is the case, soil water content is checked, and if the moisture content is enough to fill the irrigation deficit, soil water is assumed to satisfy the irrigation needs of that day. Otherwise, the irrigation time of the following day is increased to compensate for the irrigation deficit.

Real-time information about climate type, soil moisture content, solar installation and the status of the system's hydraulic devices (e.g., open valve, pressure head at the pumping station) is used to calculate all the elements described above. The information required by SPIM is obtained from the database module and the communication module with the climate web platform. A detailed description of the SPIM model can be found in (Mérida García et al., 2018).

A. 2.1.2. Irrigation Controller

In most farms, commercial irrigation controllers are used to apply the crop water requirements according to a predefined irrigation scheduling plan. Most commercial irrigation controllers are built over a database, "commercial database", which is used to operate them (reading sensor measurements and sending orders to

actuators). Remote sensors are also included in the commercial irrigation controller as an external device and their measurements are recorded in the same database. Thus, commercial irrigation controllers are just an interpreter of its database through create, read, update and delete (CRUD) queries. These CRUD queries enable the irrigation controller to read the external sensors and give any orders to filters, electro valves, etc., which control the irrigation process. Likewise, the opening or closing process of all irrigation system elements (electro valves, filters...) are also managed by the irrigation controller through its database. Consequently, irrigation controller is just a listener of its database, where the status of each field sets its behaviour.

Thus, managing the commercial database allows the irrigation controller and all their connected devices to be handled. Hence, in this work, the commercial irrigation controller was managed by RESSIM to target the commercial database through Structured Query Language (SQL) queries.

A.2.1.3. Field Sensing Module and Remote Agroclimatic Data Module

Two different ways to get and save information from field sensors were implemented in RESSIM. Most of the commercial irrigation controllers enable the integration of multiple sensors regardless of the transmission protocol. Measures from these sensors can be saved in its commercial database. Thus, RESSIM could read and operate these sensors through its database. For example, RESSIM managed in real time a pyranometer which was installed in the studied field. By RESSIM and the real time processing of pyranometer data, the smart PV irrigation management module could compute the instantaneous power available for irrigation

sectors. Alternatively, RESSIM could integrate other sensors, different from those initially included in the database. Thus, any other sensor, that can send information to a cloud repository, may be managed by the system.

The remote agroclimatic data module allowed agro-climatic information required by the smart PV irrigation management module (SPIM, in this work) to be obtained. These data are collected from a public weather stations platform. This module, developed in MATLAB™, gets information from public websites by HTTP call-backs and sent it to RESSIM as JavaScript Object Notation (JSON) format. Then, this information was managed by RESSIM and sent to the smart PV irrigation management module.

A.2.1.4. Database Module

The database module was made up by two databases: commercial and open databases. The commercial one was a relational database which resides on a separate machine from the irrigation controller. This commercial database was accessible by TCP/IP connection and SQL server. Frequently, the irrigation controller database is private. Therefore, information about username, password, database name and port where the database was running was necessary for RESSIM. In this work, the commercial database was managed by CRUD functions from RESSIM.

The open database was automatically created by RESSIM at the first-time execution. This database consisted of five relational tables and was developed in MATLAB™, using SQL server (Fig. A.2). The first table, “Farm’s Owner Table”, relates each user to their farm(s). Information about location and the number of

sectors that make up the irrigation network is required by SPIM. Thus, farm description is recorded in "Farm Description Table".

Several agroclimatic parameters, such as reference evapotranspiration, rainfall, temperature and solar radiation are required by SPIM. For each farm, these data are stored in "Agroclimatic Data Table". On the other hand, the power demand of each sector of the irrigation network computed by SPIM is saved in "Farm PV Power Table". Finally, "Operating Sector Table" stores the daily sequential operating sectors of each farm as a Boolean variable (open/close).

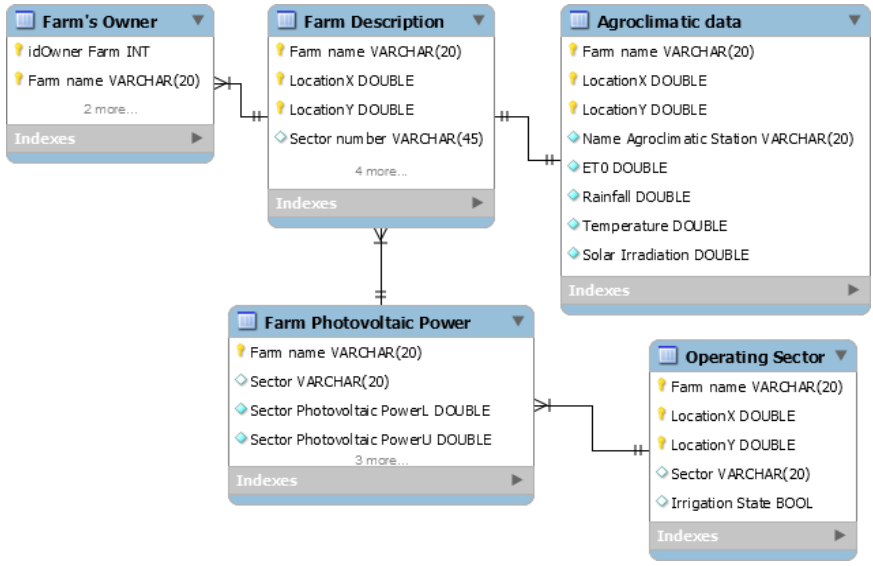

Fig. A.2. Architecture of the open database of RESSIM.

A.2.1.5. RESSIM Middleware and RESSIM GUI

RESSIM software and RESSIM GUI was developed in MATLAB™ and its flow chart is shown in Fig. A.3.

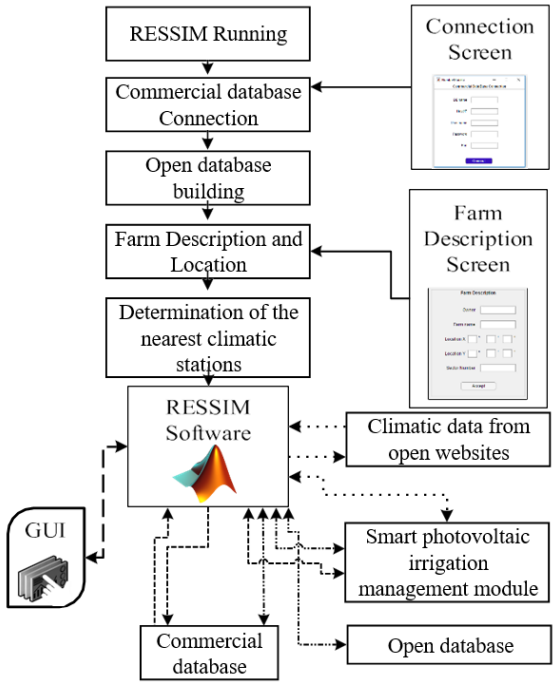

Fig. A.3. Chart flow of RESSIM.

Initially, RESSIM requires four connection parameters from the commercial database (IP, username, password and port). Then, the open database is automatically created and saved as a local database. After connection with the commercial database, which controls the irrigation controller, and once the open

database is built, information about farm description is demanded. Once the farm location is known, RESSIM automatically identifies the nearest agroclimatic stations, storing this information in the open database.

After the initial setting, RESSIM determines the inputs/outputs, as well as SPIM's variables, which are shown in the main screen of the GUI. At this point, RESSIM remains in a "listening mode" to both the GUI and SPIM model. When SPIM requires climatic information, it sends a request through RESSIM (Fig. A.3, dotted line). Via HTTP callbacks, RESSIM obtains the climatic data from open websites and this information is sent back to SPIM. By the same token, the information received by field sensors, such as pressure head at pumping station or irradiance values, is obtained by RESSIM through SQL queries, by the connection between RESSIM software, the commercial database, RESSIM GUI and SPIM (Fig. A.3, dash line).

Once the sequence of operating sectors (irrigation scheduling) is determined as described by (Mérida García, et al., 2018), this information is sent to the database module by RESSIM and stored in the open database, parallelly modifying the commercial database. Thus, the irrigation controller, which is connected to the commercial database, receives the length of the irrigation event of each sector in real time (Fig. A.3, dot and dash line).

Finally, a friendly GUI (Fig. A.4) was designed to visualize the values of the main decision variables in real time and to interact with SPIM and the irrigation controller.

Any information shown or managed by RESSIM GUI follows the path shown

in Fig. A.3 with the bold dash line. The GUI was divided into seven containers: experimental farm, pumping station-operating sector, photovoltaic plant, irrigation season, water volume records, soil water balance and irradiance threshold per sector. The experimental farm container shows the farm's layout highlighting the operating sector and the spatial hydraulic simulation of this sector in real time (pressure and flow for each emitter of the irrigation sector as well as for hydrant).

Pressure head, in m, and flow applied, in $m^3\ h^{-1}$, by the pumping station is shown in the container labelled "Pumping station-operating sector". Information related to the photovoltaic plant as irradiance, in $W\ m^{-2}$, and photovoltaic power, in W, is shown in the "Photovoltaic plant" container.

The "Irrigation season" container provides the beginning date of the irrigation season, the estimated flowering date and the real flowering date. When estimated and real flowering dates do not match, SPIM recomputes the irrigation scheduling. The "Water volume records" container provides the total amount of water applied to each irrigation sector, in m^3, the irrigation target volume in this irrigation season per irrigation sector, in m^3, the percentage of irrigation requirements which have been satisfied, in %, the date of the last irrigation event per irrigation sector and the estimated irrigation requirements for the following day. The real time value of the soil water content in each sector is displayed in the "Soil water balance container".

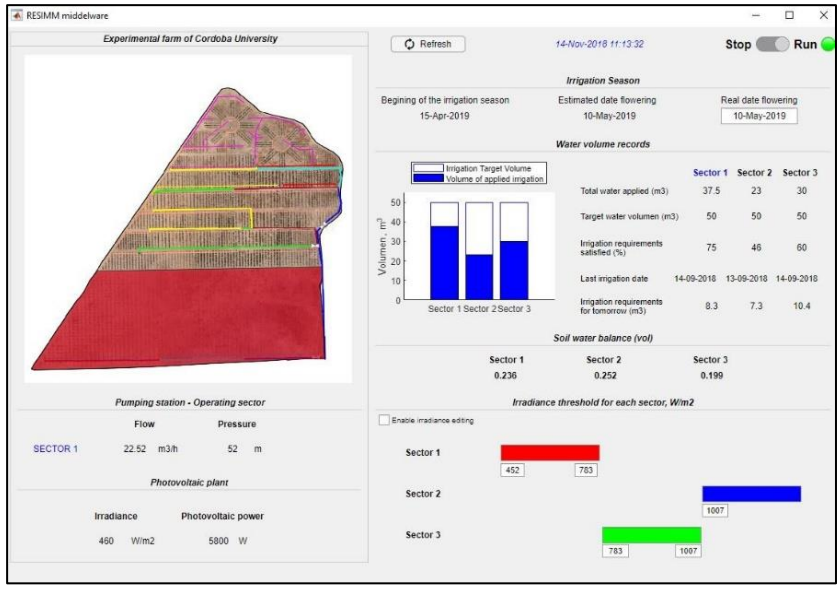

Fig. A.4. RESSIM graphical user interface (GUI).

The range of irradiance in which each sector operates, determined by SPIM, is shown in the "Irradiance threshold per sector container". Finally, the current date, and start/stop button were in the upper-right corner of the GUI.

A.3. Implementation of RESSIM in a Real Case Study

RESSIM has been designed to be implemented to the most irrigation controllers which are based on a SQL database and most smart photovoltaic irrigation managers. The implementation of RESSIM just requires a PC with an internet connection to get the full potential of the tool.

A test field of 13.4 ha located on the experimental farm of Cordoba University

(Southern Spain) was selected to test the proposed RESSIM middleware (Fig. A.5).

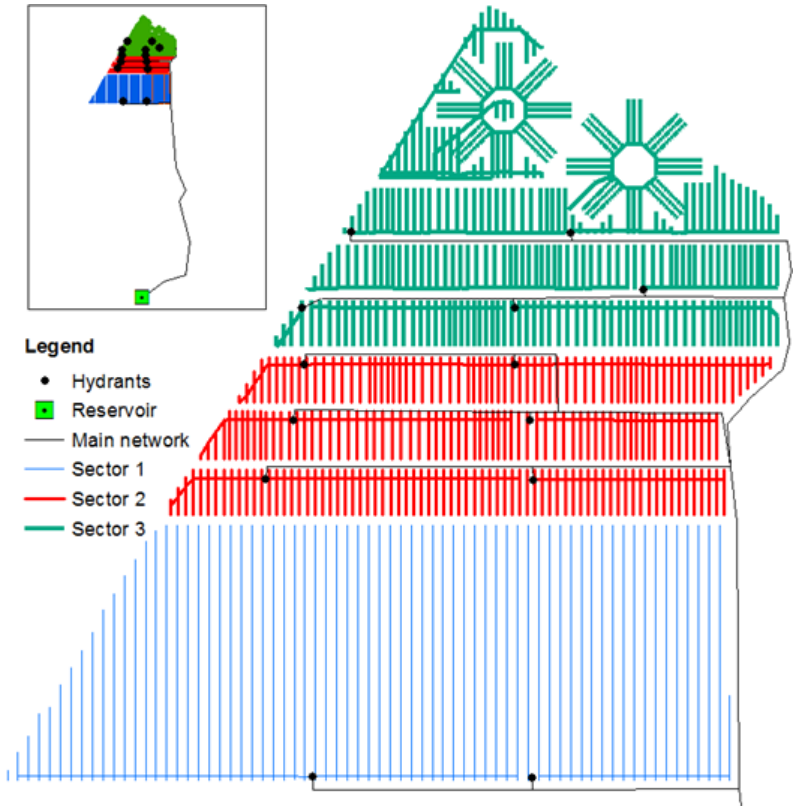

Fig. A.5. Experimental farm of Cordoba University.

The irrigation system of the experimental farm is fitted with an irradiance sensor, a flow meter, a pressure meter and a soil moisture sensor, which are connected to a commercial irrigation controller, AGRONIC 4000

(https://www.progres.es/es/agronic4000).

Historical climatic data (precipitation and evapotranspiration) were obtained from the open website of Andalusian weather stations (https://www.juntadeandalucia.es/agriculturaypesca/ifapa/ria/servlet/FrontController), while, forecasted and real time climatic data were obtained from a national open website (https://www.eltiempo.es/).

RESSIM was applied for an entire irrigation season. Thus, Fig. A.6 shows the applied irrigation depth, the required irrigation depth and the irrigation correction by SPIM model during the irrigation season. Two days (16 April and 28 July, Julian days of the year 106 and 209, respectively) were selected and marked in Fig. A.6 by asterisk in order to discuss the results with RESSIM management. The irrigation scheduling for the two selected days is shown in Fig. A.7 a, b respectively. Both figures show the synchronization of the operating sectors of the irrigation network and the photovoltaic power generation determined by SPIM and managed by RESSIM. Fig. A.7a (Julian day of the year 106) shows the synchronization of the operating sector in a typical cloudy day while RESSIM management for a sunny day is shown in Fig. A.7b. The hard task to manage in real time (manually operate) the synchronization of the irrigation operation with the photovoltaic power generation highlights the utility of RESSIM in daily irrigation scheduling.

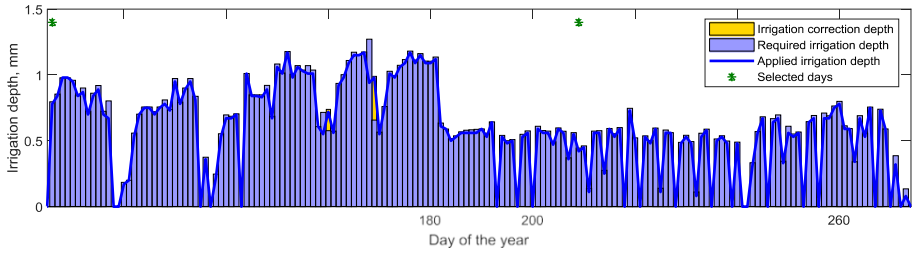

Fig. A.6. Irrigation scheduling with the smart photovoltaic irrigation manager (SPIM) and RESSIM management for a whole irrigation season.

Two different times of the day were selected in Fig. A.7a, b (red asterisk), 11 am and 12 am, respectively. For both selected time periods, RESSIM GUI is shown in Fig. A.8a, b respectively. S3 and S2 irrigation sectors were working in the selected instant, respectively. Fig. A.8a highlights the first day of the irrigation season in which S2 irrigation sector was working at 12:00 h. Thus, the total water volume applied until that day was 0.3%, 0.4% and 0.5% for the three irrigation sectors, respectively. The volume applied at the studied hour on that day (Julian day of the year 106) was 15.9 m^3, 20.8 m^3 and 39.6 m^3 for S1, S2 and S3, respectively, and the total water volume required on that day was 48.7 m^3, 41.8 m^3 and 60.7 m^3, respectively. The estimated water volume for the following day (day of the year 107) was 52.3 m^3, 44.9 m^3 and 65.1 m^3, for the three irrigation sectors, respectively.

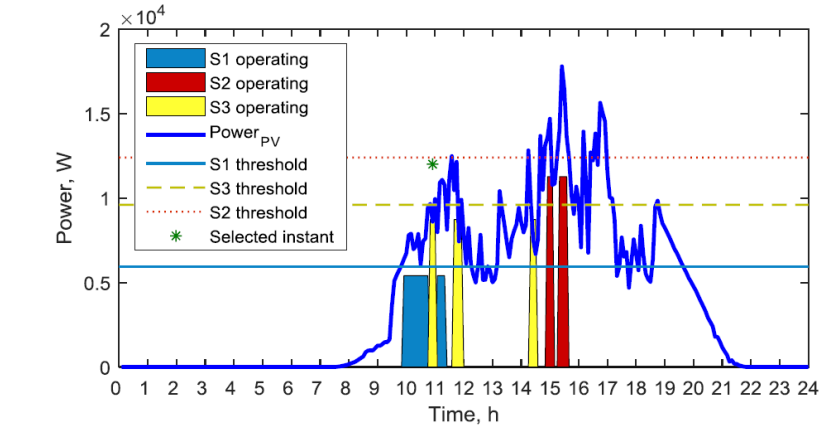

(**a**)

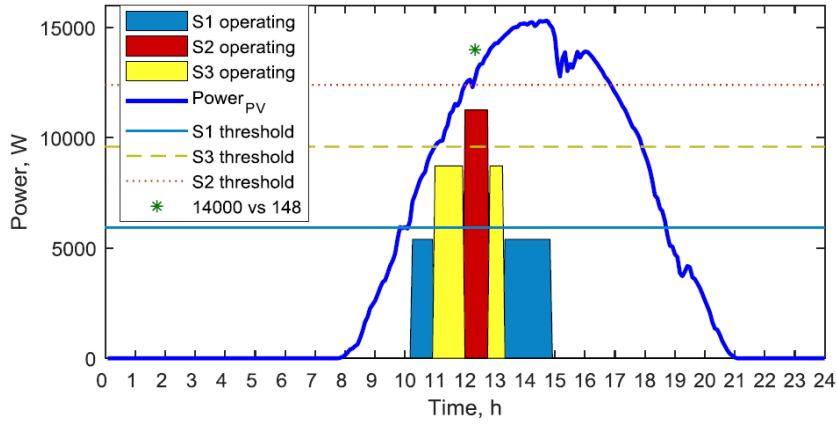

(**b**)

Fig. A.7. Photovoltaic power generation, power threshold and operation sequence of sectors of the irrigation network in the Julian day of the year 106 (**a**) and 209 (**b**) of the irrigation seasons.

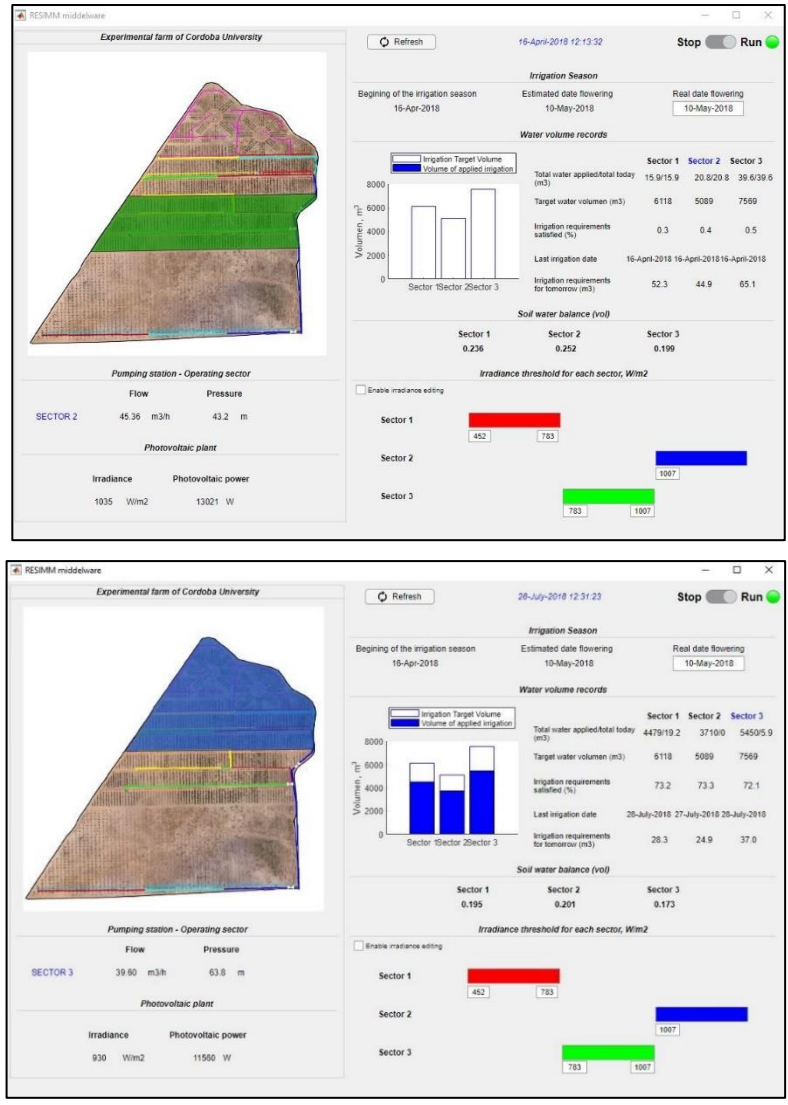

Fig. A.8. Screenshots of the RESSIM model on the Julian day of the year 106 (a) and 209 (b).

For the day of the year 209 (Fig. A.8b), the percentage of water applied until that day was 73.2%, 73.3%, and 72.1% of the total water requirements of the irrigation season, for the three irrigation sectors, respectively. At that moment, the daily applied water volume for S1, S2 and S3 was 4479 m^3, 3710 m^3 and 5450 m^3, respectively. According to SPIM model, the estimated water volume for the following day (Julian day of the year 210) was 28.3 m^3, 24.9 m^3 and 37.0 m^3, for the three irrigation sectors, respectively. Both scenarios (Fig. A8a, b) show the high synchronization determined by SPIM and carried out by RESSIM between the operation of the irrigation sectors and photovoltaic power generation linked to irrigation requirements.

Although the SPIM model could be run manually, the daily synchronization and the daily irrigation scheduling based on solar irrigation would be impossible without RESSIM middleware.

A.4. Conclusions

Due to the variability of power production during the day, the irrigation management with water pumped with PV energy is a complex task. As power production is variable, heterogeneous elements like sensors, countless web platforms and commercial irrigation controllers must be used co-ordinately. The integration of all these elements is essential to ensure the success of this technology, which is more complicated to manage than systems based on conventional energies where the availability of power is constant.

Thus, RESSIM is a friendly tool that facilitates the management of PV irrigation systems, since it gathers information from different data sources and models and automatically apply the previously calculated irrigation depths to all the sectors depending on the instant power production of the solar panels.

RESSIM was successfully tested in an experimental field for olive trees irrigation. The system managed automatically the solar irrigation system during one full irrigation season, without any major incident.

The first version of the RESSIM model have allowed the optimum synchronization between the solar energy production and the irrigation requirements and the operation with the pumping station. By this optimal synchronization, the investment cost of the photovoltaic plant can also be reduced, optimizing the size and consequently reducing the greenhouse gases emissions. In future versions of the tool, dynamic models of crop growth, predictive models of daily water demand at farm level as well as the possibility of fitting the pumping station with variable speed drives will be implemented in order to improve the synchronization between the photovoltaic energy production and water demand both at farm and at water user association levels.

A.5. References

Bhattacharjee, B.; Chakrabarti, A.; Sadhu, P.K. Solar photovoltaic integrated pump for advanced irrigation system. Int. J. Innov. Technol. Explor. Eng. 2019, 8, 3246–3250.

Bouchakour, A.; Borni, A.; Zaghba, L.; Boukebbous, S.E.; Fazzani, A. Fuzzy logic controller to improve photovoltaic water pumping system performance. In Proceedings of the 2018 6th International Renewable and Sustainable Energy Conference (IRSEC), Rabat, Morocco, 5–8 December 2018; IEEE: Piscataway, NJ, USA, 2019.

Corominas, J. Agua y energía en el riego en la época de la sostenibilidad. Ing. del agua 2010, 17, 219–233.

Fernández García, I.; Rodríguez Díaz, J.A.; Camacho Poyato, E.; Montesinos, P.; Berbel, J. Effects of modernization and medium term perspectives on water and energy use in irrigation districts. Agric. Syst. 2014, 131, 56–63.

García Morillo, J.; Martín, M.; Camacho, E.; Díaz, J.A.R.; Montesinos, P. Toward precision irrigation for intensive strawberry cultivation. Agric. Water Manag. 2015, 151, 43–51.

González Perea, R.; Daccache, A.; Rodríguez Díaz, J.A.; Poyato, E.C.; Knox, J. Modelling impacts of precision irrigation on crop yield and in-field water management. Precis. Agric. 2017, 19, 497–512.

Hamidat, A.; Benyoucef, B.; Hartani, T. Small-scale irrigation with photovoltaic water pumping system in Sahara regions. Renew. Energy 2003, 28, 1081–1096.

López-Luque, R.; Reca, J.; Martínez, J. Optimal design of a standalone direct pumping photovoltaic system for deficit irrigation of olive orchards. Appl. Energy 2015, 149, 13–23.

Mérida García, A.; Fernández García, I.; Camacho Poyato, E.; Montesinos Barrios, P.; Rodríguez Díaz, J.A. Coupling irrigation scheduling with solar energy production in a smart irrigation management system. J. Clean. Prod. 2018, 175, 670–682.

Murakami, E.; Saraiva, A.M.; Ribeiro, L.C.M.; Cugnasca, C.E.; Hirakawa, A.R.; Correa, P.L.P. An infrastructure for the development of distributed serviceoriented information systems for precision agriculture. Comput. Electron. Agric. 2007, 58, 37–48.

Peres, E.; Fernandes, M.A.; Morais, R.; Cunha, C.R.; López, J.A.; Matos, S.R.; Ferreira, P.J.S.G.; Reis, M.J.C.S. An autonomous intelligent gateway infrastructure for in-field processing in precision viticulture. Comput. Electron. Agric. 2011, 78, 176–187.

Vick, B.D.; Almas, L.K. Developing a hybrid solar/wind powered irrigation system for crops in the Great Plains. Appl. Eng. Agric. 2011, 27, 235–245.

Wang, N.; Zhang, N.; Wang, M. Wireless sensors in agriculture and food industry—recent development and future perspective. Comput. Electron. Agric. 2006, 50, 1–14.